

CFD STUDY ON THE EFFECT OF VELOCITY AND TEMPERATURE TOWARD  
THE PERFORMANCE ON PARTIAL COMBUSTION UNIT

NURUL SYAZWANI BINTI ROHAIMI

Thesis submitted in fulfillment of the requirements  
for the award of the degree of  
Bachelor of Chemical Engineering (Gas Technology)

Faculty of Chemical and Natural Resources Engineering  
UNIVERSITI MALAYSIA PAHANG

JANUARY 2012

### **SUPERVISOR'S DECLARATION**

We hereby declare that we have checked this thesis and in our opinion, this thesis is adequate in terms of scope and quality for the award of the degree of Bachelor of Chemical Engineering (Gas Technology).

Signature :  
Name of Supervisor : ASSOCIATE PROFESSOR ZULKAFI BIN HASSAN  
Date : 27<sup>th</sup> JANUARY 2012

Signature :  
Name of Co – Supervisor : MR MD. NOOR BIN ARIFIN  
Date : 27<sup>th</sup> JANUARY 2012

### **STUDENT'S DECLARATION**

I hereby declare that the work in this thesis is my own except for quotation and summaries which have been duly acknowledged. The thesis has not been accepted for any degree and is not concurrently submitted for award of other degree.

Signature :  
Name : NURUL SYAZWANI BINTI ROHAIMI  
ID Number : KC08052  
Date : 27<sup>th</sup> JANUARY 2012

*Dedicated specially for my beloved mother, father, sister and brother,  
thanks for supportive and encouragement.  
And for the one, thank you for understanding.*

## ACKNOWLEDGEMENTS

First and foremost, thank and praise the Almighty God, Allah S.W.T. for giving me good health, a clear mind and determination to complete this thesis for Undergraduate Research Projects successfully.

I am grateful and would like to express my sincere gratitude to my Supervisor, Associate Professor. Zulkafli bin Hassan and Co-Supervisor, Mr Md. Noor bin Arifin for their idea and advising me in preparing this thesis and guiding me on the workflow of the overall project.

My sincere thanks go to Dr Jolius Bin Gim bun and my friend Norliyana Binti Erain for sharing their knowledge and experience in conducting simulation via Computational Fluid Dynamics (CFD). They spent most of their valuable time in guiding me a basic in CFD and monitoring the simulation.

Unforgotten, Tn. Hj. Amirudin Bin Safie, the Head of Ironmaking Process Research and Development of Perwaja Steel Sdn. Bhd. as my industrial supervisor for providing valuable feedbacks on the study approach and supports.

I also like to take this golden opportunity to express my feeling of gratitude to my beloved family members and friends for the moral support and consistently encouraged me to complete this thesis.

Thank you.

## ABSTRACT

In the iron and steel making process, Direct Reduction Plant (DRP) is the most important components which are consist of Partial Combustion Unit (PCU). PCU take place in between the process gas heater and the oxides removal reactor. The PCU consists of one transfer line and two oxygen lances. On the oxygen lances, there is a nozzle attached to each of it. The simulation via Computation Fluid Dynamics (CFD) to validate the performance of the PCU with current installation by analyzing the profile of the temperature was performed using standard k- $\epsilon$  (SKE) viscous model and Eddy Dissipation (ED) turbulence-chemistry interaction model. The heated natural gas (NG) from the heater will be supplied to the transfer line. The performance of PCU using current process was compared with the new process scheme which consists of different mass fraction of the process gasses, temperature and velocity of process gasses and oxygen to identify the most effective process in term of the temperature used in PCU by using CFD. The simulation also was performed to detect either the boundary refractory in the simulation will influence the temperature profile obtain. These should be design using GAMBIT 2.4 and simulation should be run to compute the solution using FLUENT 6.3.26. From this study, the new process scheme show the temperature profile at the validation point is high compare to the current process scheme even though the percentage error is much higher in the new process scheme compare to current process scheme. Thus, further study on design and data modification should be done to get more accurate result.

## ABSTRAK

Dalam proses penghasilan besi dan keluli, 'Direct Reduction Plant' (DRP) adalah salah satu komponen penting yang terdiri daripada Unit Pembakaran Separa (PCU). PCU ini terletak di antara pemanas proses gas dan reaktor penyingkiran oksida. Di dalam PCU ini terdapat satu 'transfer line' dan dua 'oxygen lances'. Terdapat satu 'nozzle' pada setiap satu 'oxygen lances' tersebut. Simulasi yang dijalankan menggunakan alatan pengkomputeran 'Computation Fluid Dynamics' (CFD) adalah untuk membandingkan prestasi PCU dengan pelan sebenar dengan menganalisis penghasilan haba dengan menggunakan 'standard k- $\epsilon$ ' (SKE) model kelikatan dan Eddy Dissipation (ED) model pergolakan interaksi kimia. Gas asli (NG) yang telah dipanaskan di dalam pemanas akan di salurkan ke dalam 'transfer line'. Prestasi PCU yang menggunakan proses semasa dibandingkan dengan yang menggunakan proses yang mempunyai perbezaan dalam pecahan jisim proses gas, suhu dan halaju proses gas dan oksigen untuk mengetahui proses yang efektif dengan membandingkan suhu yang terhasil di dalam PCU dengan menggunakan CFD. Simulasi ini juga dilakukan untuk melihat kesan modifikasi terhadap reka bentuk dengan penambahan 'boundary refractory'. Reka bentuk 'transfer line' ini harus dilukis menggunakan GAMBIT 2.4 dan simulasi dijalankan untuk mendapatkan keputusan menggunakan FLUENT 6.3.26. Menerusi keputusan yang diperolehi, proses baru menunjukkan peningkatan suhu yang ketara pada titik yang mempunyai 'thermocouple' berbanding dengan proses semasa yang menunjukkan peningkatan yang sedikit walaupun peratusan ralat proses baru lebih tinggi daripada proses semasa. Justeru itu, modifikasi terhadap data dan reka bentuk sepatutnya dijalankan demi untuk mendapat keputusan yang memberangsangkan.

## TABLE OF CONTENTS

	<b>Page</b>
<b>SUPERVISOR’S DECLARATION</b>	ii
<b>STUDENT’S DECLARATION</b>	iii
<b>DEDICATION</b>	iv
<b>ACKNOWLEDGEMENT</b>	v
<b>ABSTRACT</b>	vi
<b>ABSTRAK</b>	vii
<b>TABLE OF CONTENTS</b>	viii
<b>LIST OF TABLES</b>	xi
<b>LIST OF FIGURES</b>	xii
<b>LIST OF SYMBOLS</b>	xiv
<b>LIST OF ABBREVIATIONS</b>	xv
<b>LIST OF APPENDIXES</b>	xvi
 <b>CHAPTER 1            INTRODUCTION</b>	
 1.1            Background of Study	1
1.2            Overview of Direct Reduction Plant	2
1.3            Problem Statement	3
1.4            Objectives of study	3
1.5            Scope of Study	4
1.6            Rationale & Significance	4
 <b>CHAPTER 2            LITERATURE REVIEW</b>	
 2.1            Introduction	5
2.2            Fundamental Theory of Partial Combustion	5
2.2.1    Introduction to Partial Combustion	13



	2.2.2	Reduction Process	18
	2.2.3	Advantages of Hot and High Carbon DRI	19
2.3		Introduction of Computational Fluid Dynamic	20
	2.3.1	CFD Approach	25
	2.3.1.1	Gambit 2.4.6	25
	2.3.1.2	Fluent 6.3.26	26
2.4		Fundamental of CFD	26
	2.4.1	Turbulence Modeling	26
	2.4.2	Transport Equation	26
	2.4.3	Mass Transfer and Species Transport Equation	26
	2.4.4	The Eddy-Dissipation Modeling	28
	2.4.5	Convection and Mass Transfer Equation	28
	2.4.6	The Energy Equation	29
2.5		Transfer Line Boundary Refractory	29

### **CHAPTER 3            METHODOLOGY**

3.1		Introduction	31
3.2		Computational Tools	31
3.3		Detail Steps	31
3.4		Simulation procedure	35
	3.3.1	Modeling using Gambit 2.4.6	35
	3.3.2	Fluent data setting	36
	3.3.3	Simulation on existing lance configuration	36
	3.3.4	Detail in setting the data	37

### **CHAPTER 4            RESULT AND DISCUSSION**

4.1		Data Collection	44
4.2		Current Process Scheme	44
4.3		New Process Scheme	44
4.4		Process Schemes with Refractory	45

### **CHAPTER 5            CONCLUSION**

5.1		Conclusion	55
-----	--	------------	----

5.2	Recommendation	56
5.2.1	Volume Meshing	56
5.2.2	Design of Oxygen Nozzle and Lance	57
5.2.3	Validation Point	57
5.2.4	Boundary Refractory	57
<b>REFERENCES</b>		58
<b>APPENDICES</b>		61
A	Contour of Simulated Results and Graph	61
B	Supportive Information for Simulation Study	72

**LIST OF TABLES**

<b>Table No.</b>	<b>Title</b>	<b>Page</b>
2.1	Composition of Gases in Natural Gas	23
2.2	Chemical analysis on the brick KX-99	29
3.1	Mass Flowrate	32
3.2	Physical Properties	32
3.3	Properties of refractory brick KX-99	34
3.4	Reaction mechanism	39
4.1	Comparison of Temperature Reading	54

## LIST OF FIGURES

<b>Figure No.</b>	<b>Title</b>	<b>Page</b>
2.1	Units of steel-making process and related CO <sub>2</sub> reducing technologies	7
2.2	CO <sub>2</sub> emission from steel production using the traditional blast furnace and basic oxygen furnace/converter	12
2.3	Process flow diagram of iron making process	15
2.4	Position of Injection Oxygen to the Transfer Line	16
2.5	Elements of the Partial Combustion or Autothermal Reforming To Occur	17
2.6	Effect of DRI Temperature and Carbon on Electricity Consumption and power on – time	20
2.7	EAF oxygen consumption using different charges of DRI With different carbon level	21
2.8	Effect of DRI temperature and carbon content on electricity consumption	21
2.9	Effect of DRI temperature and carbon on melting and refining time	22
3.1	Procedure for CFD simulation	31
3.2	Modeling using Gambit 2.4.6	34
3.3	Mesh generation of transfer line	34
3.4	Mesh generated at outlet transfer line	35
3.5	Mesh generated at nozzle and oxygen lances	35
3.6	Mesh generated at oxygen lance	36
3.7	Check the grid for mesh exported	37
3.8	Viscous model selection	38

3.9	Species model selection	38
3.10(a)	Set the material	40
3.10(b)	Choose the material (make sure the material type is correct)	40
3.11(a)	Set the reaction	41
3.11(b)	Data in Table 3.4	41
3.12	Editing the boundary condition	42
3.13	Energy relaxation factor and second – order iteration	43
4.1	Temperature profile for previous study and current study for current process	48
4.2	Graph of temperature profile for previous study and current study	48
4.3	Temperature profile for previous study and current study for new process	49
4.4	Graph of temperature profile for previous study and new study	49
4.5	Temperature profile on both processes	50
4.6	Graph of temperature profile on both processes	50
4.7	Z-axis velocity of fluid on both processes	50
4.8	Graph of z-axis velocity of fluid on both processes	51
4.9	Mass Fraction of CH <sub>4</sub> on both processes	51
4.10	Graph of Mass Fraction of CH <sub>4</sub> on both processes	52
4.11	Graph of turbulent kinetic energy on both processes	53
4.12	Graph of Temperature comparison on thermocouple line	53

## LIST OF SYMBOLS

$k$	Turbulence kinetic energy
$\varepsilon$	Dissipation rate
$G_k$	Generation of turbulence kinetic energy due to the mean velocity gradients
$G_b$	Generation of turbulence kinetic energy due to buoyancy
$Pr_t$	Prandtl number for energy
$g_i$	Component of the gravitational vector in the $i^{th}$ direction
$\beta$	Thermal expansion coefficient
$Y_M$	Contribution on fluctuation dilatation in compressible turbulence to the overall dissipation rate
$M_t$	Turbulence mach number
$\alpha$	Speed of sound
$Y_i$	Mass fraction of each species $i^{th}$ species
$R_i$	Net rate of production by chemical reaction
$S_i$	Net rate of creation by addition from the dispersed phase
$R_{i,r}$	Net rate of production of species $i$ due to reaction $r$
$Y_p$	Mass fraction of any products species $P$
$Y_R$	Mass fraction of particular reactant $R$
$k_{eff}$	Effective thermal conductivity
$E$	Total energy
$(\tau_{ij})_{eff}$	Deviatory stress tensor
$\vec{J}_j$	Diffusion flux of species $j$

## LIST OF ABBREVIATIONS

CFD	Computational Fluid Dynamics
CH <sub>4</sub>	Methane
CO <sub>2</sub>	Carbon dioxide
CO	Carbon monoxide
DR	Direct Reactor
DRI	Direct Reduce Iron
DRP	Direct Reduction Plants
EAF	Electric arc furnace
Fe	Iron
Fe <sub>3</sub> C	Iron Carbide
Fe <sub>2</sub> O <sub>3</sub>	Iron (III) Oxide
H <sub>2</sub>	Hydrogen
H <sub>2</sub> O	Water
HBI	Hot Briquetted Iron
MBF	Mini Blast Furnace
NG	Natural Gas
PCU	Partial Combustion Unit
R&D	Research and Development
SMS	Shed and Steel Melting Shop

## LIST OF APPENDIXES

<b>Figure</b>	<b>Title</b>	<b>Page</b>
A1	Contour mass fraction of CO on both process	61
A2	Graph Contour mass fraction of CO on both process	61
A3	Contour mass fraction of CO <sub>2</sub> on both process	62
A4	Graph Contour mass fraction of CO <sub>2</sub> on both process	62
A5	Contour mass fraction of H <sub>2</sub> on both process	63
A6	Graph contour mass fraction of CO <sub>2</sub> on both process	63
A7	Contour mass fraction of H <sub>2</sub> O on both process	64
A8	Graph contour mass fraction of H <sub>2</sub> O on both process	64
A9	Contour mass fraction of N <sub>2</sub> on both process	65
A10	Graph contour mass fraction of H <sub>2</sub> O on both process	65
A11	Contour mass fraction of O <sub>2</sub> on both process	66
A12	Graph contour mass fraction of H <sub>2</sub> O on both process	66
A13	Contour of reaction equation 2.1	67
A14	Graph contour of reaction equation 2.1	67
A15	Contour of reaction equation 2.2	68
A16	Graph contour of reaction equation 2.2	68
A17	Contour of reaction equation 2.3	69
A18	Graph contour of reaction equation 2.3	69
A19	Contour of reaction equation 2.4	70
A20	Graph contour of reaction equation 2.4	70



A21	Contour of reaction equation 2.5	71
A22	Graph contour of reaction equation 2.5	71
B1	Process plant flow diagram	72
B2	Details drawing of the transfer line	73
B3	Overview drawing on the transfer line	73
B4(a)	Details drawing on the oxygen lances	74
B4(b)	Details drawing on the oxygen lances	74
B5	Overview drawing on oxygen lance	75
B6	Overview drawing on nozzle oxygen lance	75
B7	Excel simulation	76
B8	Summary data from excel simulation	79

<b>Table</b>	<b>Title</b>	<b>Page</b>
B1	Mass fraction on excel simulation	77
B2	Mass balance on excel simulation	78
B3	Energy balance on excel simulation	79

## **CHAPTER I**

### **INTRODUCTION**

#### **1.1 BACKGROUND OF STUDY**

The rapid development nowadays causes the high demand of steel from the heavy industry. Thus, there are many evolution on the steel making processing in order to produce the high quality steel as required, which is also environmental friendly and have low energy consumption and investment costs. The high product value is needed to ensure the steel produce has a high resistant. Natural gas and coal plays as main utilities for plant in producing steel and iron making industry. In Malaysia, Perwaja Steel Sdn. Bhd. is the leading manufacturer company of primary steel and iron product. The process started with the production of iron by reducing the oxides inside the iron ores and steel making production as the final product and distributed in various types such as billets (Perwaja Holding Berhad, 2009). The plant consists of three main parts which are Direct Reduction Plant (DRP), Direct Reduces Iron (DRI) Shed and Steel Melting Shop (SMS). This study focuses on the first component of the plant which is DRP.

Direct Reduction (DR) reactor used by this company is HYL III which is capable to producing up to 1.5 million metric tonnes of Direct Reduced Iron (DRI) per annum. The reducing agent used in processing the DRI is natural gas-based or coal-based direct reduction process. Oxygen is removed from the iron ore by chemical reactions based on Hydrogen,  $H_2$  and Carbon Monoxide, CO for the production of DRI and Hot Briquetted Iron (HBI) (Raul & Matthias, 2002). The natural gas (NG) was firstly reformed into hot reducing gas which is known as syngas. This company is using the natural gases as a reducing agent. The natural gas will generated as self-reforming in

the reduction reactor. Through the partial oxidation of natural gases and oxygen, reducing in-situ gases which are  $H_2$  and CO will be generated. Thus, the operating temperature will increase as required for the iron ore reduction process.

In the DRP, the important unit in production of DRI is Partial Combustion Unit (PCU). PCU takes place in between the reactor and heater. The PCU consists of transfer line and two oxygen lances with nozzle attached to each of its. The transfer line is a medium to transfer the hot process gas to the reactor while the oxygen lances will supply the oxygen to the unit. The oxygen will be injected in the transfer line through the oxygen lances for partial combustion and increasing the temperature of NG. In this unit, the partial oxidation of natural gases and oxygen will generate the in-situ gases. Besides that, through this unit, the operating temperature can be increased (temperature that will enter the reactor). The high temperature of reducing gases is important in order to remove the oxides inside the iron ore to produce the DRI.

## 1.2 OVERVIEW OF DIRECT REDUCTION PLANT

The natural gas used was firstly reformed into hydrogen, carbon monoxide, carbon dioxide, methane, nitrogen and a little amount of water vapour. In the DRP, the gasses are reformed into single component of gas through gas reformer and then supplied to the gas heater to increase the temperature. The heated process gas is consists of high concentration of hydrogen and carbon monoxide. Then, it will partially react with the oxygen that supplied through the oxygen lances. Through this reaction, the heat of combustion will produce. The heat will increase the temperature of the process gases and reduced the energy consumption of the process to achieve the desire temperature.

Thus, many research had been carried out in propose of improving the PCU. There are several considerations that should take into account such as the need to be optimized to achieve higher Partial Combustion ratio (*Yun Li & Richard J. Fruehan et al.*). In this research, the consideration is about the performance of PCU with one oxygen injection since the other lance is under maintenance. Besides, in the previous study, the existent of boundary refractory is neglected. Thus, in this study, the modeling

of previous study has modified and boundary refractory is added to the PCU. In addition, to increasing the performance of the PCU, the different type of scheme is proposed by Research and Development (R&D) Unit in Perwaja Steel Sdn. Bhd.. Through this study, the effect of the new process scheme with current process which has different composition of process gas, velocity inlet for process gas and oxygen injected and temperature inlet of process gas was study. The details are shown is Chapter 3.

### **1.3 PROBLEM STATEMENT**

In the PCU, the high temperature is required in order to remove the oxide inside the iron ore by the oxidation reaction between the iron ore and the NG. It is important to ensure the temperature of the system is operating at high temperature but does not exceed the fusion point of iron ore ( $1535^{\circ}\text{C}$ ) at the reactor. Besides that, the heat transfer to the surrounding will cause the global warming. Thus, the boundary refractory material and the thickness should be identified. By performing CFD simulation, the unit performance can be investigated. Besides to identify either the boundary refractory may influence the temperature obtain or not and the amount of oxygen supplied to the unit can be investigated either the oxygen or fuel ratio can resulted in optimum performance by evaluating the temperature profile of the unit. In addition, the simulation was run by using only one lance since the other one is under maintenance.

### **1.4 OBJECTIVES OF STUDY**

The objectives of the study are:

- (i) To validate the performance of the partial oxidation unit with current installation by analyzing the profile of the temperature using CFD.
- (ii) To study the effect on designing the refractory boundary toward the simulation.
- (iii) To study the impact on oxygen flow rate and temperature inlet of process gas in the PCU via simulation using one operating oxygen lance.

## **1.5 SCOPE OF STUDY**

To achieve the objectives, scopes have been identified in this training. The scope of this training is listed as below:

- (i) Performing simulation on partial combustion reaction in PCU to identify the heat generated by the unit with current installation of oxygen lances with present of boundary refractory.
- (ii) Comparing the impact of the amount of oxygen injected and temperature of process gas supplied in the PCU via simulation.

## **1.6 RATIONALE AND SIGNIFICANCE**

The rationale of this study and the significance of the research are listed as below:

- (i) Prevent the heat to be loss to the surrounding.
- (ii) Increase the effectiveness of the system by increasing the production of DRI.

## **CHAPTER 2**

### **LITERATURE REVIEW**

#### **2.1 INTRODUCTION**

Environmental Protection Agency, 2010, the steel making process has undergoes many changes due to the most economical operating cost and the most effective production that could bring benefit for the company. Integrated steel plants produce steel from iron ore in several steps and produce very high quality steel with well controlled chemical compositions to meet all product quality requirements. In this plant, the use of furnace has identified to be the most efficient. However there are several limitations that need to be improved.

Steel is an alloy of iron that usually containing less than 1% of carbon and mostly used in the automotive and construction industries. The steel mill or also known as steel works is an industrial plant for steel manufacture. Steel is produce by two stage process. Firstly, the iron ore was reduce or smelted with coke and limestone presence in a blast furnace to produce molten iron. The molten iron will cast into pig iron or carried to the next stage which is known as steel making process. Through this process, the impurities such as sulfur, phosphorus and excess carbon will be removing. After the steel cleaned from any impurities, the alloying element will be added in order to produce the required steel (Schumacher and Sathaye, 1998).

Chunbao and Da-qiang (2010) found that, iron and steel making industry is one of the most energy-intensive industries, consuming 5% of the world's total energy consumption and emitting 3%- 4% of total world greenhouse gas emissions. The increasing of energy efficiency could be a short-term approach for the steel industry to

reduce greenhouse gas emission. However, the long-term approaches to achieve a significant reduction in CO<sub>2</sub> emissions from the steel industry would be through developing and applying CO<sub>2</sub> breakthrough technologies for iron and steel making, and through increasing the use of renewable energy for iron and steel making.

Due to the energy crisis in 1970, the blast furnace was fed with iron ore continuously in order to ensure the heat can be used more efficiently. Nevertheless, the process of steel making will emit the undesired gas which is harmful to the environment. In 1995, compliance with environmental requirements was estimated to make up 20-30% of the capital costs in new steel plants (Chatterjee, 1995).

**Figure 2.1** has shown the units of steel making process and related CO<sub>2</sub> reducing technologies. From the figure there is three path of the process. First is using the blast furnace, second is using the electric arc furnace and third is direct reduction. In the first path, the blast furnace process include the coke making, sintering and the raw material will feed to the blast furnace. Coke is a solid carbon fuel and it is used to melt and reduce iron ore. The production begins by crushing the bituminous coal. The coal is fed into a coke oven which is heated to very high temperatures for 14 to 36 hour. Heat is transferred from one oven to another in purpose of reducing the energy requirements. Then, the coke is move to a tower and cooled with water spray. After then, its move directly to an iron melting furnace or into storage for future use (Chunbao and Da-qiang, 2010).

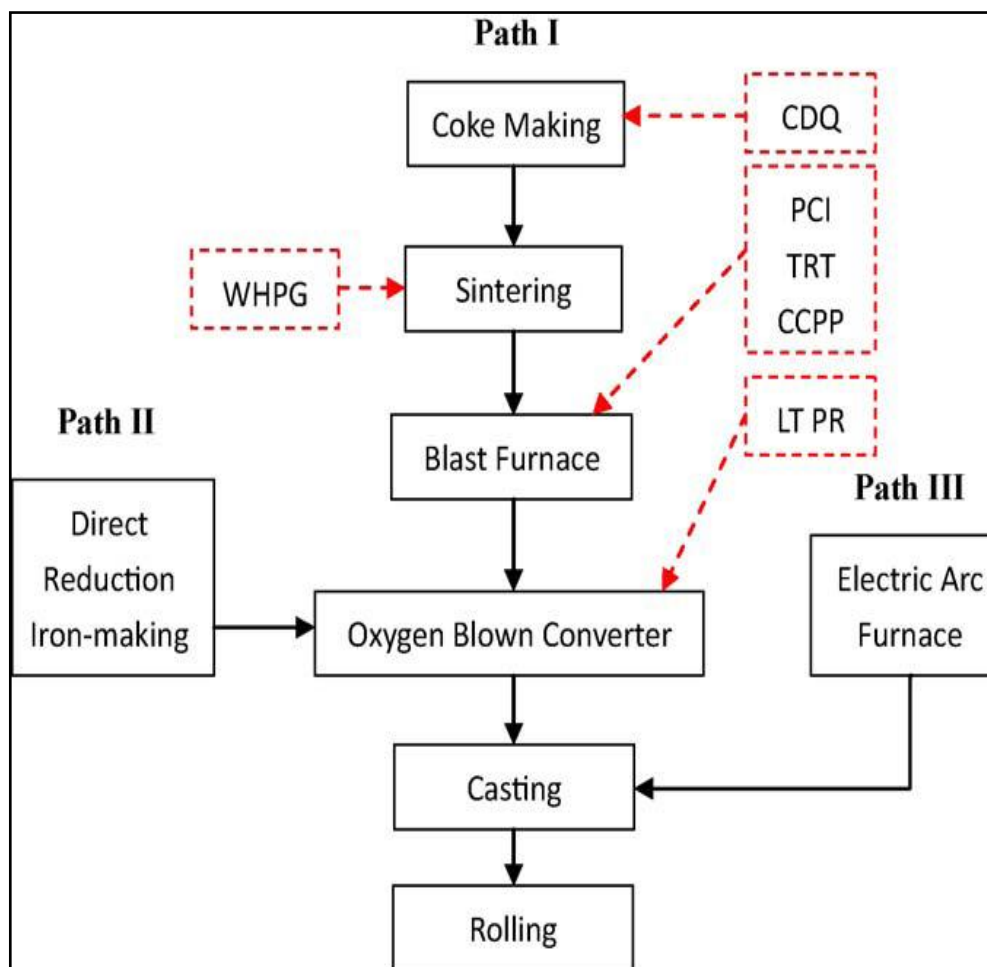


**Figure 2.1:** Units of steel-making process and related CO<sub>2</sub>-reducing technologies (dot line).

Sources: Chunbao and Da-qiang, 2010

Sintering is the heating process of iron ore with flux and coke fines or coal, to produce a semi-molten mass. It is solidified into porous pieces of sinter with the size and strength characteristics necessary for feeding into the blast furnace. The raw material of making an iron will be obtained by this process. It produces extremely consistent quality in terms of its chemical composition, grain size distribution, sinter strength and reducibility on the feed. In the process, crushed coke and limestone are mixed and granulated with fine blend ore. The raw mixture is charged as a packed bed on a continuous sinter strand, the frame for holding the wood or coal in a fireplace. A burner hood mixed the coke in the mixture at the surface of the bed. Then, the



combustion process will provide the heat for partial melting or solidifying which is leading to the agglomeration of the raw materials. To maintain the coke combustion, air is sucked down through the bed. The agglomerated bed also called as sinter cake is discharged at the end of the sinter strand where it is crushed and screened (Komarov and Kasai, 2004).

In this process, the particle size of the mixture has the major influence on the operation stability. Too small particles result in poor bed permeability and possible destabilizing of flame propagation. Nevertheless, using lower grade iron ores with very fine particle size has caused the need for improvement in the sintering process performance. The method that leads to an increase in the production cost but decrease in the operational efficiency or productivity and often deterioration of sinter quality is by granulation binder (Komarov and Kasai, 2004).

The blast furnace process is still the predominant iron production process, producing more than 92% of the world total iron which is unchallenged method of making hot metal on a large scale till 1990 (Chunbao and Da-qiang, 2010). Nevertheless, there are permanent disadvantages to the blast furnace process. The process was dependence on high-quality metallurgical-grade coke and iron oxide feed stocks instead of economic for only large capacities and emission of CO<sub>2</sub> on the coke ovens and sinter plants. Besides that, this process needs lots of assistance and supporting and cause high capital and operational intensity. Through these disadvantages, the development on iron making from blast furnace to many other alternative processes such as Shaft Furnace Direct Reduction (DR) Processes (MIDEX, HYL), Rotary Kiln DR Processes (SL/RN, CoDir, and TDR) and recently the COREX Smelting Reduction Processes.

To meet these changing needs, technology has become more prominent and integrated steel plants are being replaced with smaller plants, called mini-mills, which rely on steel scrap as a base material rather than ore. Mini-mills can never replace integrated steel plants completely because they cannot maintain the tight control over chemical composition, and thus cannot consistently produce high quality steel. Mini-mills has a narrower production line and cannot produce the specialty products

produced by integrated plants. In the mid 1990, mini-mills had been identified has less than half of the quality steel market (Chatterjee, 1995).

Mini Blast Furnace (MBF) are ideally suited to small scale operations and can be viewed as a miniature version of conventional large blast furnace which is simplicity and economy. The working volume ranges between 100-370m<sup>3</sup> and the production capacities of hot metal between 60,000-200,000T/A. The lower grade coke and iron can be used in the small scale processes compare to the blast furnace. The products qualities from mini blast furnace are same with blast furnace. The product is also free of tramp elements which are unimportant and undesirable for the product (Joardar, 2009).

This processes use only 40-50% hot metal in Electric Arc Furnace (EAF) charge thus it help in reduce the power consumption to 380-400kwh/t liquid steel from 550-600kwh/t. Besides that, the temperature used in MBF is lower than normal blast furnace and the specific heat loss is more, the coke rate tends to be 100-160kg/thm higher (thm=ton hot metal). Nevertheless, the limitation of MBF is that coal injection is normally difficult and the higher specific heat requirement has to be met entirely by coke (Joardar, 2009).

EAF is one of the alternative methods for production of steel. This furnace does not use hot metal. It is charged with manly steel scrap. Firstly, the steel scrap will tipped into the EAF by using an overhead crane. A lid comprises of three graphite electrodes which is lowered into the EAF will carefully swung into position over the EAF. Electric current passed through the lid will forms an arc that generates heat and melts the steel scrap. During this process, other metals will be added to the steel to achieve the desire composition and oxygen is blown into the EAF in order to purifying the steel. After the checked collected sample have been done, the product will be poured off by tilled the EAF to allow the slag to float on the surface of the molten steel. After then, the EAF is tilted in the other direction and the molten steel is poured into a ladle (Metallon Holdings Limited).

The EAF consists of a large shallow bath. It is either an acid or basic lining, which are carbon electrodes over the hearth and may be raised or lowered. Current is

supplied to these electrodes from special transformers. The hearth is charged with lime, and either iron ore or mill scale to remove the impurities and form a slag. The metal which forms the melt is scrapping steel of known composition. When the furnace is charged, the electrodes will be lowered and the current is switched on. The electrodes are then raised and an electric arc will jump across from the electrodes to the metal and the melting process begins. The temperature is about 3400°C. The furnace is tilted and the slag is ladled off. Lime, fluorspar, carbon and Ferro-alloys are added to de-oxidize and de-sulphurize the metal (Carty, 2007).

A sample is taken and tested and when the correct composition is achieved the furnace is tilted and the steel is poured into a ladle. The EAF is used to produce high grade alloy steels such as High Speed Steel, High Tensile Steel and Silver Steel. The greater control over impurities and also during the steel making is the reason this process became possible. Nowadays, it is increasingly being used in the production of common steel. Making steel process is very expensive due to the high cost of electricity. Arc furnaces range approximately one ton capacity used in foundries for producing cast iron products is up to about 400 ton units used for secondary steelmaking. Nevertheless, arc furnaces used in research laboratories and by dentists may have a capacity of only a few dozen grams (Carty, 2007).

Direct Reduction (DR) is an alternative iron source that produced by heating an iron ore which is generally contain 65-70% of iron at a high temperature but below its melting points, 1535°C, utilizing Carbon Monoxide, Hydrogen and Methane (CO, H<sub>2</sub> and CH<sub>4</sub>) gases and carbon-bearing materials as the reducing-carburizing agents in order to produce Direct Reduced Iron (DRI) with a porous structure or sponge iron. The demand for this process is increasing due to support the expansion of EAF steelmaking for production of new high quality product. This process is more environmental friendly in contrast with the blast furnace because they do not require high quality metallurgical-grade coke and iron oxide feed stocks but usually use fines and fine coal directly by avoiding step agglomeration and coking. The potential of decreasing the CO<sub>2</sub> had been determine to be 20%. **Figure 2.2** has shown the statistic data about the formation of CO<sub>2</sub> gasses in the blast furnace, coke making, sintering, pelletizing and steel making itself (Zeng, et al, 2009).

DR processes can be dividing into two reducing agent source, natural gas-based direct reduction process and coal-based direct reduction process. The primary DRI production processes are the natural gas-based direct reduction processes such as MIDREX and HYL using shaft furnace, and FINMET using fluidized bed. The two-stage hydrogen-based Circored process using a circulating fluidized bed system to reduce iron. The process uses pure hydrogen produced from natural gas by steam-reforming and CO shift reactions, where the highly concentrated CO<sub>2</sub> by product could be easily disposed by sequestration (Chunbao and Da-qiang, 2010).

The iron ore will be passed through several processes in the DRP. Before becoming a final product, the raw material (iron ore) must be cleaned from oxides and the process of removing the oxides is using hot reducing gases, which are Hydrogen and Carbon Monoxide gases. In the presence of high temperature of reducing gases, the additional energy is generated to the system. Firstly, the NG was passed through reformation process at high temperature of about 930°C or 1203 K. Then, from the self-reformation process, the reducing gases are generated in the reduction reactor, feeding natural gases as make-up to the reducing gas circuit and Oxygen injection at the inlet of the reactor. **Figure 2.3** describe the HYL process in detail. From **Figure 2.4**, the position of oxygen injection is shown at certain position on the transfer line.

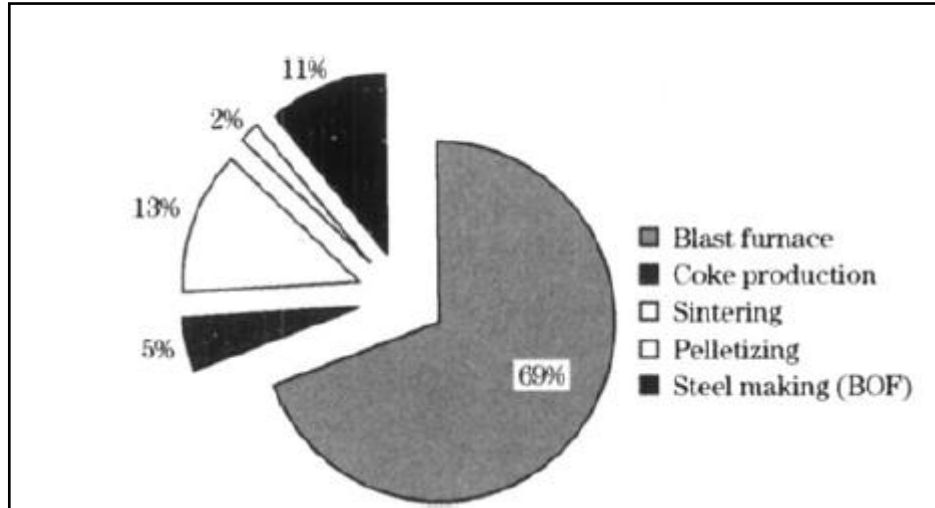
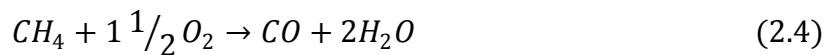


**Figure 2.2:** CO<sub>2</sub> emission from steel production using the traditional blast furnace and basic oxygen furnace/ converter.

Sources: Zeng, et al. (2009)

Below is the reaction that took place in the PO unit:



The FINMET process using natural gas and fluidized bed produced 2%, or 1.3 Mt, The remaining 20 %, or 8Mt, was made in a variety of coal-based processes involving rotary kiln/hearth. In regions where an abundant and inexpensive source of natural gas or Hydrogen exists, gas-based direct reduction of iron followed by melting in an EAF can provide a cost-competitive alternative to quality steel products. One of the constraints on the gas-based shaft furnace processes is that they require either high-grade lump ore or pellets as their iron unit raw material feed, while costs for such feeds are climbing owing to limited supply (Chunbao and Da-qiang, 2010).

The lower costs of the fine ores make the fluidized bed processes attractive. However, in areas where low cost natural gas is not available, coal-based iron reduction processes will have an advantage. Several processes based upon the direct reaction of coal and iron are in a rotary kiln, such as the SL/RN process (coal-based DRI technology of Lurgi GmbH, Germany), reached various stages of development since the 1960. Two commercial coal-based Fastmet units operates a rotary hearth furnace have been installed at Kobe Steel and Nippon Steel, both in Japan, to produce 85% of reduced iron pellets.

## 2.2 FUNDAMENTAL THEORY OF PARTIAL COMBUSTION

### 2.2.1 Introduction to Partial Combustion

Combustion is a chemical reaction between a combustible material or a fuel and oxygen releasing heat. Oxygen came from the air which is a dry basis composition is 21% of oxygen while the rest 79% is nitrogen. Carbon, hydrogen and sometimes sulfur contain in the fuel. Oxygen consumed will increase the temperature in the gases and the reactions as below with reaction (2.2):



The combustion can happen in three different grades. First is the perfect combustion. In this grade, the amount of the oxygen supplied is stoichiometry as a required to burn a fuel (2.3). Second is a complete combustion which is used an amount of oxygen bigger than the stoichiometry or known as excess air and causes the fuel to completely burn off (2.8). The last grade is incomplete combustion (2.4). Through this grade, there is no enough oxygen to be supplied and the oxygen as a limiting reactant and the fuel will be excess. It is also known as partial combustion.



Partial combustion is a process when a substantial portion of the soot that formed from the combustion reactor is separated from the Natural Gas and burned in a separate combustion zone with the presence of excess oxygen in a steam in order to yield a hot gas containing oxygen, carbon dioxide and water. The iron ore will pass through several processes in the Direct Reduction Plant which is also known as HYL III Process. The production rate of HYL plants influence by increasing the reduction temperature, as the chemical change in the reduction reactions.

Through this process, the reaction rate and the product composition influence by an absorption of heat. The oxygen is injected to the transfer line which is in between the reactor and heater (Perwaja Steel Sdn Bhd.). **Figure 2.5** show the block diagram for the necessary elements of the partial combustion or autothermal reforming to occur. The partial combustion allowed increasing the reducing gas temperature at the reactor inlet from 930-1080°C since the reducing gas temperature at the heater outlet has been decrease from 930-900°C.

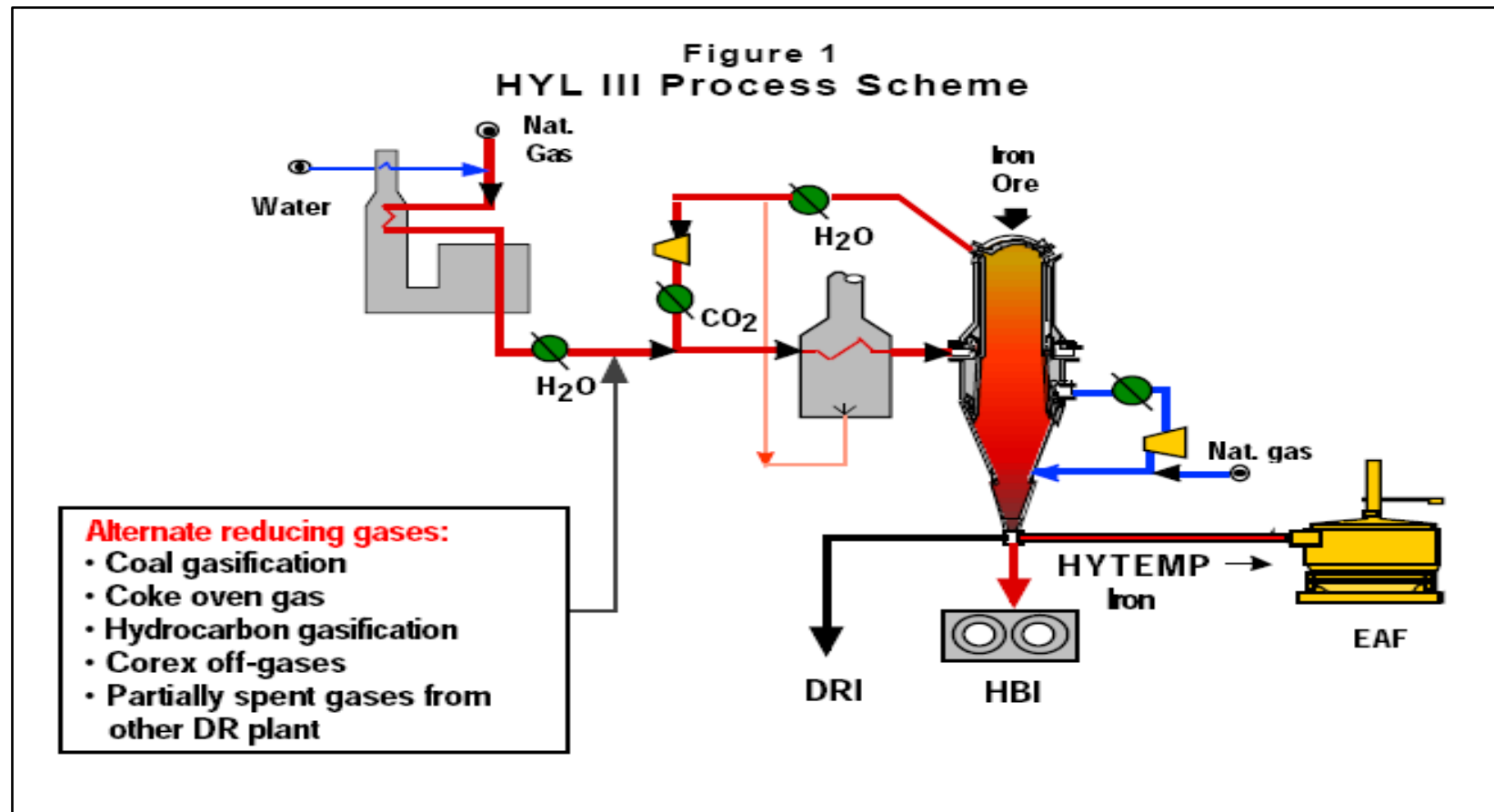


**Figure 2.3:** Process Flow Diagram of Iron Making Process

Source: HYL III: Status and Trend





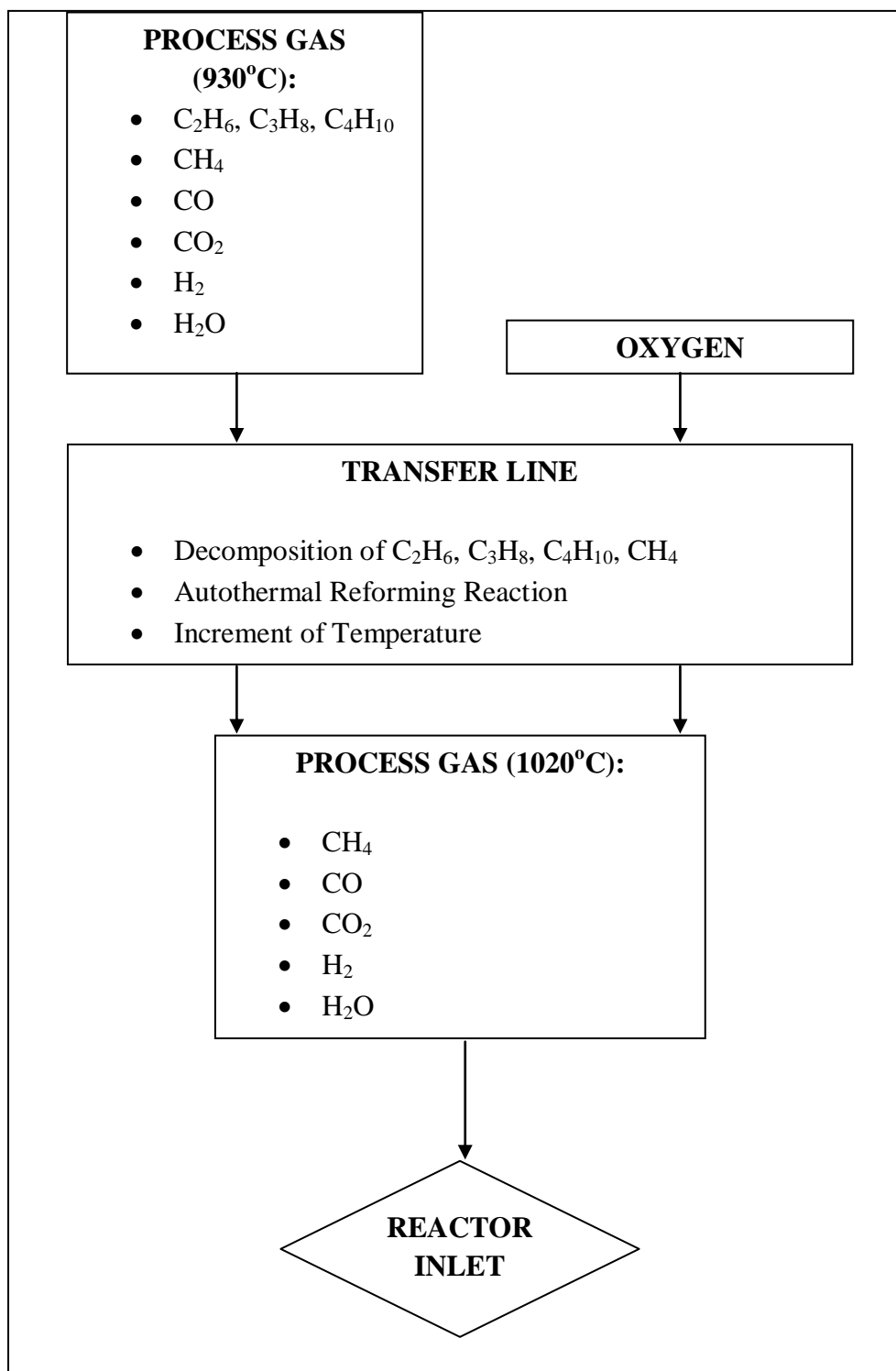


**Figure 2.5:** Elements of the Partial Combustion or Autothermal Reforming To Occur

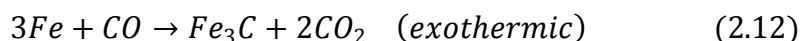
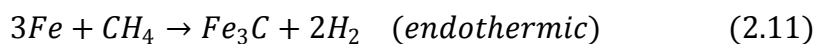
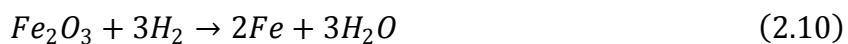
Source: Perwaja Steel Sdn. Bhd., R&D Department

### 2.2.2 Reduction Process

Chemical change in reduction reactions in HYL direct reduction process is accompanied by absorption of heat. The absorption heat will influence the reaction rate and product composition. The reduction process takes place in the reactor in which the process gasses that passed through the partial oxidation entered the reactor with high temperature. The hot process gas flow upwards as counter current to the descending moving bed of iron oxide thus, resulting the reduction of iron oxides to iron. This is due to optimizing the resident time between the contacts of the gases and solid and thus resulted in optimize reduction rate process (Manning and Fruehan, 2001).

The reducing gas is produce from the mixture of the reducing gas at the recycles stream. Then, it will pass through the reducing gas heat exchanger and then through the gas heater in where the reducing gas will heat up to 930°C. The exhaust reducing gas which also known as top gas will leaves the reactor at the top gas heat recuperator at temperature 400°C. Here, the energy is recovered to produce steam or alternatively to preheat the reducing gas stream and then it will passes through the quenching or scrubbing system. In these units, the water produced during the reduction process was condensed and remove from the gas stream. Most of the dust carried with the gas is also eliminated. Compressed gas that sent to the carbon dioxide removal unit will mix with the natural gas make up then closing the reducing gas circuit (Danieli and Tenova)

Currently, most of the DR plant operates at high temperature which is 920°C-950°C. Thus, this research is carried out to lower the operating temperature which is possible hence resulted in higher cost effective. In optimizing the rate of DRI production, the hot reducing gases is needed since carburization process is varied with the temperature of the reducing gases. The exact nature of the reaction of iron through the reduction process and the carburization process occurred in the reactor as below:



Equation 2.9 and 2.10 are presenting the reaction on reduction process while equation 2.11 and 2.12 are carburization process. In the carburization process through  $\text{CH}_4$ , the temperature of the reducing gas became lower due to the endothermic nature of the reaction, if higher amount of NG fed into the reactor (Raul, 1995). These lower reducing gases gave lower productivity of DRI and affected the low level of metallization. Therefore, the additional energy is provided by the Partial Oxidation of NG and thus improved the carburizing quality gases which are required for the carburization of the metallic iron. Reaction 2.13 is part of the in situ reforming process.

### 2.2.3 Advantages of Hot and High Carbon DRI

Partial oxidation process is important in increasing the temperature of the reducing gases entered the reactor. High temperature is needed because the heated gases is needed to remove oxides in the iron ore during the reduction process and the process will happened at the high temperature of DRI leaving the reactor. Hot DRI feed will provide additional sensible heat to the EAF and the power consumption will be reduced and tap-to-tap times which are reflected in increasing the productivity (Danieli and Tenova).

**Figure 2.6**, showed that the higher temperature of the DRI and higher carbon content, the lower electricity consumption for operating the plant. The same relation goes to the power on-time which is shown the less time needed to operate the plant at the high temperature with high carbon content. This is also a part of the reason why it is important to increase the temperature of the process gases entering the reactor since it can affected the DRI temperature and carbon content of the DRI too. By designing the boundary refractory, it is believe to prevent the heat on the partial oxidation unit from loss to the surrounding thus, the NG will enter the reactor at high temperature.

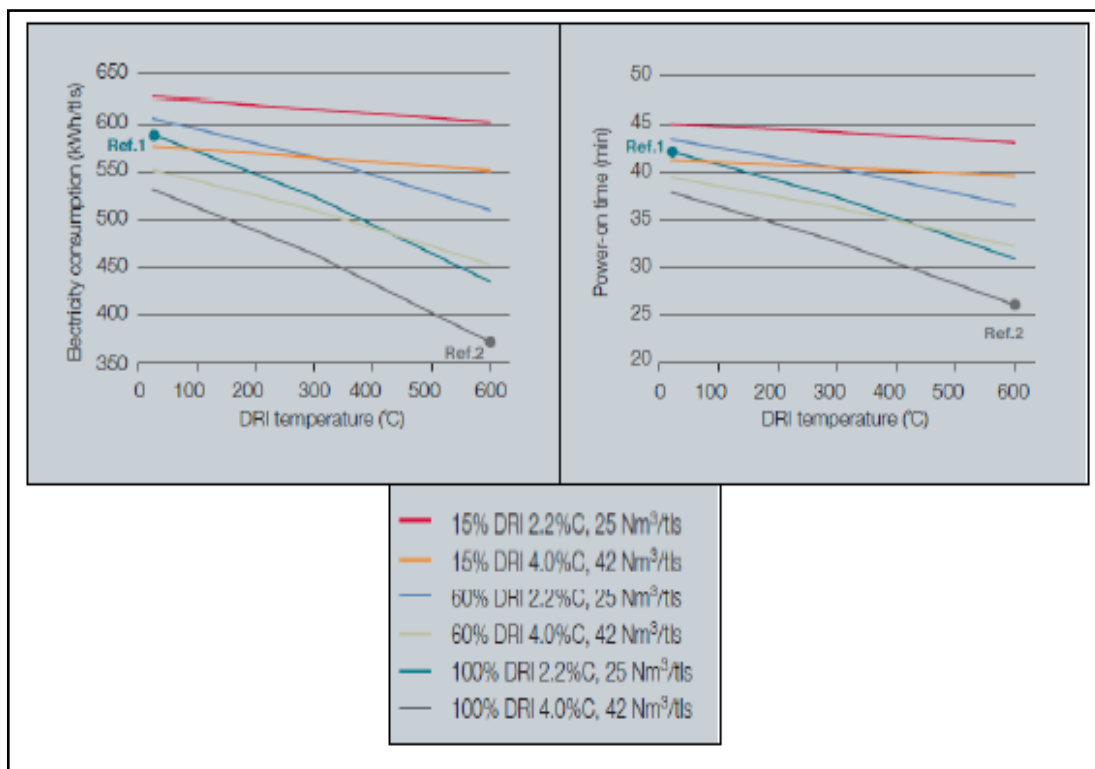


**Figure: 2.6:** Effect of DRI temperature and carbon on electricity consumption and power on-time

Sources: Danieli and Tenova

The combine effects of high temperature and high carbon content of DRI are also influenced the productivity rate of the EAF corresponding to decreasing of the electric energy required to melt the charge (Raul, 1995). The sensible heat of the DRI production from the reactor will result the lower electric energy consumption for the furnace to increase the productivity and minimizing other related operating cost such as electrodes, refractory and flux.

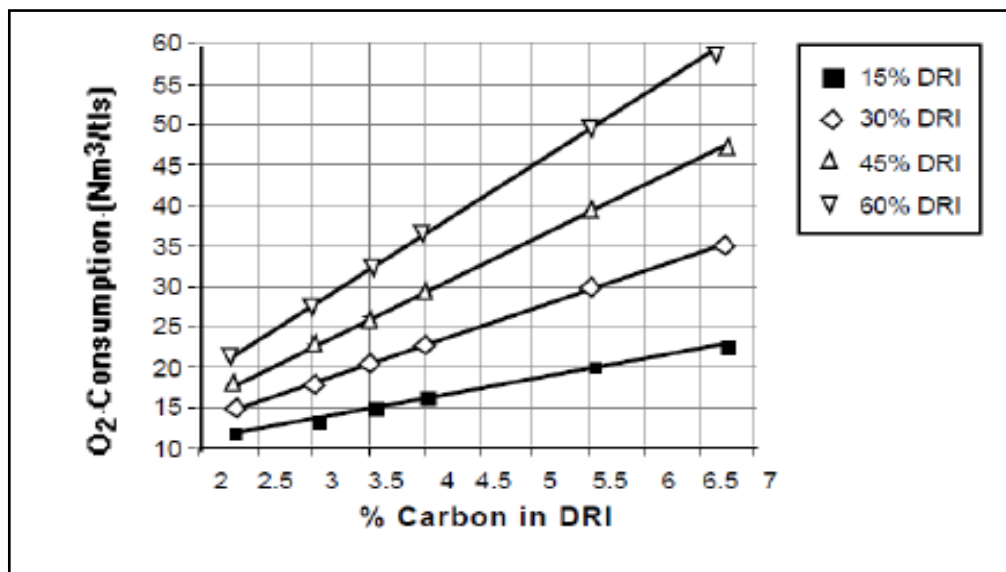


**Figure 2.7:** EAF oxygen consumption using different charges of DRI with different carbon level

Sources: HYL III: Status and Trend

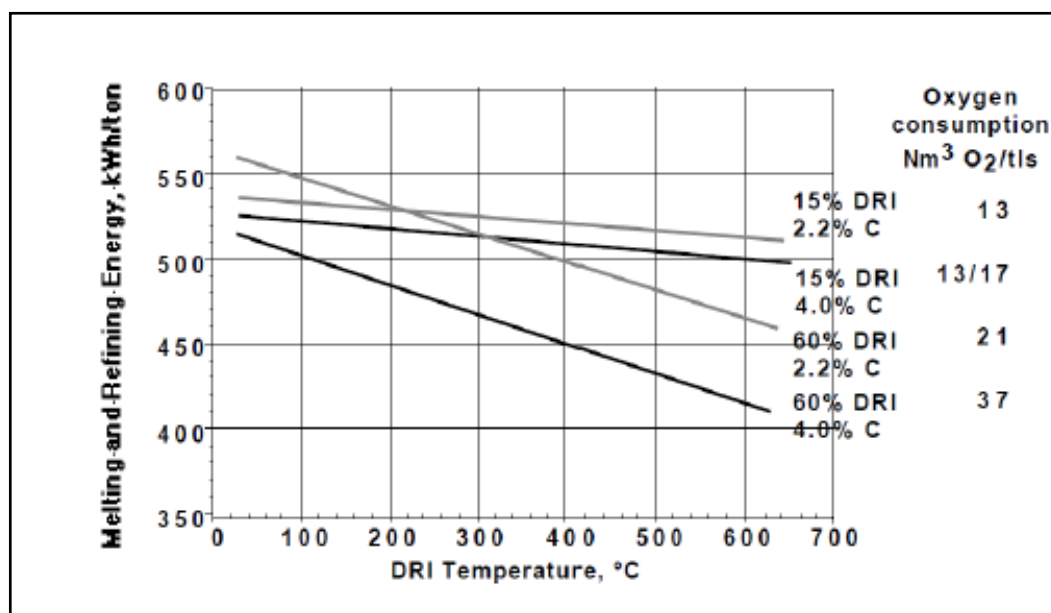


**Figure 2.8:** Effect of DRI temperature and carbon content on electricity consumption

Sources: HYL III: Status and Trend

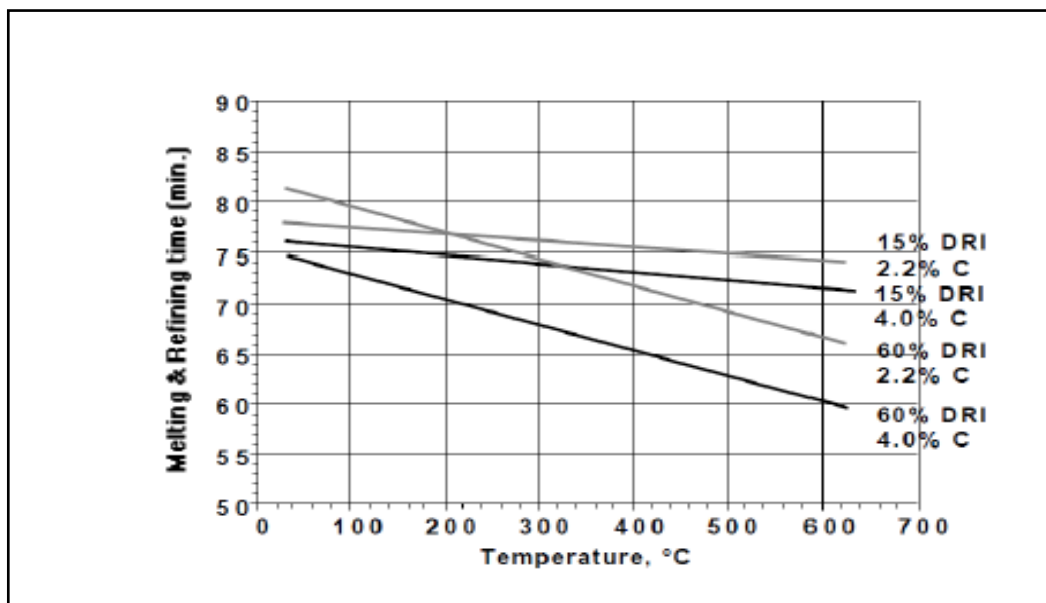


**Figure 2.9:** Effect of DRI temperature and carbon on melting and refining time

Sources: HYL III: Status and Trend

Natural gas is generally long chain of hydrocarbon which consisted of mainly methane and a little amount of ethane and other inert gases. It is considered as non-renewable fossil fuel. Natural gas is hard to find since it is usually trapped in porous rocks deep underground. There are many methods used by the geologists to find this gas deposits such as looking at the surface rocks to find the clues about underground formations. Besides, small explosion or by dropping heavy weights on the earth's surface also can be set off. In addition, the NG also can be traced by recording the sound waves as it can be bounced back from the sedimentary rock layers underground.

In chemical industries, NG is usually used with the purpose of heating, and also as the electricity sources. In iron making and steelmaking industries, NG is reformed in order to generate high concentration of reducing gases which are hydrogen and carbon monoxide. In local company, the NG is supplied from Gas Malaysia Berhad. This source of gas is manufactured by Petronas Gas Berhad and imported by GSB. In the **Table 2.1** below stated the composition of gases in NG used in Perwaja Steel.

Furthermore, NG is a colourless gas. Since it is cannot be detected if leaking, Merchantan mixture is added as odorant which makes it easily be detected when leaking. At the temperature of 537°C, the NG is predicted to be auto ignited and easily to combustible with the presence of oxygen although without any ignition. In this study, the presence of other gas is negligible except for methane since the portion of methane in this NG is in large amount. Therefore, the combustion reaction for other gases besides methane is neglected.

**Table 2.1:** Composition of gases in natural gas

<b>Gases</b>	<b>Composition (%)</b>
Methane	92.73
Ethane	4.07
Other Hydrocarbon	3.20

Source: Chemical Safety Data Sheet, Gas Malaysia Berhad

## **2.3 INTRODUCTION OF COMPUTATIONAL FLUID DYNAMIC**

### **2.3.1 CFD Approach**

Computational Fluid Dynamic is a branch of fluid mechanics that uses to analyze problem that involve fluid flows. It is use to perform the calculations required to simulate the performance of fluid flow in the system. Through CFD, the modeling design can be use exactly like an actual. This software offers the unparallel fluid flow analysis capabilities, providing the entire tool needed to design and optimize the model (Ansys, Fluent 12.1).

The fluid flow's physics and chemistry are applied to this virtual prototype and the software will provide a prediction of the fluid dynamics and related physical phenomena. Therefore, CFD is a sophisticated computationally which is based on design and analysis technique. CFD software give the capabilities to simulate flows of gases and liquids, heat and mass transfer, moving bodies, multiphase physics, chemical



reaction, fluid-structure interaction and acoustics through computer modeling. Using CFD software, a virtual prototype of a system or device can be built accordingly to analyze and then apply in real-world physics and chemistry of the model and the software will provide images and data, which predict the performance of that design (Ansys, Fluent 12.1).

Besides that, through the modeling design of transfer line, the volume meshing process can be done. Meshing is an integral part of the computer-aided engineering (CAE) analysis process. The mesh influences the accuracy, convergence and speed of the solution. Furthermore, the time it takes to create a mesh model is often a significant portion of the time it takes to get results from a CAE solution. Therefore, the better and more automated the meshing tools, the better the solution (Ansys, Fluent 12.1).

#### **2.3.1.1 Gambit 2.4.6**

Gambit is non solver software which is used for modeling purpose and meshing. Correct meshing is needed to get an accurate result.

#### **2.3.1.2 Fluent 6.3.26**

Fluent is a state-of-the-art computer program for modeling fluid flow and heat transfer in complex geometries using computational tools. Fluent provides complete mesh flexibility, including the ability to solve flow problem.

## 2.4 FUNDAMENTAL OF CFD

### 2.4.1 Turbulence Modeling

Deriving  $k - \varepsilon$ , it is assumed that the flows are fully turbulent and the effects of molecular viscosity are neglected. Therefore, it is only valid for fully turbulent flows such as this study (Stefanidis.G.D, et al, 2005).

### 2.4.2 Transport Equation

For turbulence kinetic energy,  $k$  and its dissipation rate  $\varepsilon$ , both are obtained from the following equations:

$$\frac{\partial}{\partial t}(\rho k) + \frac{\partial}{\partial x_i}(\rho k u_i) = \frac{\partial}{\partial x_j} \left[ \left( \mu + \frac{\mu_\tau}{\sigma_k} \right) \frac{\partial k}{\partial x_j} \right] + G_k + G_b - \rho \varepsilon - Y_M + S_k \quad (2.13)$$

$$\begin{aligned} \frac{\partial}{\partial t}(\rho \varepsilon) + \frac{\partial}{\partial x_i}(\rho \varepsilon u_i) \\ = \frac{\partial}{\partial x_j} \left[ \left( \mu + \frac{\mu_\tau}{\sigma_\varepsilon} \right) \frac{\partial \varepsilon}{\partial x_j} \right] + C_{1\varepsilon} \frac{\varepsilon}{k} (G_k + C_{3\varepsilon} G_b) - C_{2\varepsilon} \rho \frac{\varepsilon^2}{k} + S_\varepsilon \end{aligned} \quad (2.14)$$

Where  $G_k$  is the generation of turbulence kinetic energy due to the mean velocity gradients and was calculated as follows:

$$G_k = -\overline{\rho u_i' u_j'} \frac{\partial u_j}{\partial x_i} \quad (2.15)$$

From equation (2.13) and (2.14),  $G_b$  represents generation of turbulence kinetic energy due to buoyancy and is calculated as follows:

$$G_k = \beta g_i \frac{\mu_\tau \partial T}{P_{rt} \partial x_i} \quad (2.16)$$

Where  $P_{rt}$  is the turbulent Prandtl Number for energy and  $g_i$  is the component of the gravitational vector in the  $i^{th}$  direction. For this study, the default value of  $P_{rt}$  is to be set as 0.85. From equation (2.16), the thermal expansion coefficient,  $\beta$  is defined as:

$$\beta = -\frac{1}{\rho} \left( \frac{\partial P}{\partial T} \right)_P \quad (2.17)$$

$Y_M$  in equation (2.13) represents the contribution of the fluctuating dilatation in compressible turbulence to the overall dissipation rate and defined as:

$$Y_M = 2\rho\epsilon M_t^2 \quad (2.18)$$

Where  $M_t$  is the Turbulent Mach number and defined as:

$$M_t = \sqrt{\frac{k}{a^2}}$$

Where  $a(\equiv \sqrt{\gamma RT})$ , is the speed of sound.

### 2.4.3 Mass Transfer and Species Transport Equation

The local mass fraction of each species  $Y_i$  can be predicted through the solution of a convection-diffusion equation for  $i^{th}$  species. This conservation equation takes the following general form:

$$\frac{\partial}{\partial t} (\rho Y_i) + \nabla \cdot (\rho \vec{v} Y_i) = -\nabla \cdot \vec{J}_i + R_i + S_i \quad (2.19)$$

Where  $R_i$  is the net rate production by chemical reaction and  $S_i$  is the net rate of creation by addition from the dispersed phase. An equation of this form will be solved for  $N-1$  where  $N$  is the total number of fluid phase chemical species present in the system. Since the mass fraction of the species must sum to unity, the  $N^{th}$  mass fraction is determined as one minus the sum of the  $N-1$  solved mass fraction (Gupta, 2010).

#### 2.4.4 The Eddy-Dissipation Modelling

In combustion, most of the fuels are burning quickly and the turbulent mixing will control the overall rate of reaction. For this premixed flames, the turbulence slowly convects/mixes cold reactants and produced hot products into the reaction zones where reaction occurs rapidly. In this transport phenomena, the net rate of production of species  $i$  due to reaction  $r$ ,  $R_{i,r}$  is given as follows:

$$R_{i,r} = v'_{i,r} M_{w,i} A \rho \frac{\epsilon}{k} \min \left( \frac{Y_R}{v'_{R,r} M_{w,R}} \right) \quad (2.20)$$

$$R_{i,r} = v'_{i,r} M_{w,i} A \rho \frac{\epsilon}{k} \left( \frac{\sum_P Y_R}{\sum_j^N v''_{j,r} M_{w,j}} \right) \quad (2.21)$$

Where  $Y_p$  is the mass fraction of any products species,  $P$ ,  $Y_R$  is the mass fraction of a particular reactant,  $R$  while  $A$  and  $B$  are empirical constants which equals to 4.0 and 0.5 respectively.

#### 2.4.5 Convective Heat and Mass Transfer Equation

For this study, the heat transport is modeled using the concept of Reynold's analogy to turbulent momentum transfer. The modeled energy equation is thus given by the following:

$$\frac{\partial}{\partial t}(\rho E) + \frac{\partial}{\partial x_i} [u_i(\rho E + p)] = \frac{\partial}{\partial x_j} \left( k_{eff} \frac{\partial T}{\partial x_j} + u_i(\tau_{ij})_{eff} \right) + S_h \quad (2.22)$$

Where  $E$  is the total energy,  $k_{eff}$  is the effective thermal conductivity and (2.22) is the deviatoric stress tensor which is being defined as:

$$(\tau_{ij})_{eff} = \mu_{eff} \left( \frac{\partial u_j}{\partial x_i} + \frac{\partial u_i}{\partial x_j} \right) - \frac{2}{3} \mu_{eff} \frac{\partial u_k}{\partial x_k} \delta_{ij} \quad (2.23)$$

### 2.4.6 The Energy Equation

Generally, FLUENT solves the energy equation as follows:

$$\frac{\partial}{\partial t}(\rho E) + \nabla \cdot (\vec{v}(\rho E + p)) = \nabla \cdot (k_{eff} \nabla T - \sum_j h_j \vec{J}_j + (\bar{\tau}_{eff} \cdot \vec{v})) + S_h \quad (2.24)$$

Where  $\vec{J}_j$  is the diffusion flux of species  $j$ .

In equation (2.24),  $E$  is defined as:

$$E = h - \frac{p}{\rho} + \frac{v^2}{2} \quad (2.25)$$

Where sensible enthalpy for incompressible flows is defined as:

$$h = \sum_j Y_j h_j + \frac{p}{\rho} \quad (2.26)$$

## 2.5 TRANSFER LINE BOUNDARY REFRACTORY

Silicon Nitride Ceramics have been studied extensively in recent years on account of their potential application as high-temperature engineering materials (Maeda.M, et al, 1989). The experimental done by using three different specimens at same operating hours. The weight product gain by using Magnesium Oxide, MgO and Aluminum Oxide, Al<sub>2</sub>O<sub>3</sub> is lesser than specimens contain Yttrium Oxide, Y<sub>2</sub>O<sub>3</sub> and Aluminum Oxide, Al<sub>2</sub>O<sub>3</sub>. Nevertheless, the different bulk density and porosity in the specimens also will cause a different weight of product gain. The highest Yttrium and bulk density with lower porosity will produce higher weight gain product.

The other two commercial refractory bricks are Mullitic (3Al<sub>2</sub>O<sub>3</sub>.2SiO<sub>2</sub>) and Andalusite (Al<sub>2</sub>O<sub>3</sub>.SiO<sub>2</sub>). Both bricks contain some sillimanite and bulk density. The porosity of Mullitic is lower than Andalusite. From the result obtain, it can be conclude that the Andalusite specimens will have a high potential to melt at the higher temperature due to the higher area loss had been observe. Due to the less resistance of

the specimens, the thickness of the wall should be taking accounted. It is because to avoid any leaking and problem on the system instead of for the long used and most economical since the earth material is quite expensive (Seung Jae Lee and Kyu Tae Kim, 1997).

In Perwaja Steel Sdn. Bhd., the type of refractory used is a Brick KX-99 (brand name). It is a super duty firebrick which has an ability to fire resistance on temperature 1760°C. Heat containment solutions are available in a variety of high alumina silica and superduty fireclay bricks. **Table 2.2** below show the chemical analysis on the brick KX-99. High contaminant of silica and alumina cause this brick have a high fire resistance upon temperature.

**Table 2.2:** Chemical analysis on the brick KX-99

Chemical	Percentage %
Silica (SiO <sub>2</sub> )	39.4
Alumina (Al <sub>2</sub> O <sub>3</sub> )	55.2
Titania (TiO <sub>2</sub> )	2.0
Iron Oxide (Fe <sub>2</sub> O <sub>3</sub> )	1.1
Lime (CaO)	0.2
Magnesia (MgO)	0.2
Alkalies (Na <sub>2</sub> O+K <sub>2</sub> O)	1.9

Source: Perwaja Steel Sdn. Bhd.

## **CHAPTER 3**

### **METHODOLOGY**

#### **3.1 INTRODUCTION**

This study is involving the modeling and simulation of the partial combustion performance via CFD. Comparison of the performance is done between current scheme and new scheme with the present of boundary refractory. Some validation being performed using the real – plant data taken at Perwaja Steel Direct Reduction Plant (R&D Department).

#### **3.2 COMPUTATIONAL TOOLS**

There is many type of software used for the designing and CFD simulation. Gambit version 2.4.6 is used in modeling and meshing purpose. For the process which include chemical reaction, CFX, Fluent and ANSYS was used. For this study, Fluent version 6.3.26 is used.

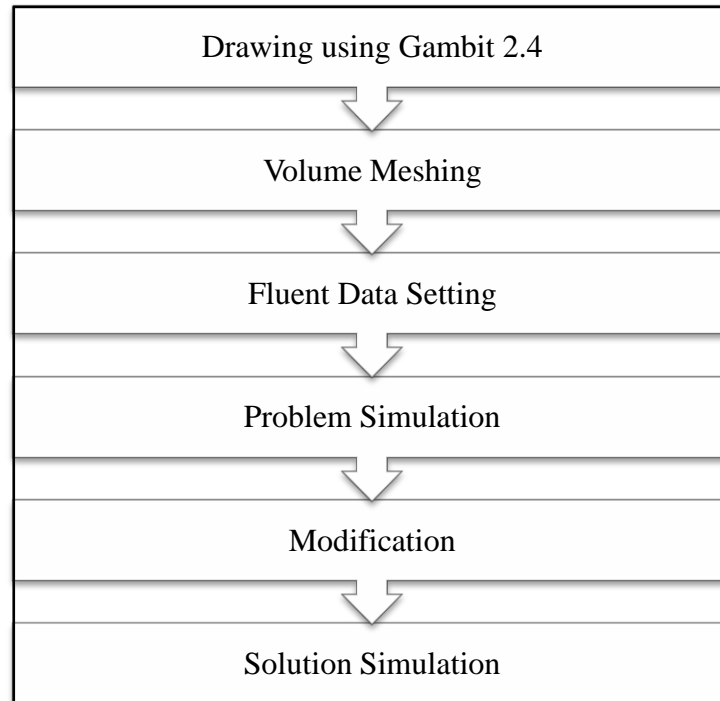


**Figure 3.1:** Procedure for simulation CFD

Source: Perwaja Steel R&D Department

### 3.3 DETAIL STEPS

Firstly, the necessary technical drawing is to be accomplished in Gambit 2.4.6. Then, the meshing strategies should be applied in order to get the best result of the meshed volume. The boundary layer must be created, with the following defined parameters, algorithm, dimensions, internal continuity option and corner shape option. The physics create in Gambit is dividing into two, first is boundary types and second is continuum types. The boundary types give a command for a flow (inlet and outlet) inside the technical drawing while the continuum types will set the phase condition of the technical drawing.

Secondly, the fluent data setting should be done. The conversion of process gas analysis in terms of volumetric percentage/mole fraction into mass fraction is needed since the fluent data setting is based on this unit, refer **Table 3.1** below:



**Table 3.1:** Mass Flowrate

Process Gas Components	Current Scheme		New Scheme	
	Mole	Mass	Mole	Mass
	fraction	fraction	fraction	fraction
Hydrogen (H <sub>2</sub> )	0.696	0.154	0.730	0.182
Carbon Monoxide (CO)	0.158	0.486	0.120	0.417
Carbon Dioxide (CO <sub>2</sub> )	0.015	0.072	0.015	0.083
Methane (CH <sub>4</sub> )	0.075	0.132	0.090	0.180
Nitrogen (N <sub>2</sub> )	0.041	0.126	0.030	0.104
Water (H <sub>2</sub> O)	0.015	0.029	0.015	0.034
Total	1.000	1.000	1.000	1.000

Source: Perwaja Steel Sdn. Bhd

Further, in setting the data for Fluent, there are some important physical properties of the respective materials that need to be defined. The properties include density, molecular weight, viscosity, heat capacity, thermal conductivity, UDS diffusion coefficients, mass diffusion coefficients, standard state enthalpies, and kinetic theory parameters. The other parameter setting values are outlined in **Table 3.2**. The properties of the refractory brick are found from the web site. The properties are present in **Table 3.3** Properties of refractory brick KX-99

**Table 3.2:** Physical Properties

No.	Items	Setting Value	
		Current Scheme	New Scheme
1.	Velocity of process gas at transfer line inlet	117.11 m/s	178.61 m/s
2.	Velocity of oxygen gas inlet at nozzle	101.34 m/s	232.25 m/s
3.	Heater outlet temperature	915°C	810°C

**Table 3.3** Properties of refractory brick KX-99

Items	Setting value
Density ( $\text{kg/m}^3$ )	2290
$C_p$ (J/kg. K)	910
Thermal Conductivity (W/m. K)	17.8

### 3.4 SIMULATION PROCEDURE

#### 3.4.1 Modeling using Gambit version 2.4.6

The most important step in this study is modeling using Gambit. The modeling size used in this software was exactly same as the real plant as show in the Appendixes. After the modeling step is done, the volume meshing should be done in order to get the best result. In this step, the boundary layer must be created. The following parameter should be specified in order to define the boundary layer:

- i. Algorithm
- ii. Dimension
- iii. Internal continuity option
- iv. Corner shape option

**Figure 3.2** below show the modeling figure in Gambit while **Figure 3.3** is a modeling figure in the fluent for previous design and current design. The node was at least 261,593 nodes for transfer line design with refractory and 357,345 nodes for transfer line design without refractory to yield reasonable prediction. Nevertheless, the greater the value of the nodes, more accurate result obtained and more time taken for the iteration. In this case, the high performance computer is needed to simulate in the range of time.

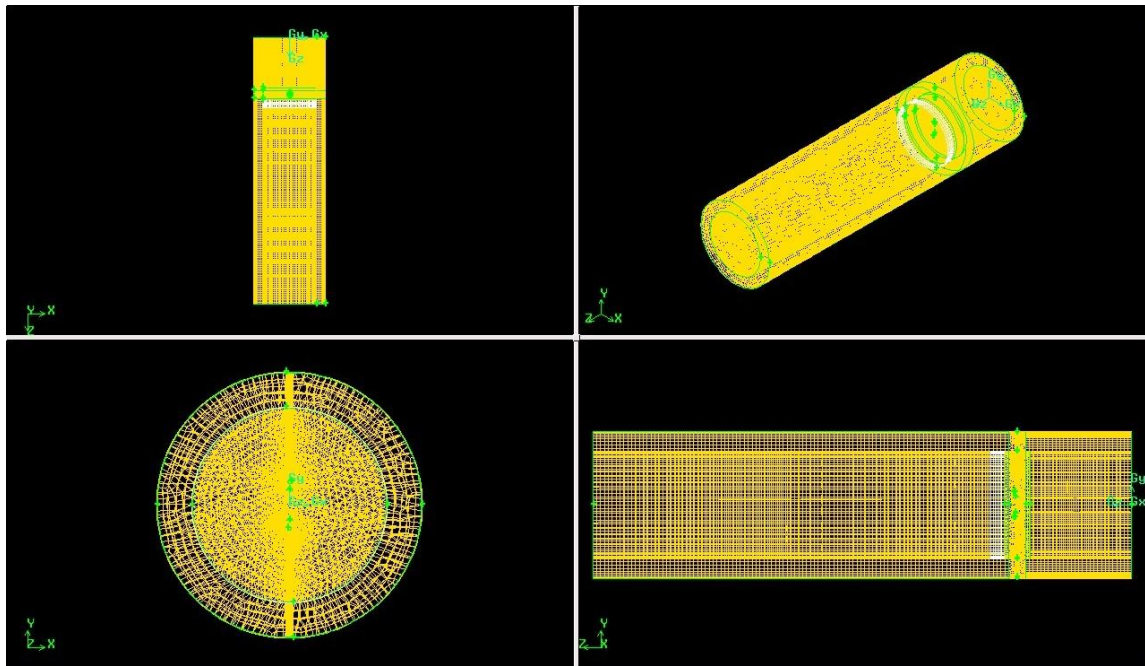


**Figure 3.2:** Modeling using Gambit 2.4.6

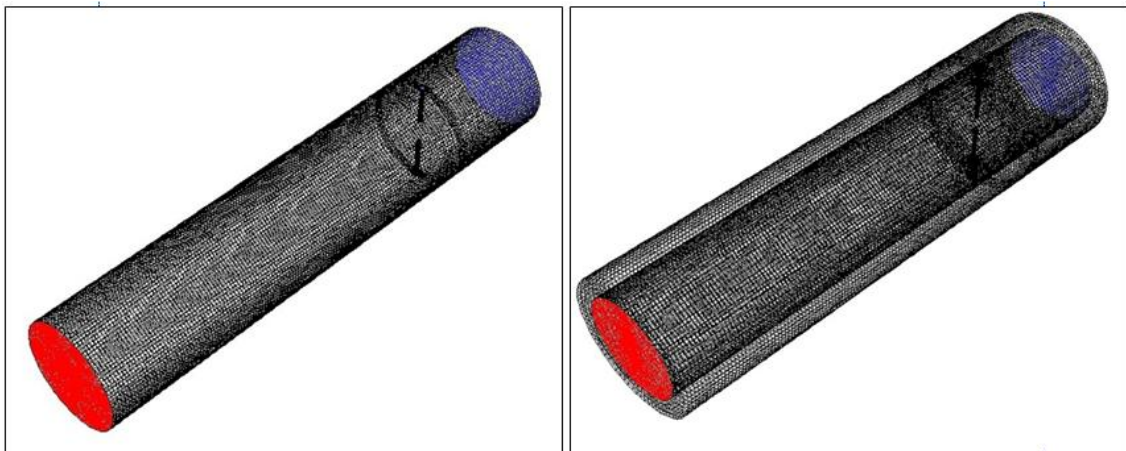


**Figure 3.3:** Mesh generation of transfer line  
(left is a previous design, right is a current design)



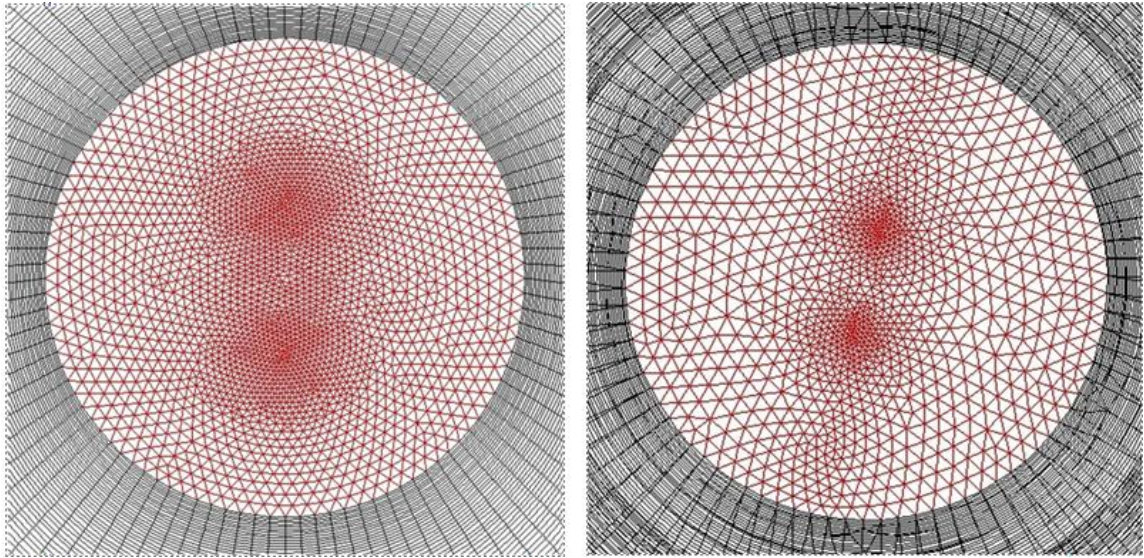


**Figure 3.4:** Mesh generation at outlet transfer line  
(left is a previous design, right is a current design)

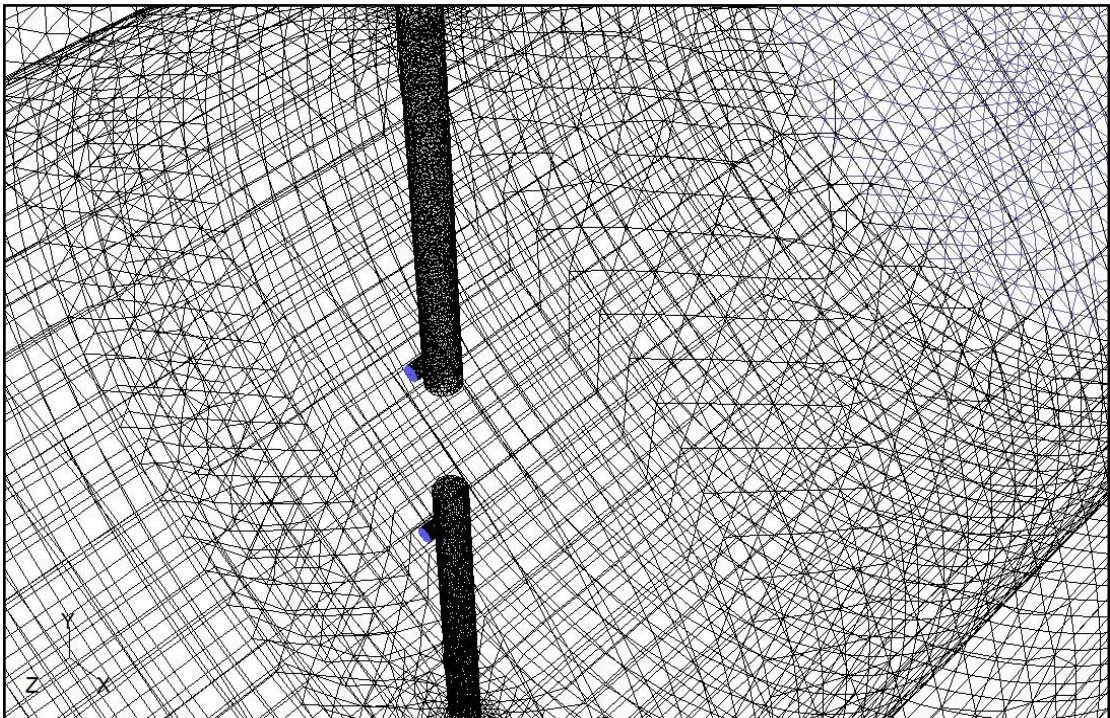


**Figure 3.5:** Mesh generated at nozzle and oxygen lances



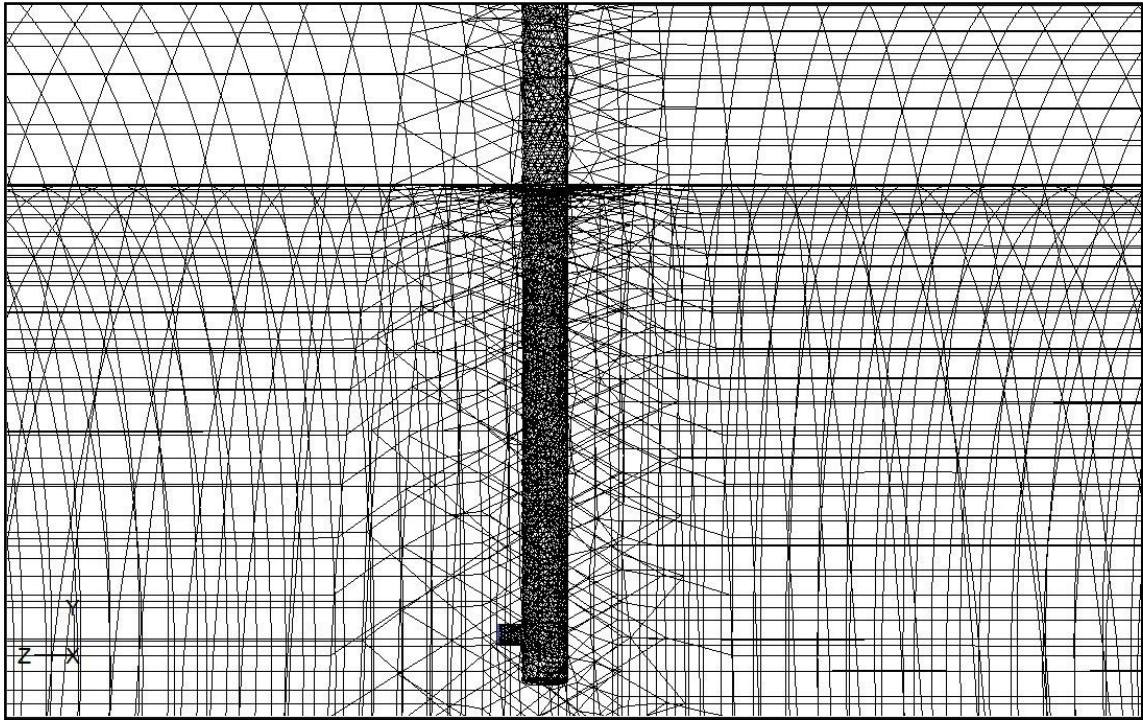


**Figure 3.6:** Mesh generated at oxygen lance

### **3.4.2 Fluent data setting**

In Fluent, there are many properties of mixture, fluid and solid those have been set. The properties of items can be set by user if Fluent does not have the data. The detail in setting the data was shown in section 3.3.4

### **3.4.3 Simulation on existing lance configuration**

After finished with the data setting and parameters needed, simulation then can be run in Fluent. Next, at a certain number of iteration, the drawing contour displayed by the simulation and the profile of certain parameters such as Temperature, Turbulent Kinetic Energy and Species Concentration also can be determined. Every single observation should be recorded for further reference during the modification and troubleshooting.

### 3.4.4 Detail in setting the data

After the modeling and volume meshed is done, export the mesh (.msh). Then, open the Fluent and choose the 3ddp version. In the menu bar, click the file and read the case of the export mesh. After then, click the grid and check.

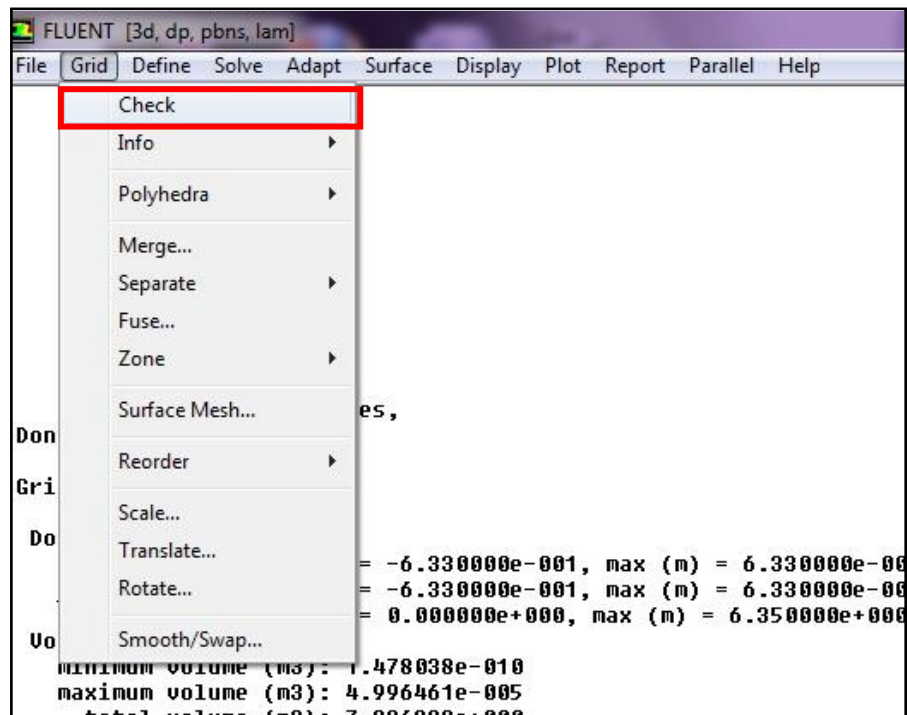


**Figure 3.7:** Check the grid for the mesh exported

After check the grid, the energy, viscous and species model need to be defined. First, the energy needs to be enabled. Then, set the viscous model as a standard k-epsilon. In the defining the species model, the volumetric reaction, inlet diffusion, diffusion energy source, thermal diffusion and finite rate/Eddy – dissipation need to be enable.

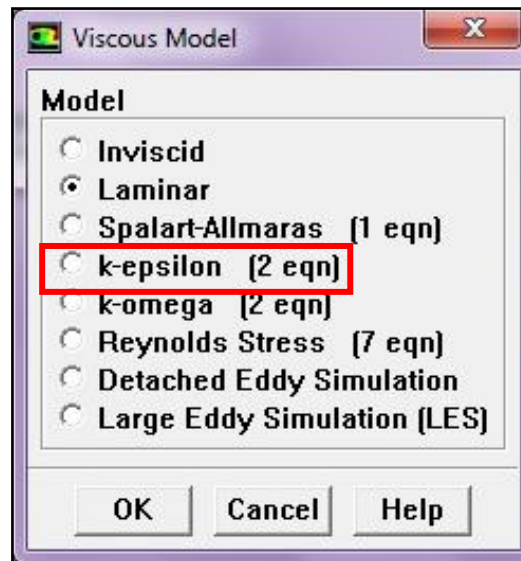


Figure 3.8: Viscous model selection

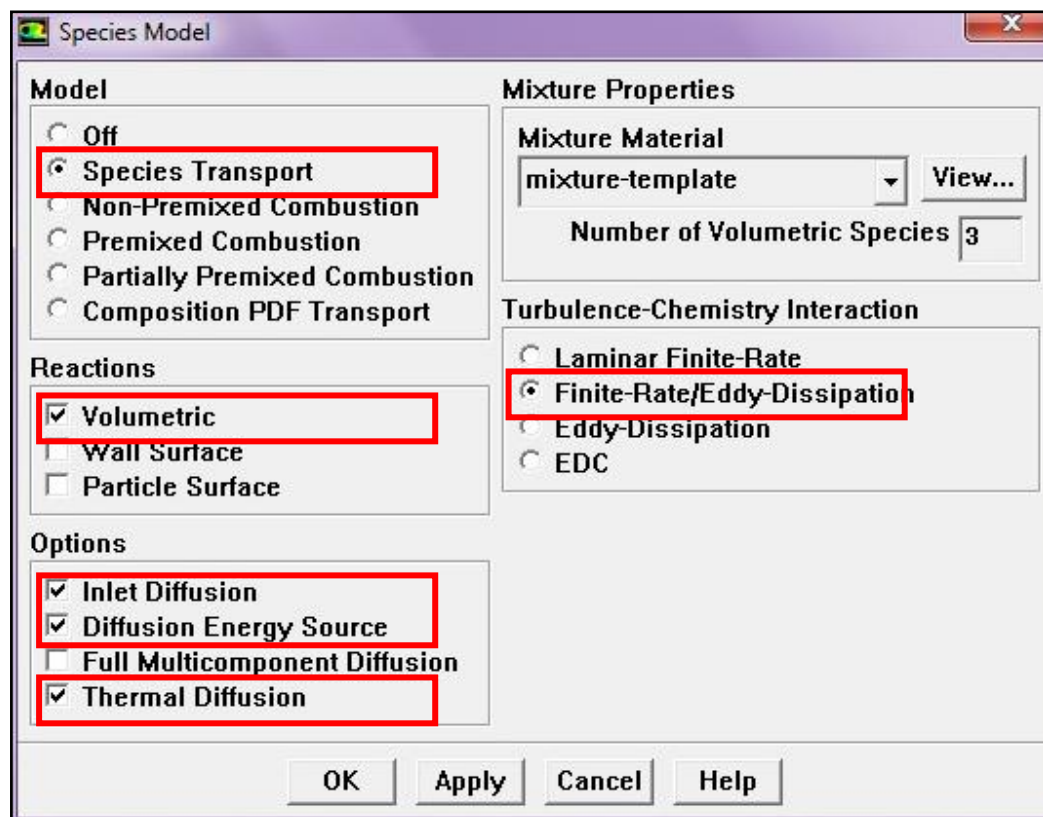


Figure 3.9: Species model selection

After defining the energy, viscous and species model, a window of information appear and state regarding the changes properties or methods. Thus, the materials of mixture, fluid and solid need to be set.

First set the mixture as a methane air – 2 – step. Then, set the fluid gas as a methane, hydrogen, oxygen, carbon dioxide, carbon monoxide, nitrogen, water vapor and air. Set the solid as aluminum, steel and brick KX-99. Since there is no property of the brick in the Fluent, thus, the data need to be set. The procedure to set the data was shown in **Figure 3.10(a)** and **Figure 3.10(b)** and it same for fluid and solid. The After done, mixture species of the mixture need to be edited and air should be on the last in the list. Then, the reaction of the mixture need to be set as shown in **Table 3.4** Reaction Mechanism. **Figure 3.11(a)** and **Figure 3.11(b)** below shown the procedure needed to key in the data presented in **Table 3.4**.

**Table 3.4:** Reaction Mechanism

Reaction (as shown in Chapter 2)	Exponential Factor	Activation Energy	Temperature Exponent	Mixing Rate		Rate Exponent
				A	B	
Equation (1)	$2.239 \times 10^{12}$	$1.70 \times 10^{08}$	0	4	0.5	CO:1, O <sub>2</sub> :0.25
Equation (2)	$9.870 \times 10^{08}$	$3.10 \times 10^{07}$	0	4	0.5	H <sub>2</sub> :1, O <sub>2</sub> :1
Equation (3)	$2.119 \times 10^{11}$	$2.03 \times 10^{08}$	0	4	0.5	CH <sub>4</sub> :0.7, O <sub>2</sub> :1.3
Equation (4)	$5.012 \times 10^{11}$	$2.00 \times 10^{08}$	0	4	0.5	CH <sub>4</sub> :0.7, O <sub>2</sub> :0.8
Equation (5)	$5.000 \times 10^{08}$	$1.70 \times 10^{08}$	0	4	0.5	CO <sub>2</sub> :1



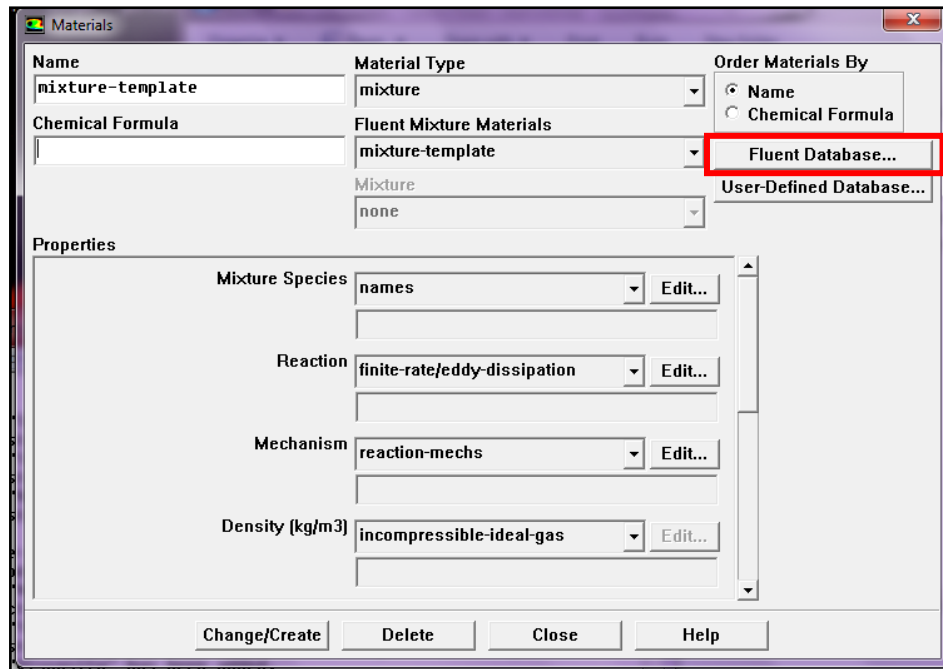


Figure 3.10(a): Set the material

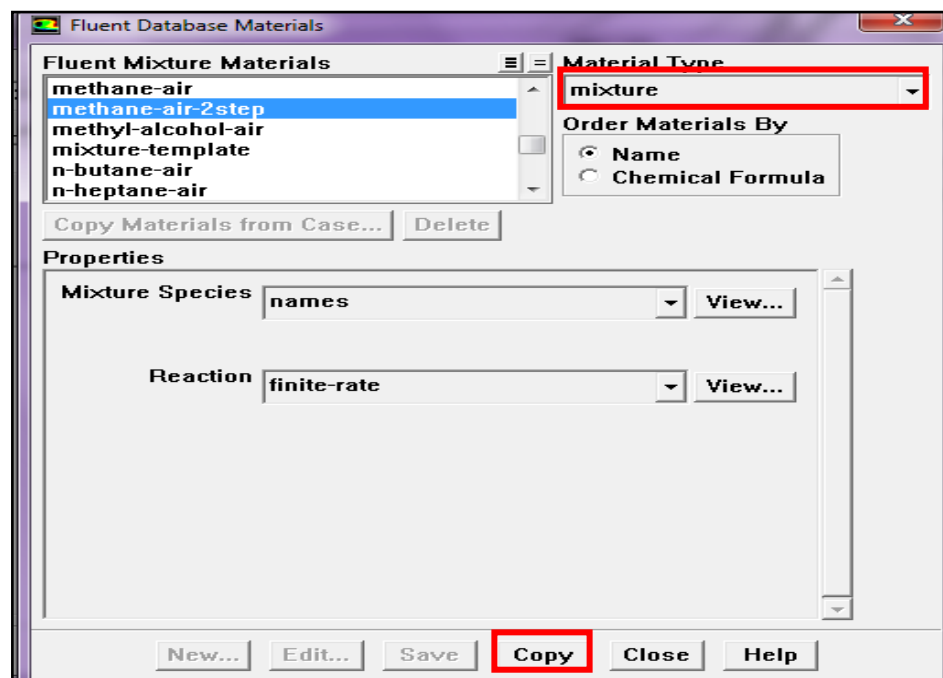


Figure 3.10(b): Choose the material (Make sure the material type is correct)

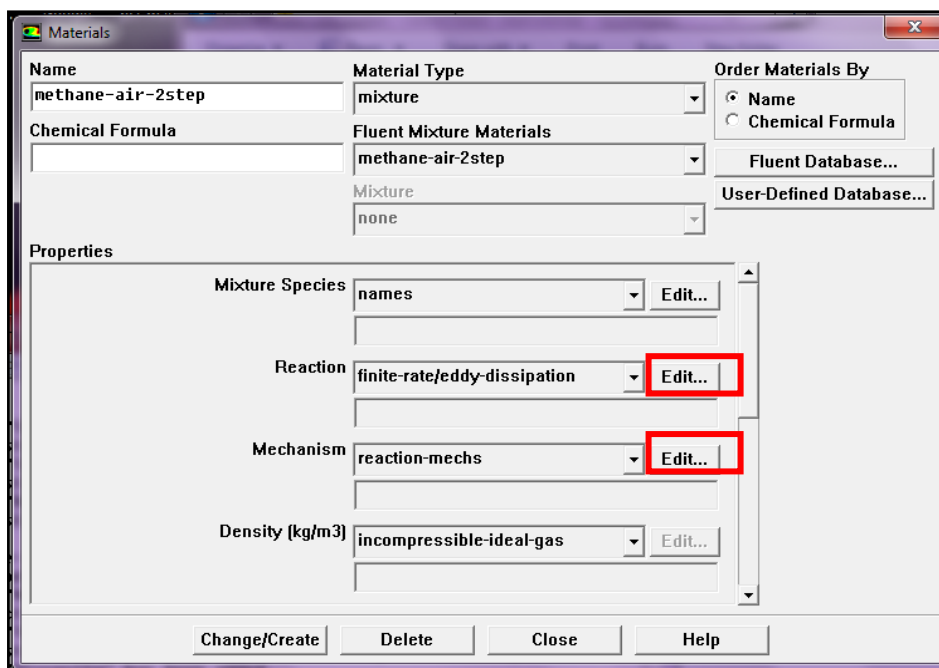


Figure 3.11(a): Set the reaction

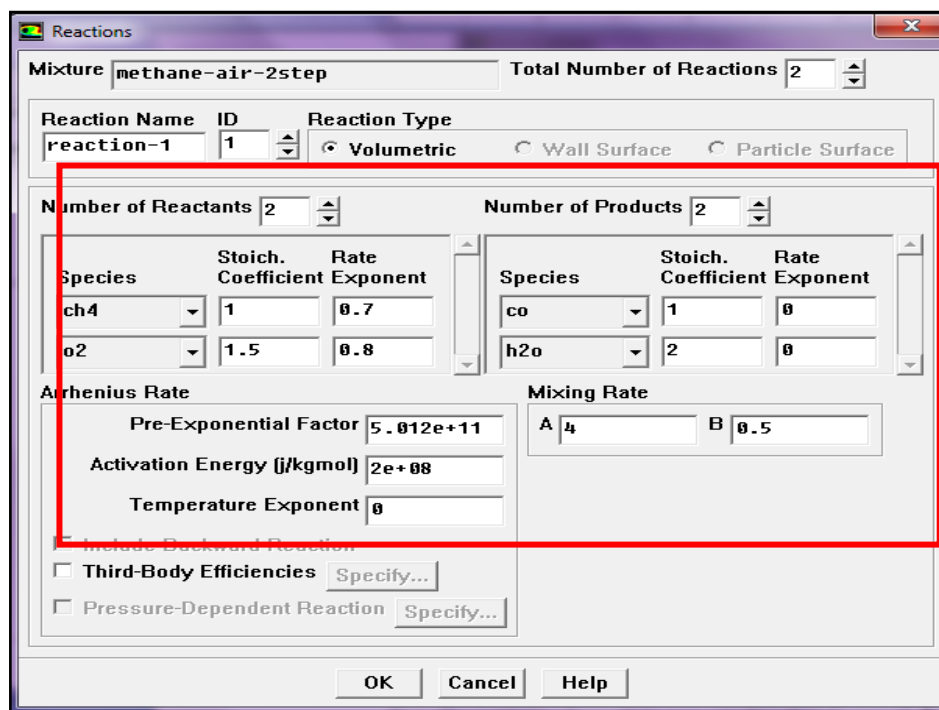
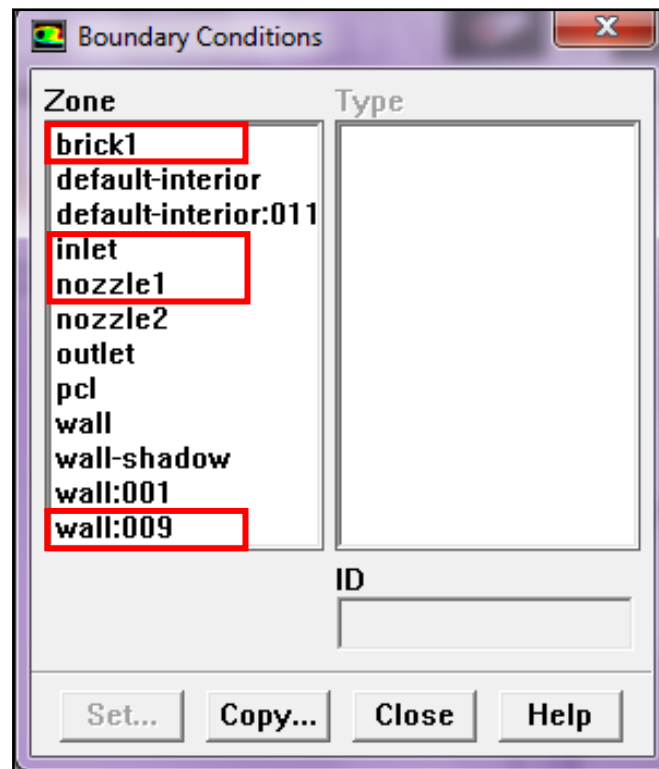


Figure 3.11(b): Set data in Table 3.4

As shown in **Figure 3.10(a)**, the Fluent Mixture Material is mixture – template. This mixture need to be deleted and replace with Methane air – 2 – step. Click the data in **Figure 3.10(b)** change it to the Methane air – 2 – step. Then, in **Figure 3.10(a)**, select the mixture – template and click the delete button on the bottom.

After done, define the operating condition and boundary condition. In the operating condition, the gravity is set at x – axis. Nevertheless, the axis of the gravity is base on the modeling. Boundary condition was set according to **Table 3.1** and **Table 3.2**. **Figure 3.12** presented the boundary condition that need to be set.



**Figure 3.12:** Editing the boundary condition

Than, click the solve button on the menu bar search for monitor, than residual and thick the plot. All the iteration data will be display during iteration. On the same tab menu, search for the initialize to set the flow to be start at the inlet. Then set the energy of Relaxation Factor to 0.7 under the same tab menu on the control solution.

Lastly, iterate the simulation after set the number of iteration. Nevertheless, the iteration needs to be done in 3 stages. First stage is unable all the reaction to check the flow in the transfer line. To unable the reaction, click the mechanism tab in **Figure 3.11(a)** and unselect all the reaction. After certain iteration and the flow are stable, select all the reaction and continue the iteration until it stable. Then, change the data into second – order reaction. It because, the discrete of viscous is always accurate in second order while first – order discrete yields more robust convergence. **Figure 3.13** below shown the energy Relaxation Factor that need to be change and changes need for second order iteration.

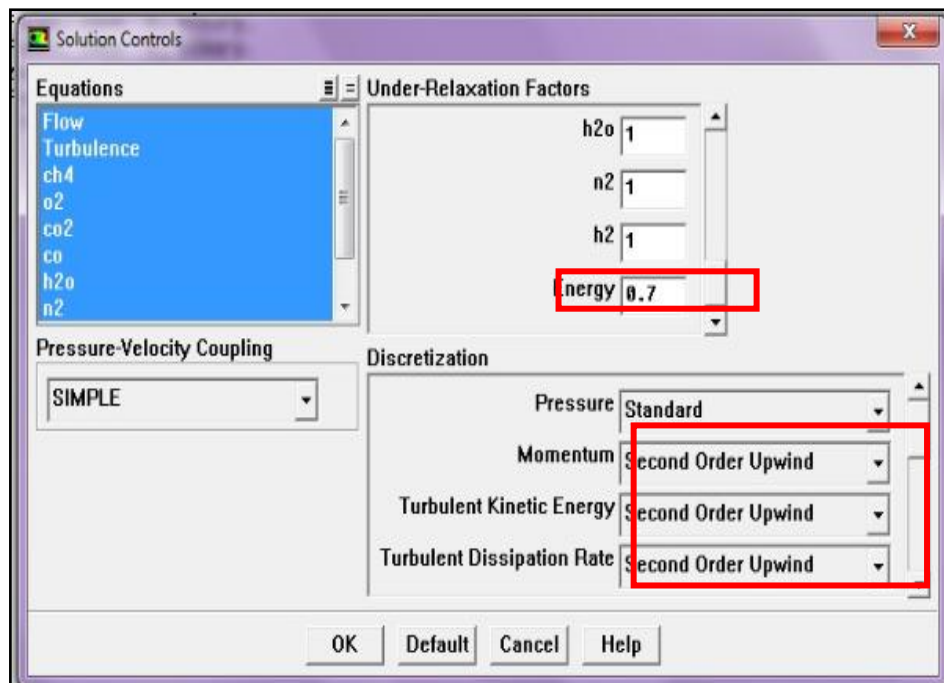


**Figure 3.13:** Energy relaxation factor and second – order iteration.

## CHAPTER 4

### RESULT AND DISCUSSION

#### 4.1 DATA COLLECTION

The temperature profile for the partial combustion unit in the transfer line of Direct Reduction plant was determined by analyzing the contour of the unit obtained using the CFD. The centre line of the transfer line was created as the reference line to read the Parameters for the analysis. Then, validation being made using the data obtained using CFD, Excel Simulation and real plant data.

The data comparison was divided into three. First is on current scheme process which, comparison between transfer line without refractory (previous study) and with refractory. Second is on new scheme process with same comparison as the first discussion. Third is the comparison between these two different process schemes with refractory existent.

#### 4.2 CURRENT SCHEME PROCESS

According to contour for current scheme process for previous design and current design, the temperature profile for previous study is higher compare to the current study, the design of PCU with boundary refractory. The contours were shown is **Figure 4.1** and **Figure 4.2** present the temperature profile for both study in the graph.

As stated in previous chapter, the amount of nodes for previous study is higher compare to the new study. As mention before, the amount of nodes may influence the results where the higher amount of nodes will give more accurate result. At the

validation point, the temperature measure for the previous study is 8.89% error with a real plant compare to the current study, the error is 7.58%. The error for both study are slightly different.

Besides that, the type of modeling used for these two designs is totally different. As shown in **Figure 4.1**, for the previous study contour, one of the lances (the lance at the bottom) does not appear on the figure compare to the current study, both lances are shown clearly on the contour. Through this figure, the injection of oxygen is not on the nozzle for the previous study. It shown that, there is a flow in the oxygen lance. Since the diameter for the nozzle is smaller than the oxygen lance, thus, based on fluid dynamics principal, the velocity of fluid from the larger surface area to smaller surface area will be increase. This factor may influence the higher temperature obtain in the previous study. Thus, further study based on design modeling should be done to improve this study.

### 4.3 NEW SCHEME PROCESS

In new process scheme, the design used is same as mention in sub chapter 4.2. The contours were shown is **Figure 4.3** and **Figure 4.4** present the temperature profile for both study in the graph. At the validation point, the temperature measure for the previous design is 1.44% error with a real plant compare to the current study, the error is 15.92%. The error for both study are totally different. Nevertheless, in the new process scheme for previous study give a low percentage error because of the modeling design used for the simulation as mention in sub chapter 4.2.

In the previous design, the simulation from first order to second order cannot be change suddenly. It is because, at certain iteration at the certain nodes, there is turbulent viscosity limited occurred. As mention in chapter 3, there are three discretizations need to be change (**Figure 3.9**). Thus, the momentum was firstly change into second order upwind, followed by turbulent kinetic energy and lastly turbulent dissipation rate. This turbulent viscosity limited occur might be because the differential of oxygen injection on the lance.

#### 4.4 PROCESS SCHEMES WITH REFRACTORY

**Figure 4.5** show the temperature profile on the transfer line for both processes. Through the contour that forms from the simulation, it is difficult to determine the temperature at certain point. Thus, the graph was plot in **Figure 4.6** that show the differential of these two process schemes. As shown in the graph, the temperature on the new process scheme increase highly in contrast with the current process scheme. It is because the velocity of process gas inlet and oxygen injection are higher for new process scheme even the temperature of process gas inlet used is lower.

**Figure 4.7** show the velocity contour of both processes in transfer line. The detail of velocity is shown through the **Figure 4.8**. Through the data plot in the graph, the velocity of fluid flow in the new process scheme is increasing 5% while current process increases only 3%. The high velocity may reduce the time needed to oxidize the iron ore. Nevertheless, this factor needs to have a supporting result in term of cost effectiveness of natural gas used.

As the contour of mass fraction of  $\text{CH}_4$  presented in **Figure 4.9** and the detail in **Figure 4.10**, it shows that the mass fraction of  $\text{CH}_4$  in new scheme is higher as the fraction of  $\text{CH}_4$  in inlet is high compare to current scheme. By referring to these two figures, just a little amount of  $\text{CH}_4$  reacts with oxygen supplied in current process while in new process more amount of  $\text{CH}_4$  will reacts with oxygen supplied due to the higher velocity in the new process scheme. Nevertheless, the small amount  $\text{CH}_4$  can favor better partial combustion reaction. Since  $\text{CH}_4$  favor an endothermic process, it may cause Temperature drop in the reactor.

According to **Figure 4.11**, the new process scheme will gave better turbulence for the process gases to mix properly. Proper missing of the process gases gave better condition for the combustion and partial combustion reaction to take place. Due to high velocity of process gas in inlet and oxygen on the lance nozzle give high constraint to the process gas. Therefore the temperature reading for the new process scheme is better since it shown to increase highly as shown in **Figure 4.6**.

**Figure 4.12** show the temperature profile on the thermocouple as located at position  $Z=5.85\text{m}$  from the inlet of the transfer line, and the reading is taken at the point  $Y=0.373\text{m}$  from the center of the transfer line. Since the data cannot be taken from many point, therefore, this validation only take 1 exact point. In addition, for accurate validation, the data simulated from MS Excel also inserted and compared by considering the same operating condition. The summary of the validation is stated in the **Table 4.1** below.

From the data in the table, the calculated error for both current process for real plant and CFD simulation data is about 7.58%. While using the new process scheme, from the CFD simulation data, 15.92% of the temperature can be increased thus might give the increasing in temperature of the real plant to  $1293\text{K}$  @  $1020^{\circ}\text{C}$  for current process and  $1318.00\text{K}$  @  $1045^{\circ}\text{C}$ .

The small value of error which is around 10% is acceptable. From this study, the error is occurred when some of the parameters only set at the default value. Therefore, for better and accurate result, further study on this simulation case study can be performed with further details consideration taken. Although MS Excel and real plant data recorded the same value, the MS Excel simulation is inaccurate since the reaction is not all considerable and include in the simulation. Only the major reaction which is water-shift reaction is considered.



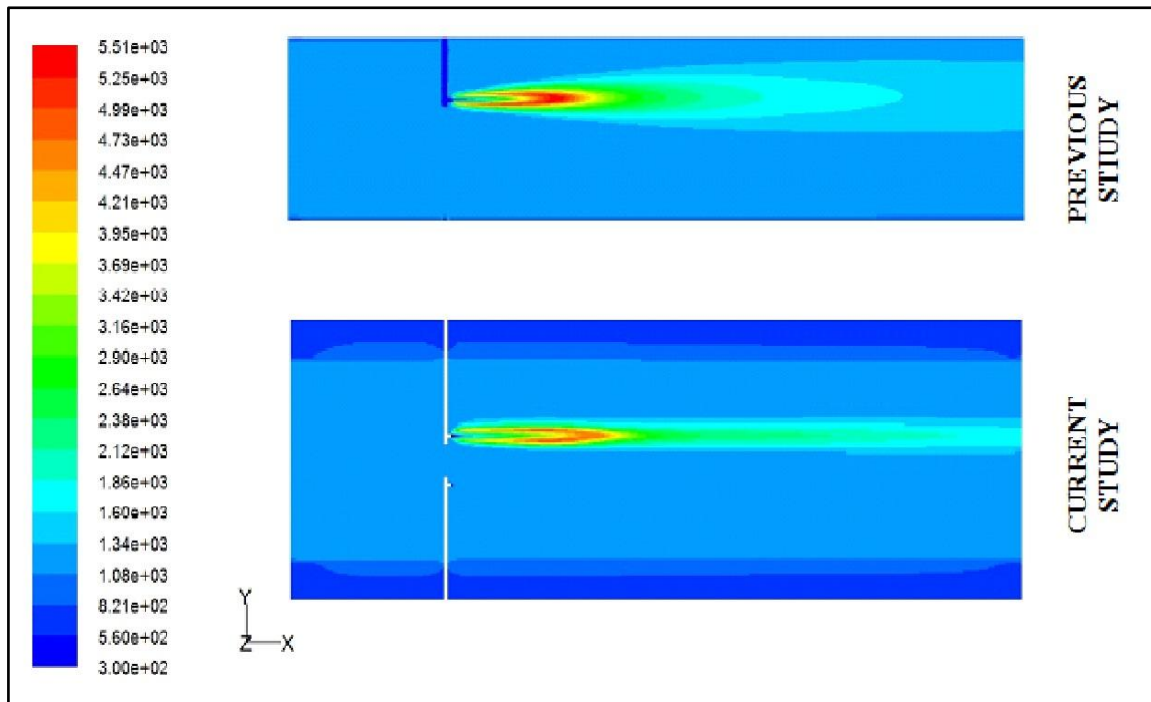


**Figure 4.1:** Temperature profile for previous study and current study for current process

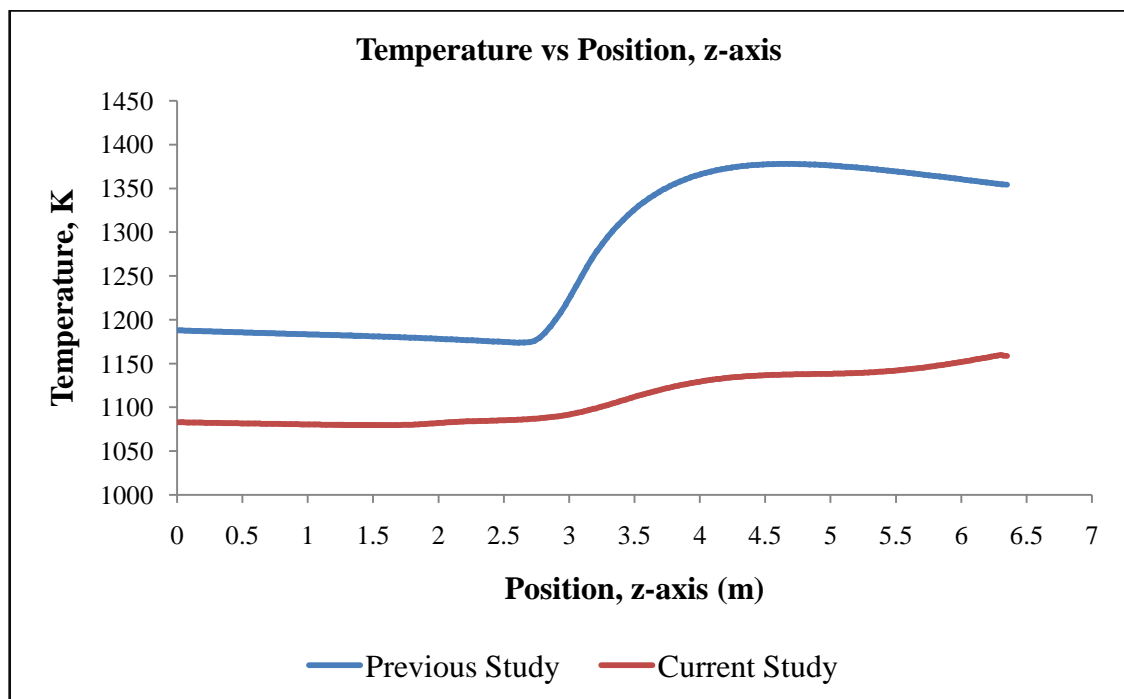


**Figure 4.2:** Graph temperature profile for previous study and current study

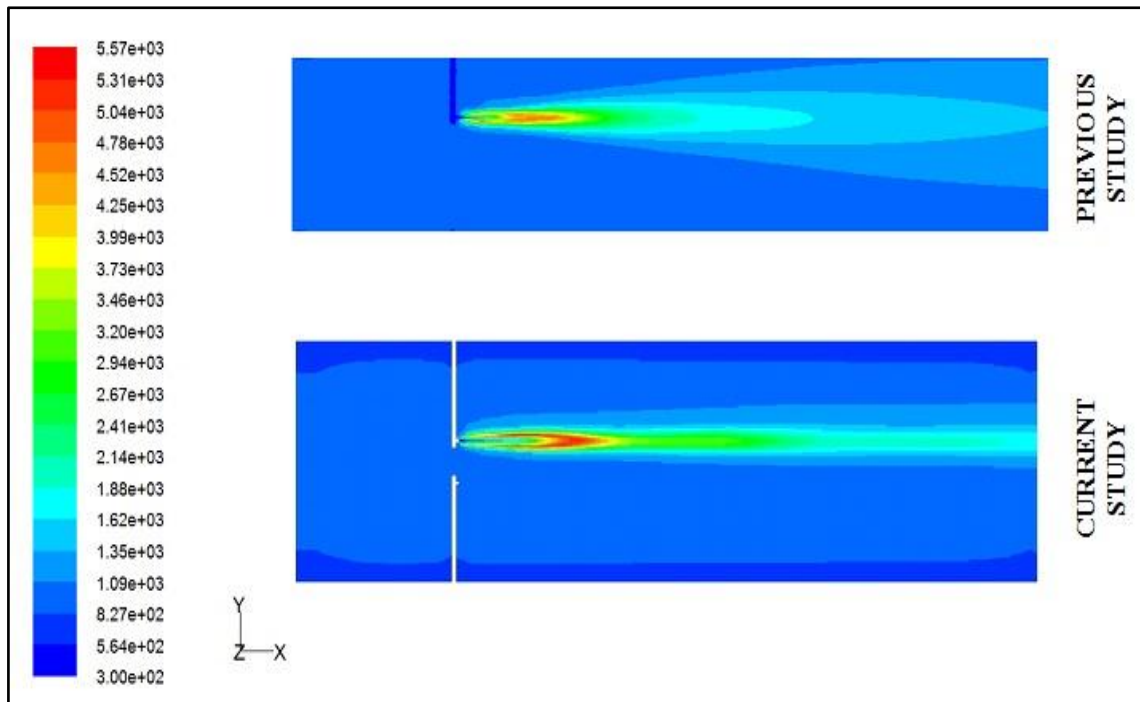


**Figure 4.3:** Temperature profile for previous study and current study for new process

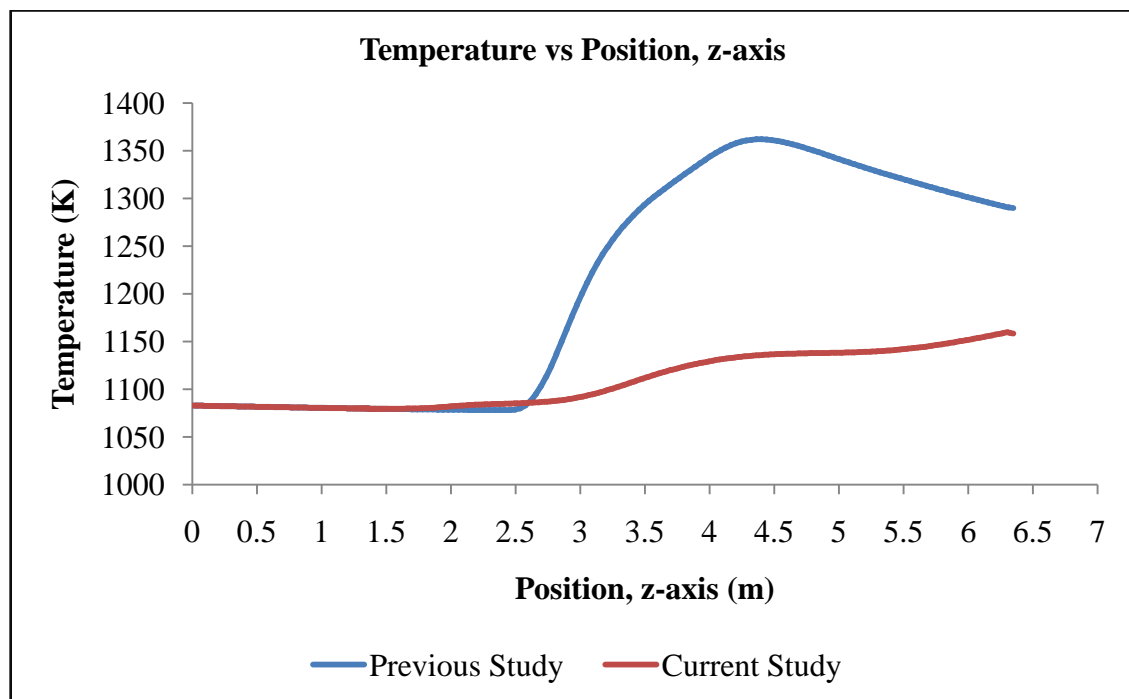


**Figure 4.4:** Graph temperature profile for previous study and current study

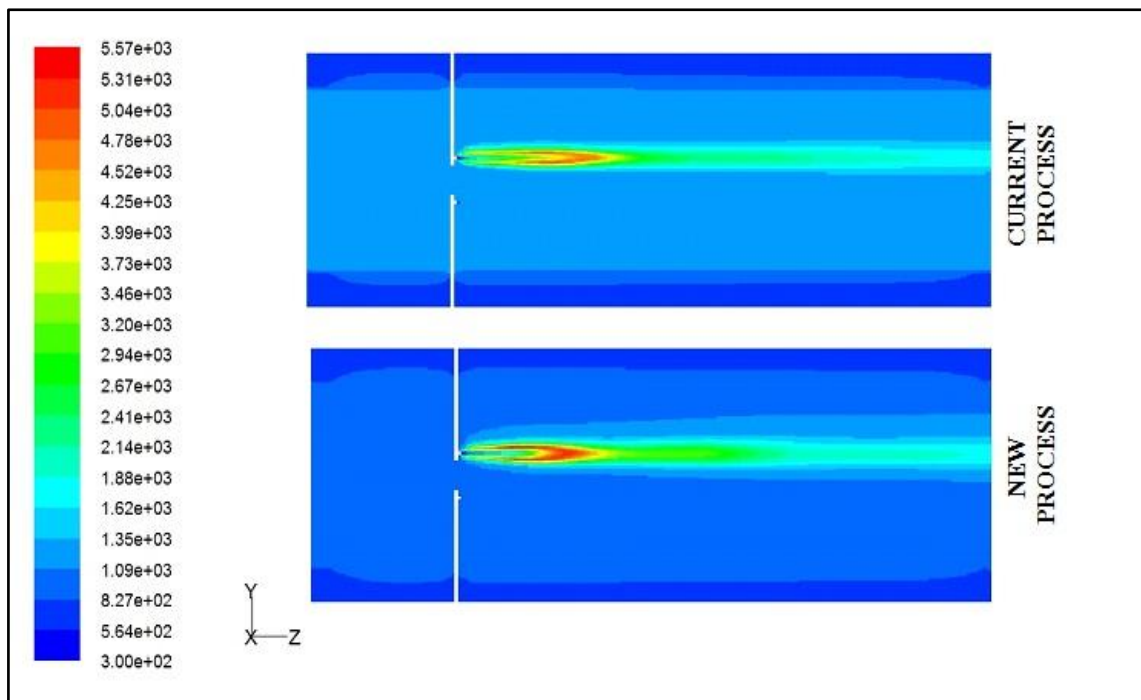


**Figure 4.5:** Temperature profile on both processes

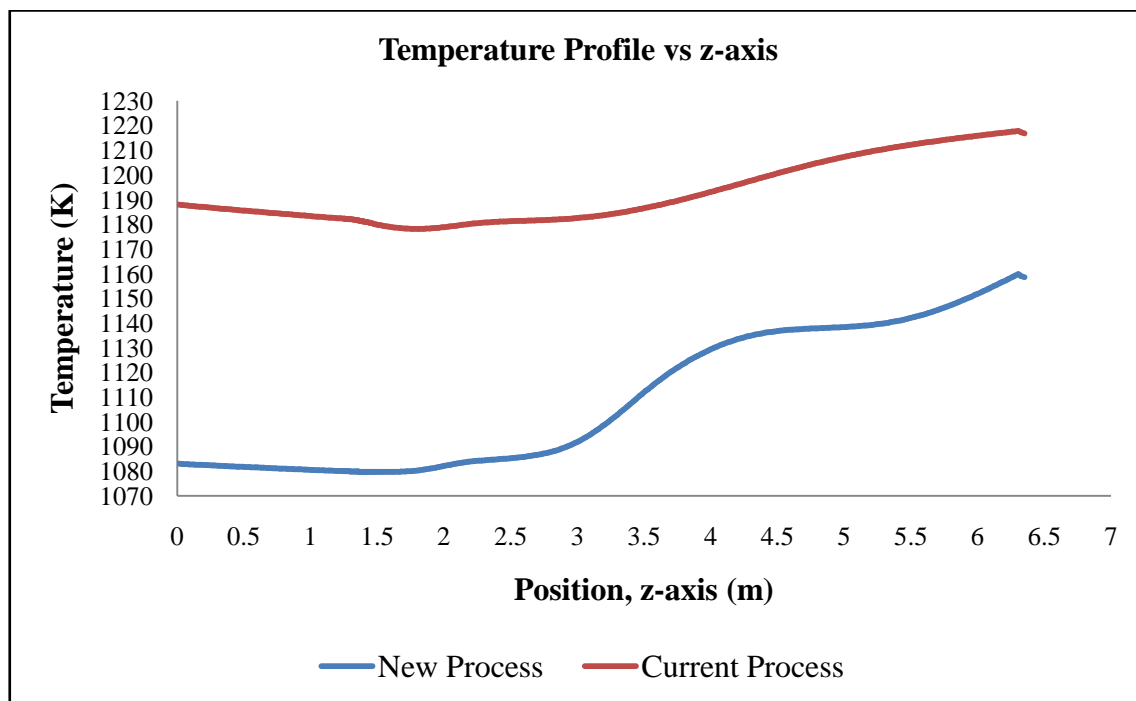


**Figure 4.6:** Temperature profile on both processes

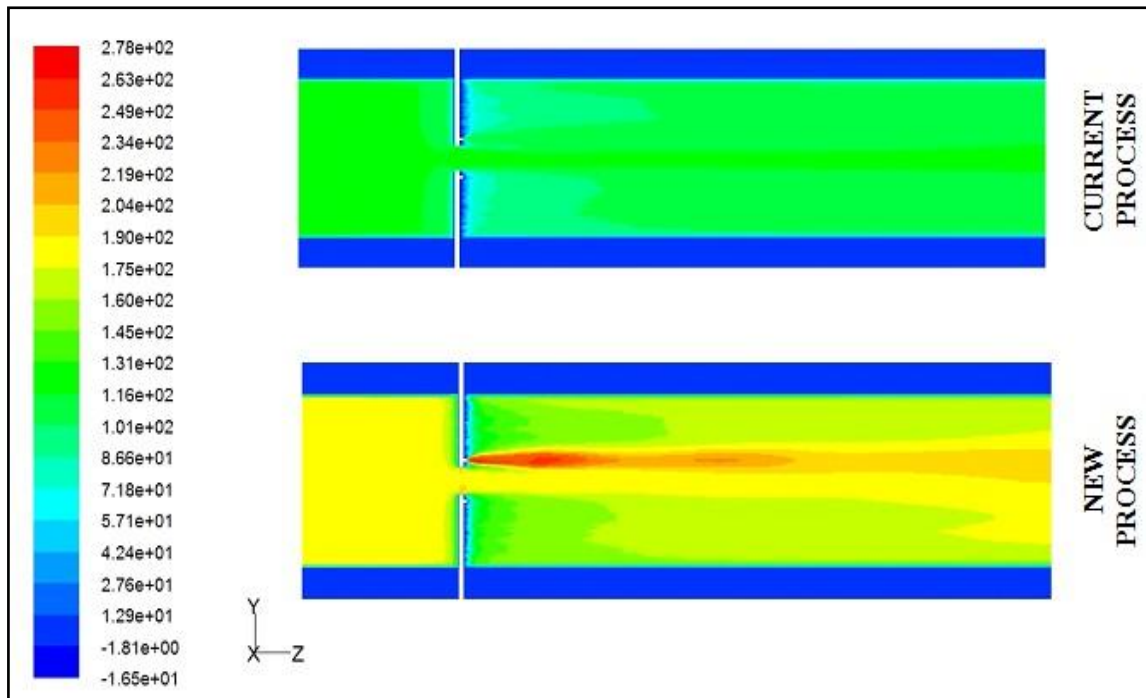


**Figure 4.7:** Z – axis velocity of fluid on both processes

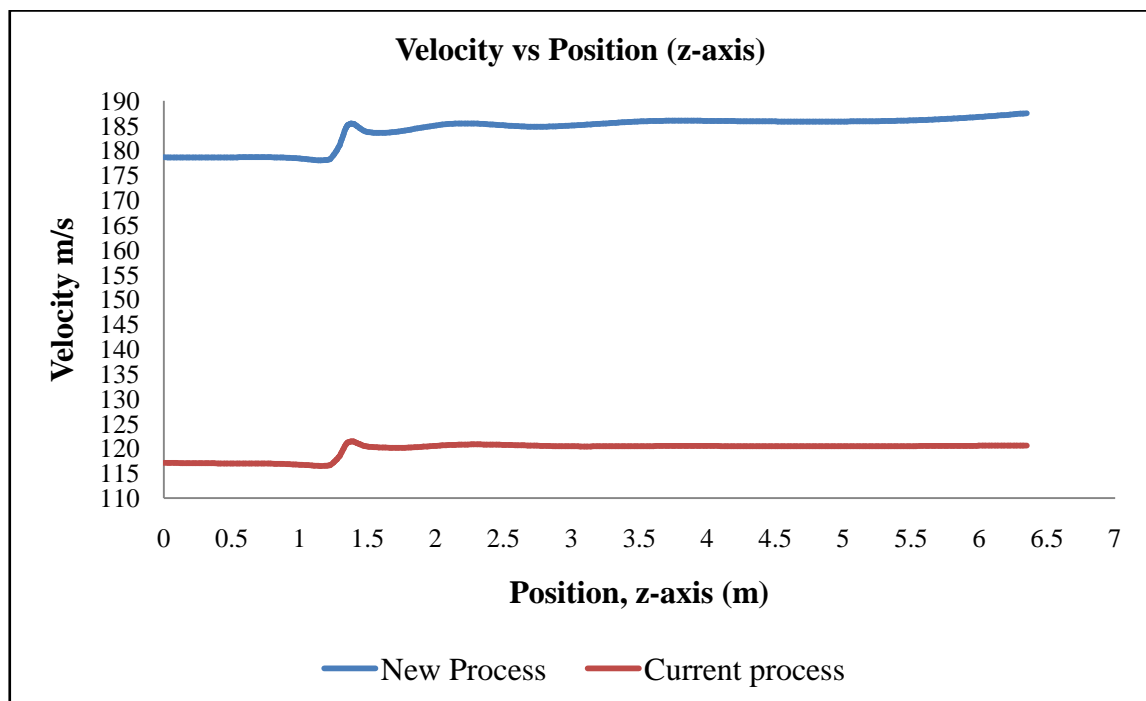


**Figure 4.8:** Graph of Z – axis velocity of fluid on both processes

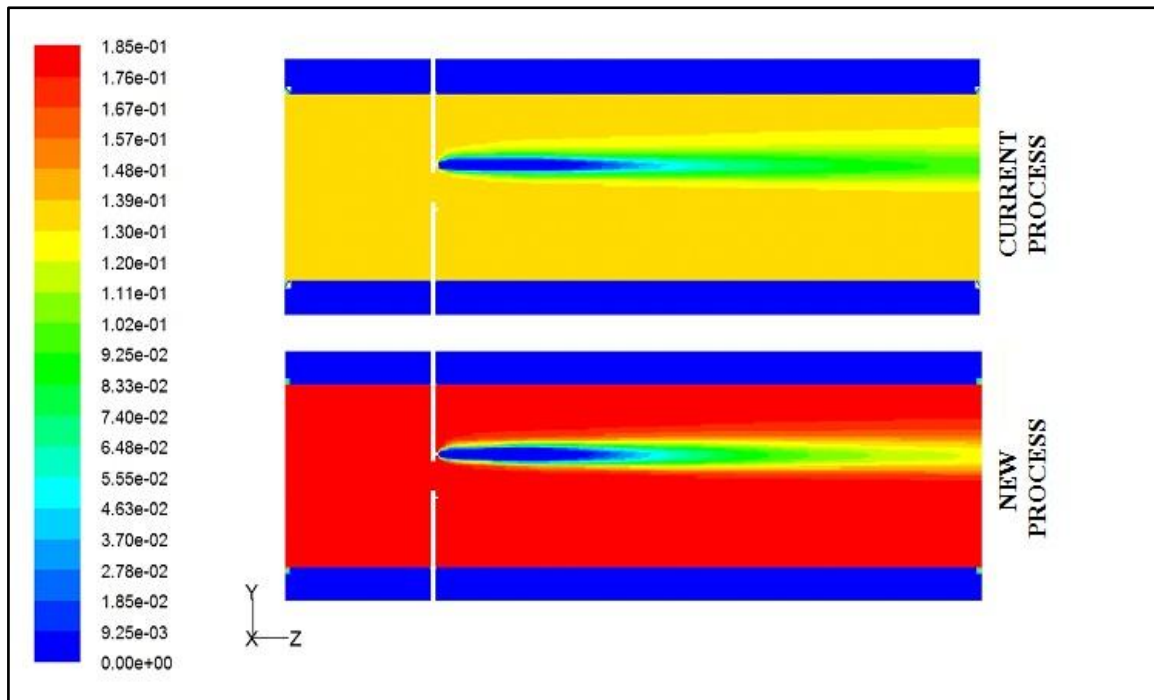


**Figure 4.9:** Mass fraction of  $\text{CH}_4$  on both processes

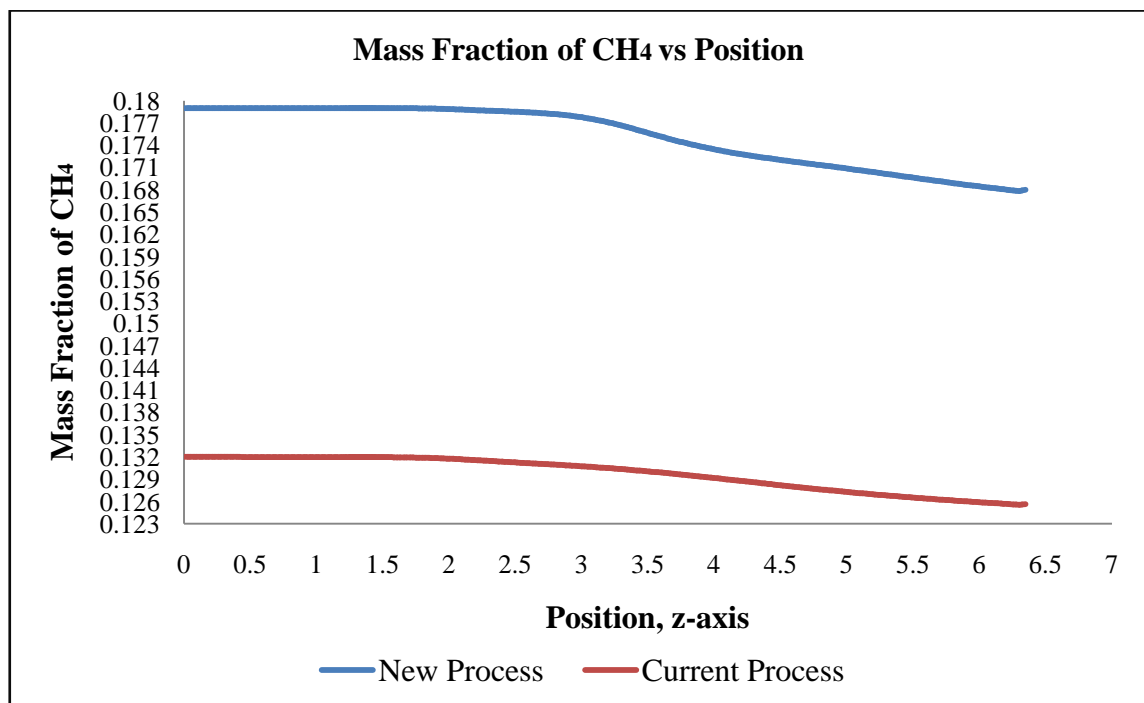


**Figure 4.10:** Mass fraction of  $\text{CH}_4$  on both processes

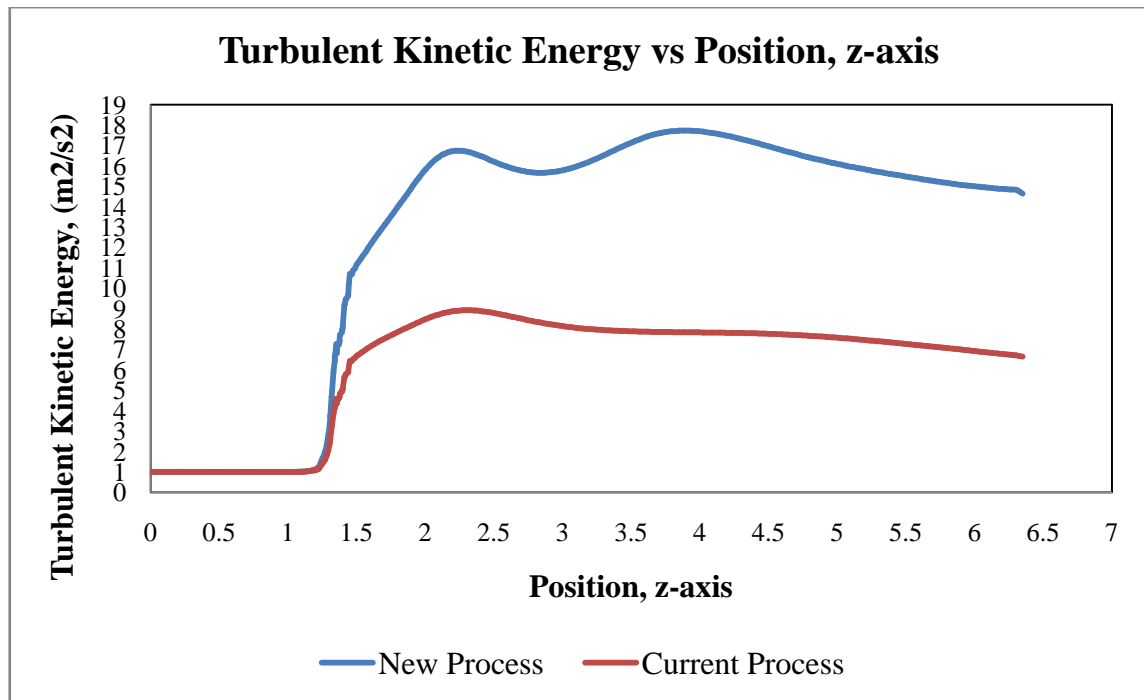


**Figure 4.11:** Graph of turbulent kinetic energy on both processes

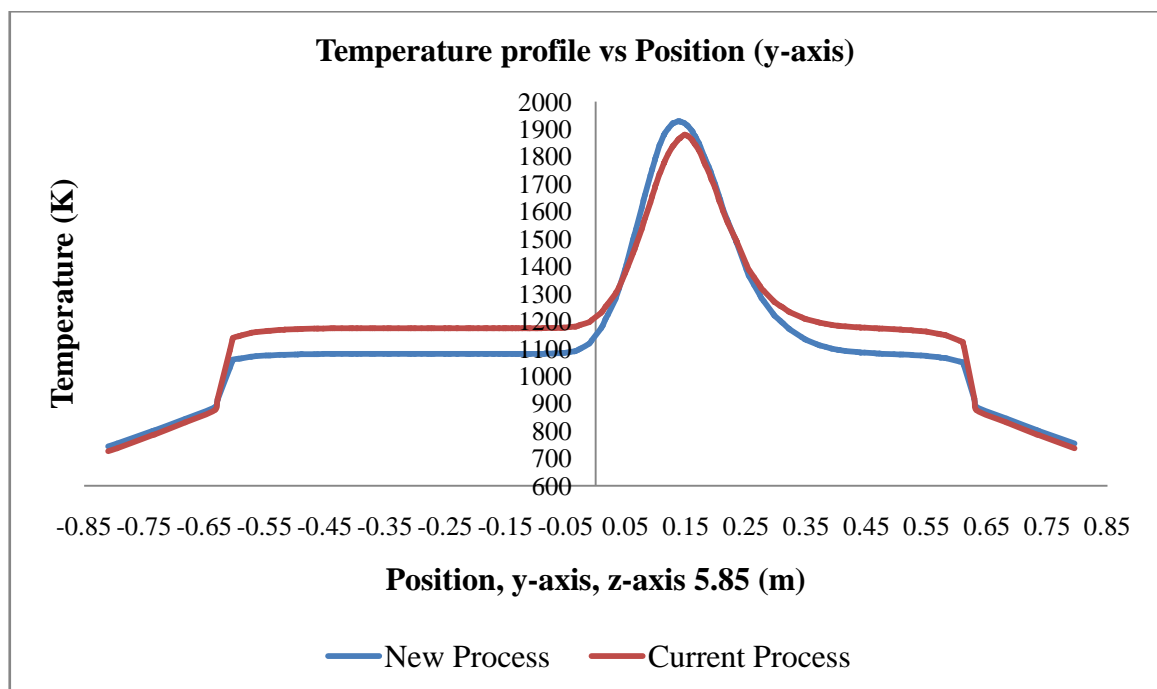


**Figure 4.12:** Graph of temperature comparison on thermocouple line

**Table 4.1:** Comparison of Temperature Reading

Items	Temperature (K/°C)	
	Current Process	New Process
	Scheme	Scheme
Real Plant	1293.00/1020.00	1318.00/1045.00
Excel	1289.00/1016.00	1387.00/1114.00
CFD (previous study)	1407.98/1134.98	1338.56/1065.56
CFD (current study)	1191.27/918.27	1108.12/835.12

## **CHAPTER 5**

### **CONCLUSION**

#### **5.1 CONCLUSION**

The performance of partial combustion unit in direct reduction plant was studied numerically using a CFD in purpose to make a validation with a real plant. In this studied, the improvement of design from previous studied is made by adding a boundary refractory with a same condition with an existing plant. Through this new design, the temperature obtain is assume to be more acceptable in purpose of validation since the design used is exactly same as the real plant. Besides, with the existent of boundary refractory, the temperature obtain is lower than without the refractory.

Unfortunately, the temperature at validation point has an error 7.85% for current process and 15.92% for the new process. Even though the temperature obtain in new process has a high percentage error, improvement can be done in term of volume meshing, temperature inlet of process gas and mass fraction of  $\text{CH}_4$  at initial. It is because,  $\text{CH}_4$  can favor carburization process but the process of  $\text{CH}_4$  itself is endothermic. Thus, the temperature drop may be occurring. Since the fraction of  $\text{CH}_4$  is higher in new process scheme, it may be influence the temperature obtains.

The temperature in new process increase highly as the  $\text{CH}_4$  is used up more in this scheme. It shown that, the product can be increased as the temperature of process gas is increasing. When the process gas temperature is increased, less energy consumed and thus gave better and costly efficient. From the turbulent kinetic graph it shown that the turbulent flow in new process scheme is higher compare to current scheme.



Nevertheless, the figure of validation point show that the temperature at an injection oxygen point which is the highest peak on the graph obtain a high temperature. For current process 1900K @ 1627°C and new process 1950K @ 1677°C. It can be prove that the temperature of process gas enter the reactor in high temperature for both process. From this figure also, it shown that the different temperature will be obtained in the different point in the system and the temperature in the transfer line is not same at all point. The amount of oxygen lance used also may be one of the factors. In this study, the lance used is only one out of two since the other lance is under the maintenance.

## **5.2 RECOMMENDATION**

Through out this study, the result obtain can be improve. For the improvement, there are many scopes for further research in order to improve the studied via CFD. The recommendation is divided and discuss according to the scope in this sub – chapter.

### **5.2.1 Volume meshing**

This simulation is run with less quality of meshing for the system model. It is because, the nodes for the transfer line with refractory is less compare to the without refractory. The nodes should be proportional to the volume of the design. Thus, it will affect the result since better quality of meshing will gave more accurate results. For higher volume meshing, the quality is higher thus, more time needed for the iteration to finish.

### **5.2.2 Design of the oxygen nozzle and lance**

From this study, it shows that the velocity of process gas and oxygen can influence the turbulent kinetic energy, the percentage of temperature increase and the amount of CH<sub>4</sub> used up. Thus, further research toward the design of oxygen nozzle for effective injection can be done. The improvement of lance and nozzle may consume in increasing the velocity of oxygen. Besides that, the position of oxygen injection point

should be studied in order to identify the most suitable point for the injection to be set in the fluent.

### **5.2.3 Oxygen lance injection position**

It is believe that the injection position of oxygen will influence the temperature profile along the transfer line. Thus, further study regarding the most effective injection position of oxygen should be studied.

### **5.2.4 Boundary refractory**

The boundary refractory used is high duty brick. Nevertheless, the temperature release by the boundary refractory can be considered high. Thus, there will be some addition on the boundary refractory can be done. Besides that, the accurate surrounding temperature is needed so the data temperature of boundary refractory that had been set in the fluent should be same as the real plants.

### **5.2.5 Validation point**

Since the temperature in the PCU is not same at every point, thus, further analysis toward the position to determine the most effective point should be done. It also to ensure the most suitable position of the temperature detected on the system. Besides, the validation at only one point may not be so accurate. Thus, the variation position of thermocouple for validation should be done.

### **5.2.6 Option for simulation**

The type of solver is focusing in this study is steady state solver. By referring to the graph presenting in chapter 3, the temperature of the fluid flow inside the transfer line is at steady flow. Thus, to gain more accurate results, this study should be done in unsteady state where it is a dynamics simulation with the integrated of time.

## REFERENCES

Ansys, Fluent 1.21, Ansys Inc.

Armando.G.M, Armando.B.B.J, Christian.V.C, Rangel-Hernandez.V.H (2010). Analysis of the Conjugate Heat Transfer in a Multi-Layer Wall Including an Air Layer. *Journal of Applied Thermal Engineering*, 30: 599-604

Armando.B.B.J, Armando.G.M, Riesco Ávila J.M, Christian.V.C, Zaleta Aguilar A (2007). Analysis of the conjugate heat transfer in a multi-layer wall: industrial application. *Proceedings of the XIII International Annual Congress of the SOMIM*. México, September 2007, Durango, Dgo.

Balikoglu.F, Akkurt.S (2009). Isothermal Corrosion Testing of Frit Furnace Refractories *Ceramics International*. 35: 3411–3419

Carty.A Furnaces (2007), Steels-Irons, Heat Treatments, Metals.

Cheely R., 'Gasification and The Midrex Direct Reduction Process', Midrex Direct Reduction Corporation, (1999)

Chatterjee, Amit (1995). Recent Developments in Iron making and Steelmaking. *Iron and Steelmaking*. 22:2, 100-104

Chunbao (Charles), Da-qiang.C (2010). A Brief Overview of Low CO<sub>2</sub> Emission Technologies for Iron and Steel Making. *Journal of Iron and Steel Research, International*, 17(3): 01-07

Duarte.PE, *Energiron Direct Reduction Technology – Economical, Flexible, Environmentally Friendly*, Tenova HYL, (2008).

Fluent 6.3, 'Getting Started Guide', User Manual, Fluent Inc.,(2006)

Gas Malaysia Berhad, '*Chemical Safety Data Sheet*', Natural Gas, Revision 3 (2007)

Gupta.R, Fletcher.D.F , Haynes.B.S. (2010). CFD modeling off low and heat transfer in the Taylor flow regime. *Journal of Chemical Engineering Science*, 65: 2094-2107  
 Maeda.M, Nakamura.K, Tsuge.A (1989). Scale Effect of the testing furnace on the oxidation of the silicon nitride ceramics. *Journal of Materials Science Letters* 8: 195-197.

Joardar, A. 2009, *Iron Making in Mini Blast Furnace (MBF)*, Blast Furnace, Iron and Steel, MBF, Mini Blast Furnace.

Komarov, S.V and Kasai, E. 2004, *Simulation of sintering or iron bed with variable porosity*. Slide. Melbourne: Institute of Multidisciplinary Research for Advanced Materials, Tohoku University

López, G.G and Noriega, E. *Intech Hot Iron, Iron Reduction Technology Keeps Plant Shutdown Safe, Trip Free*.

*Metallon Holding Limited*, Mishra Ispat Private Limited.

Morales R.G., '*Flexibility in Using Iron Ores For Direct Reduction*', HYLSA Technology Division, Metal Bulletin 2<sup>nd</sup>, (2000)

Morales R.D., Conejo A.N., Rodriguez H.H., '*Process Dynamics of Electric Arc Furnace during Direct Reduced Iron Melting*', Matallurgical and Materials Transactions B, (2002)

Morris A.E., '*Computer Modeling and Analysis of Processes for the Production and Use of DRI*', Thermart Software, San Diego California, USA, (1999)

Perwaja Steel Sdn. Bhd., '*Partial Combustion Operation and Maintenance Manual*', Perwaja Steel HYL III Plant.

- Quintero R., '*HYL III: Status and Trends*', HYL Technology Division, (1995)
- Raúl Quintero, HYL Technology Division, Hylsa, S.A. de C.V. (1995). HYL III: Status and Trend. *Gorham/Intertech Conference on Iron & Steel Scrap, Scrap Substitutes and Direct Steel Making*. Atlanta, Georgia March 21-23, 1995.
- Shawcross P. World DRI Output in 2003 Just Missed 50m Tonnes [NJ. Metal Bulletin. 2004-04-15(32).
- Stefanidis.G.D, Merci.B, Heynderickx.G.J, Marin.G.B, (2005), CFD simulations of steam cracking furnaces using detailed combustion mechanisms. *Computers and Chemical Engineering*, 30: 635-649
- Seung Jae Lee and Kyu Tae Kim (1997). The Seminar on the New Fuel Technology Toward the 21<sup>st</sup> Century, November 25 - 26, 1997, KAERI, Taejon, Korea. *The Influence of the Sintering Atmosphere on Properties of Refractory for UO<sub>2</sub> Sintering Furnace and Microstructure of UO<sub>2</sub> Pellets*, 305-353
- Tenova HYL and Danieli, *JSPL Selects Energiron for Four New DR Plants*, Tenova HYL Press Release.
- Zeng.S, Lan.Y, Huang.J, (2009). Mitigation paths for Chinese iron and steel industry to tackle global climate change. *International Journal of Greenhouse Gas Control*, 3:675-682

## APPENDICES A

### Contour of Simulated Results

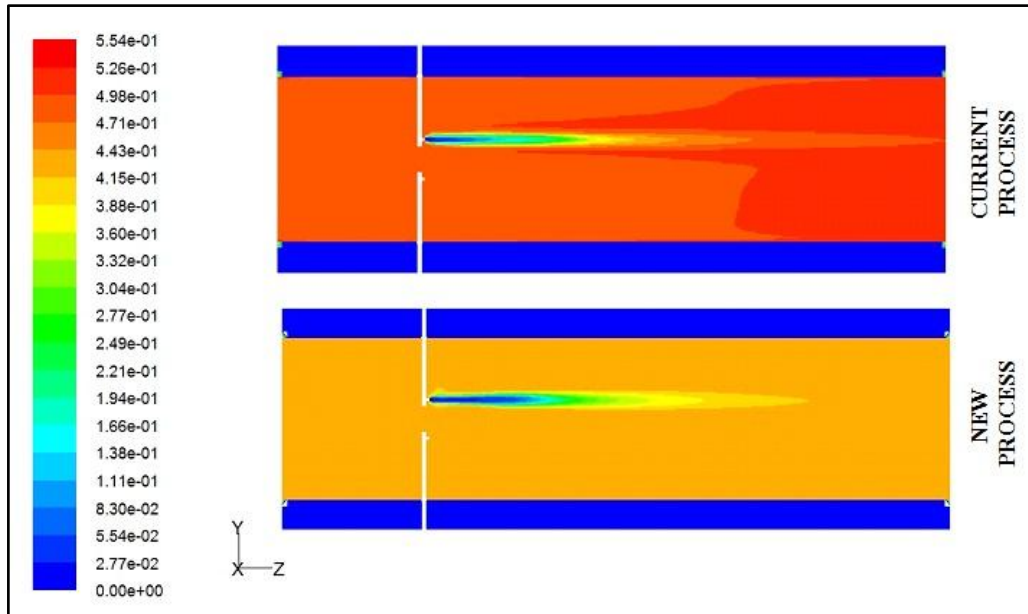


**Figure A1:** Contour mass fraction of CO on both processes

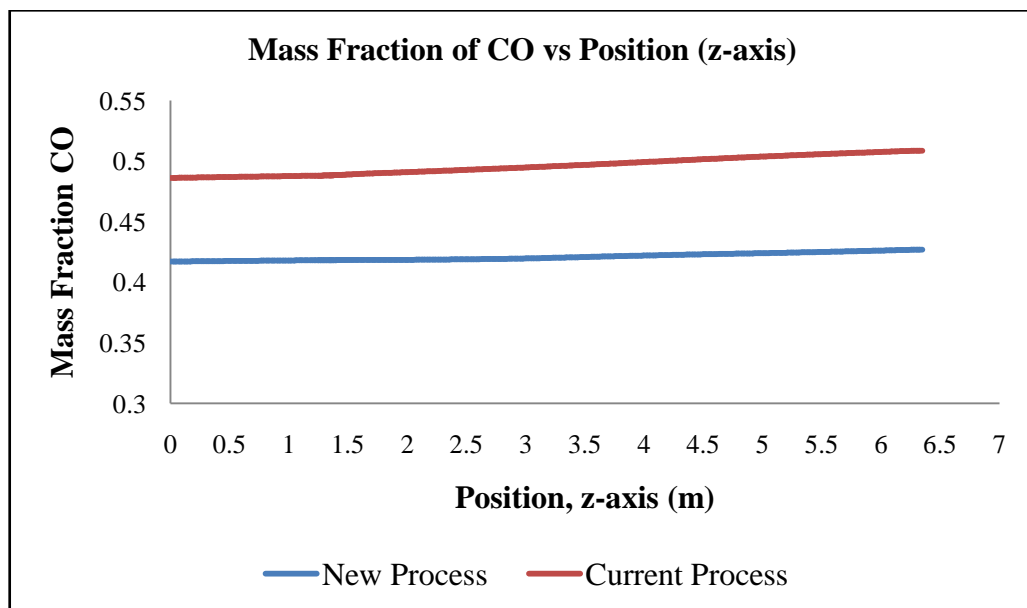


**Figure A2:** Graph of CO mass fraction for both processes

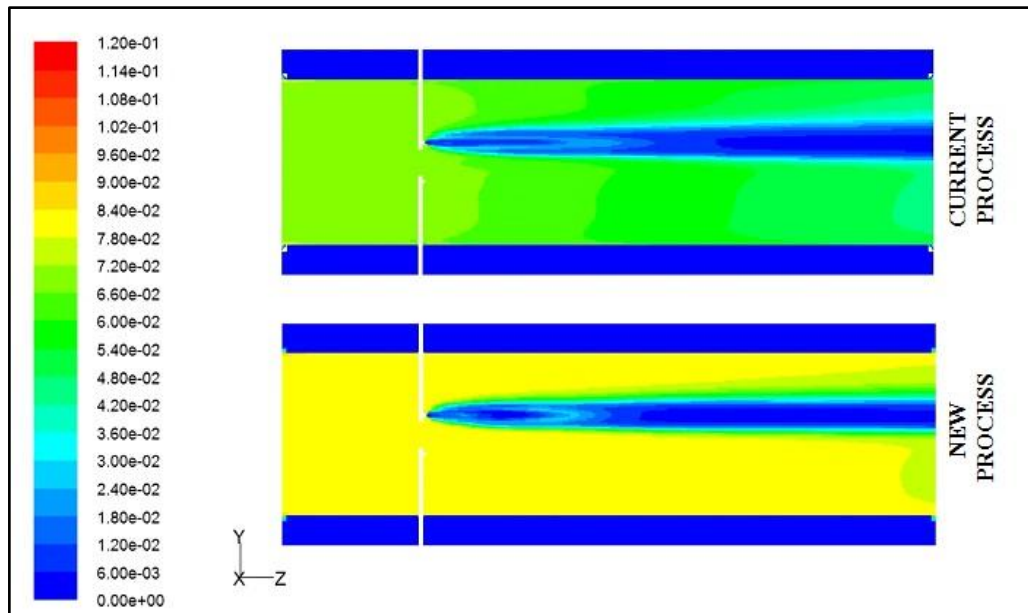


**Figure A3:** Contour mass fraction of CO<sub>2</sub> on both processes

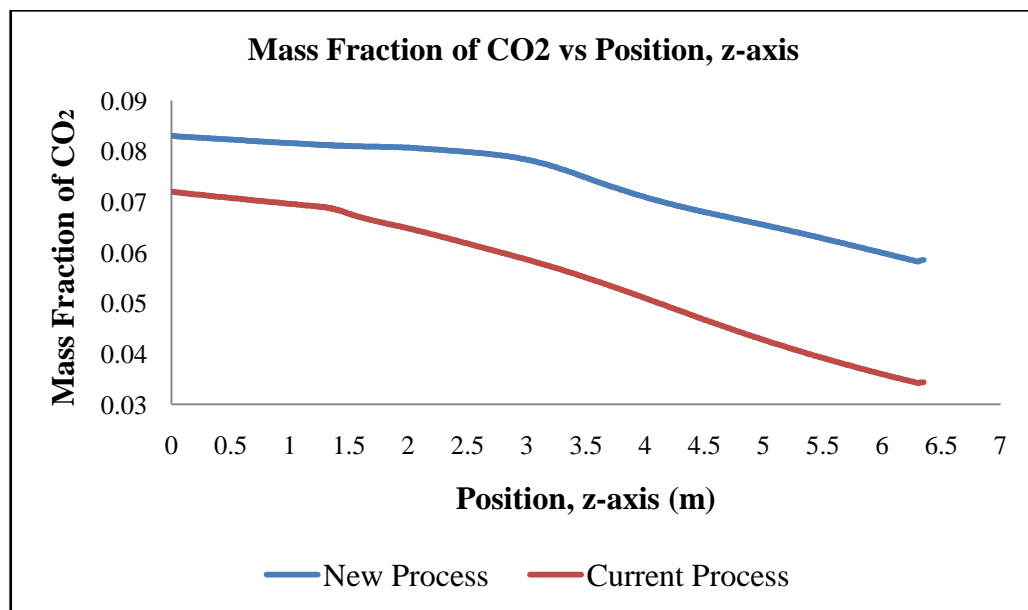


**Figure A4:** Graph of CO<sub>2</sub> mass fraction for both processes

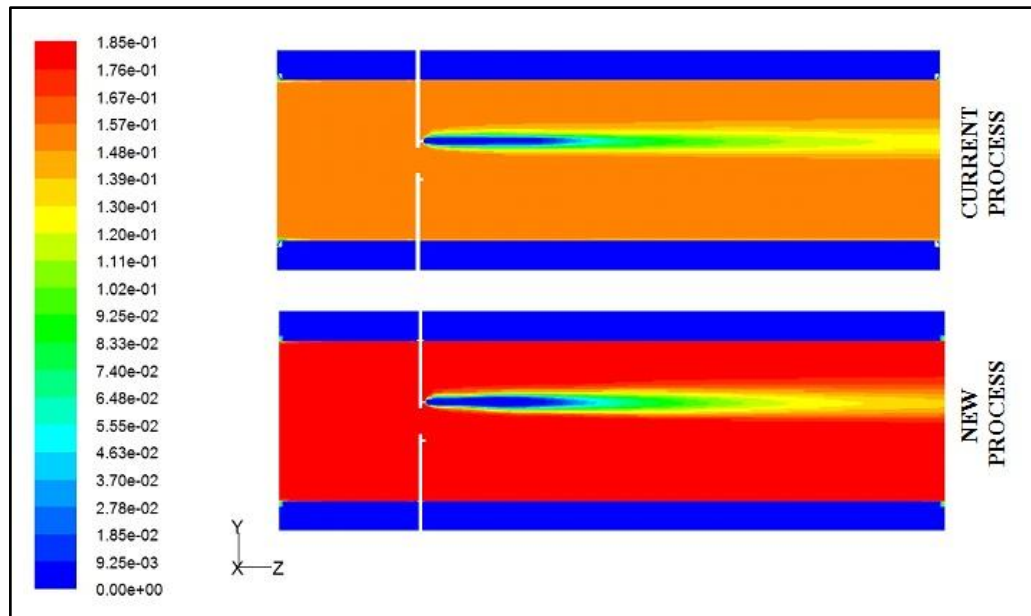


**Figure A5:** Contour of mass fraction of  $H_2$  on both processes

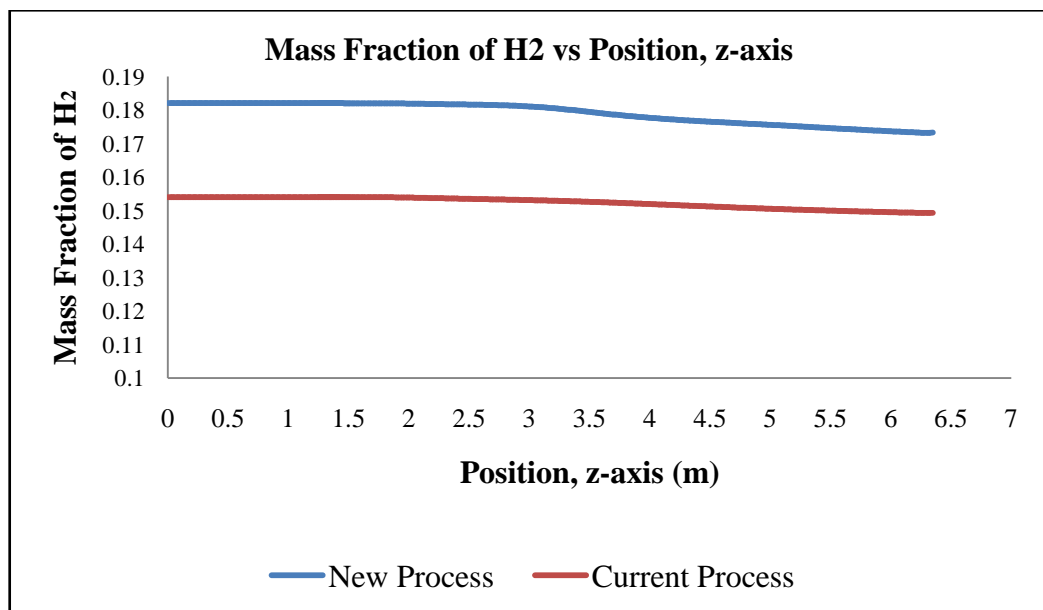


**Figure A6:** Graph of  $H_2$  mass fraction for both processes



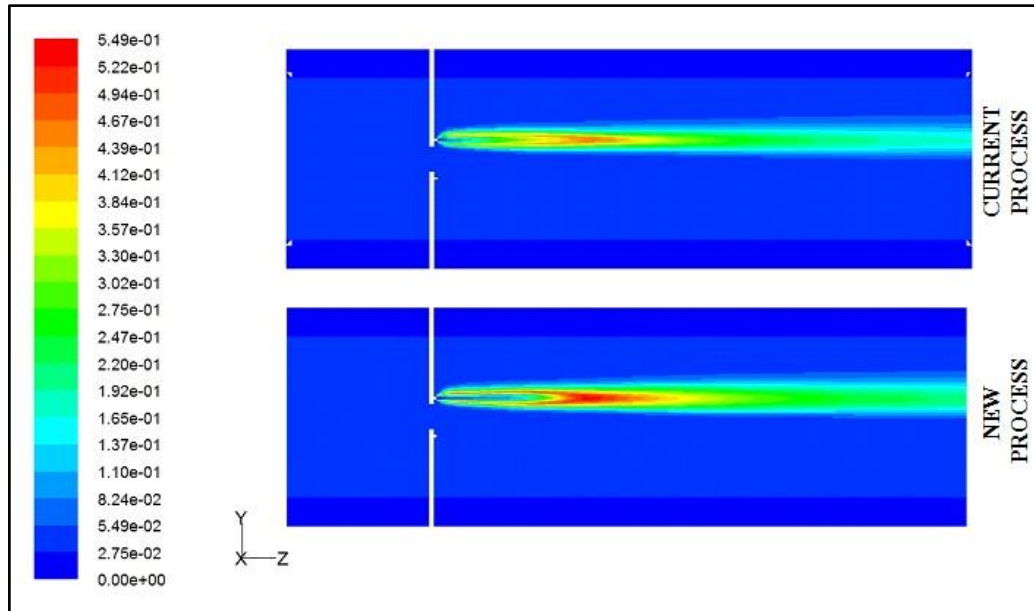


**Figure A7:** Contour of mass fraction of  $H_2O$  on both processes

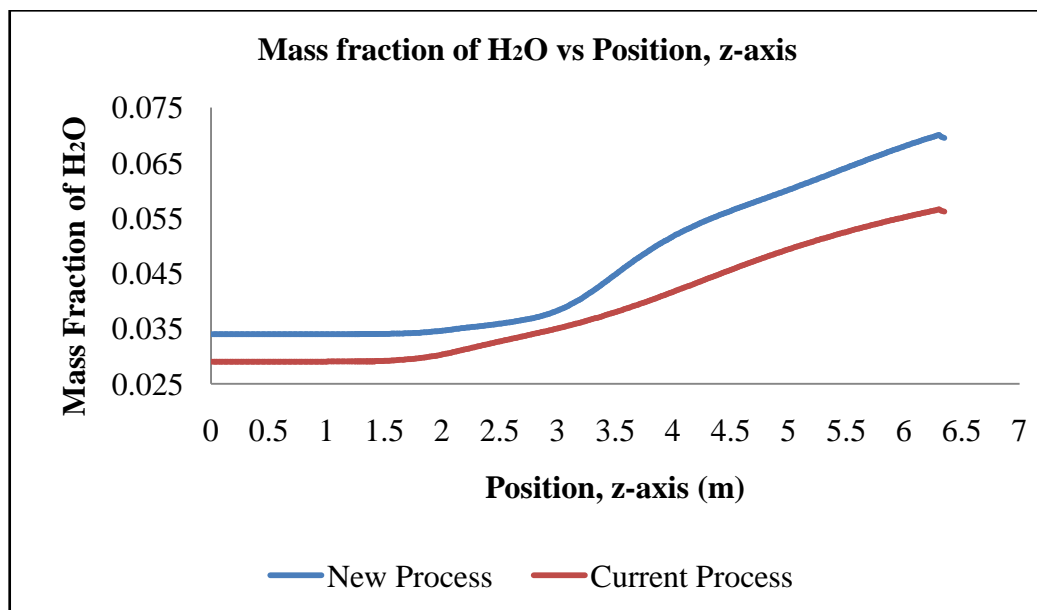


**Figure A8:** Graph of  $H_2O$  mass fraction for both processes

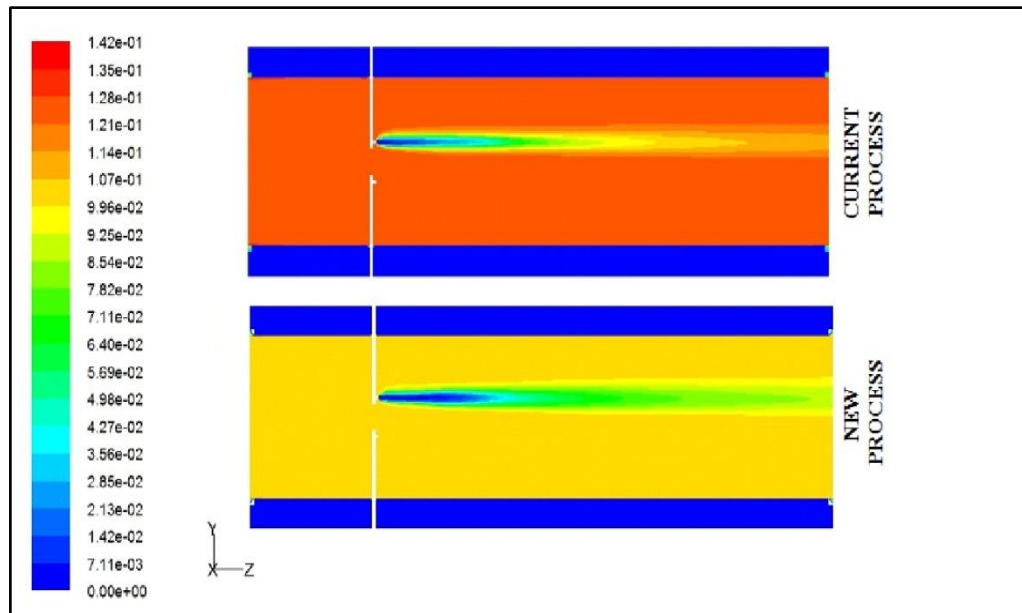


**Figure A9:** Contour of mass fraction of  $N_2$  on both processes

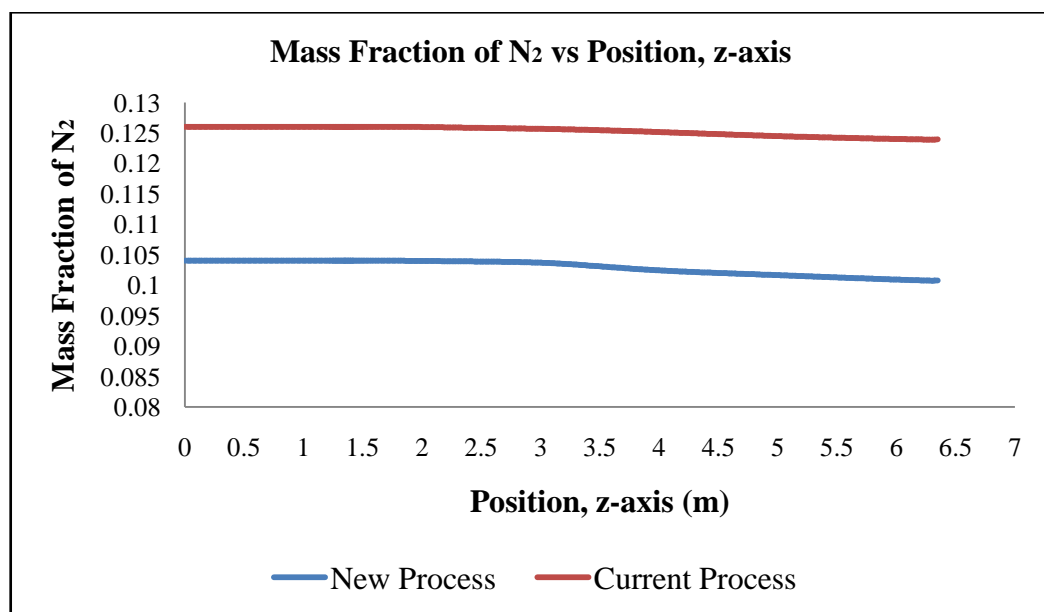


**Figure A10:** Graph of  $N_2$  mass fraction for both processes

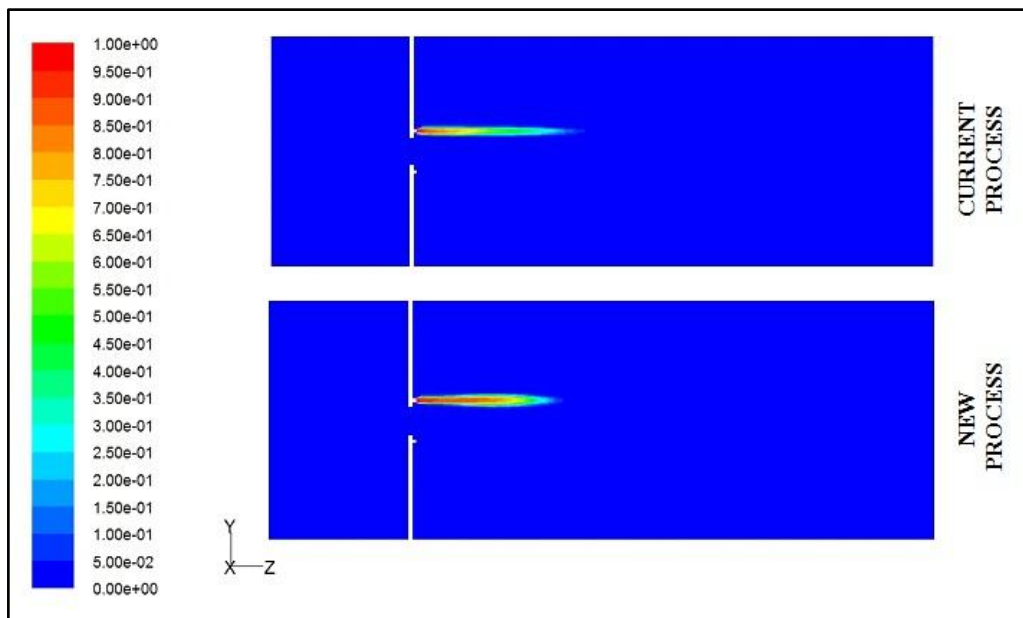


**Figure A11:** Contour of mass fraction of  $O_2$  on both processes

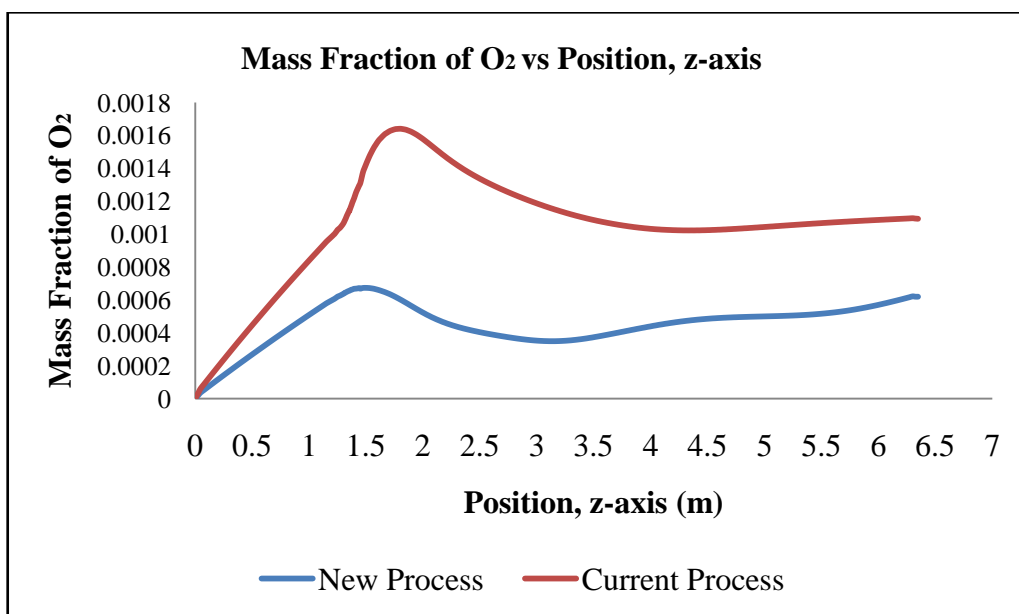


**Figure A12:** Graph of  $O_2$  mass fraction for both processes

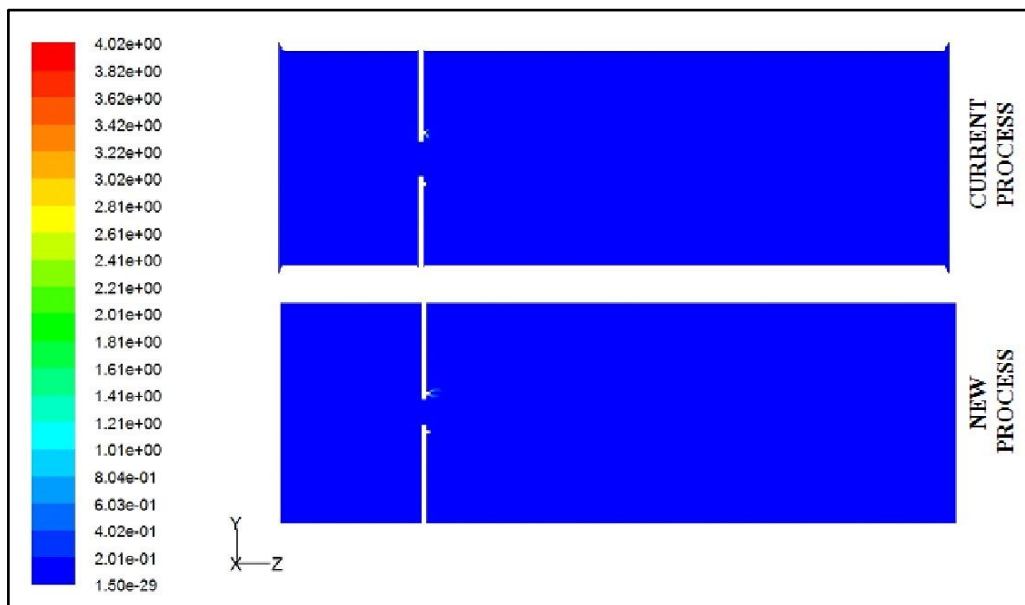


**Figure A13:** Contour for reaction equation (2.1)

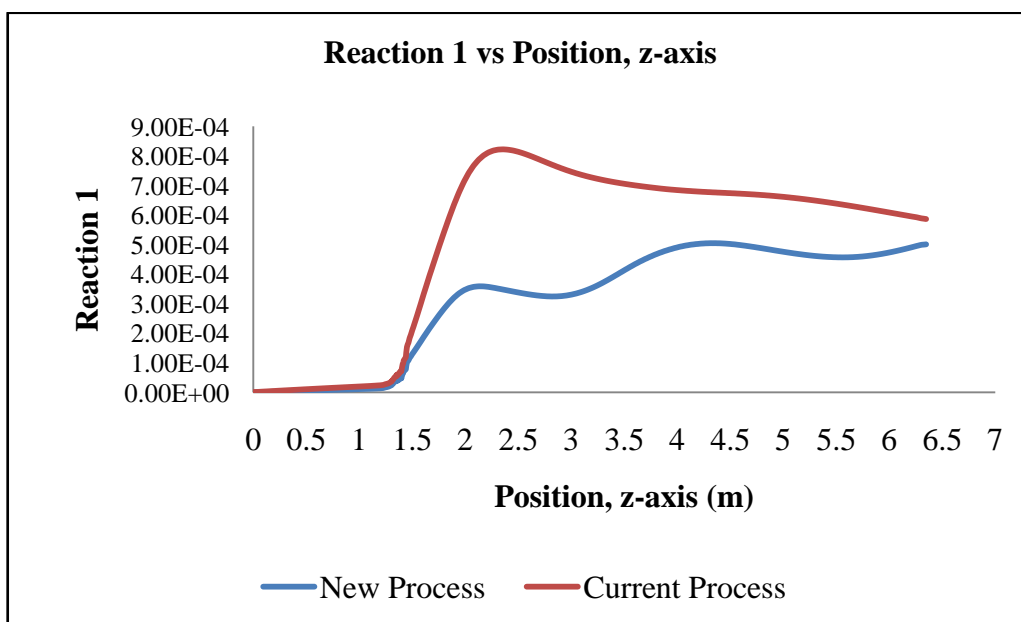


**Figure A14:** Graph for reaction equation (2.1)

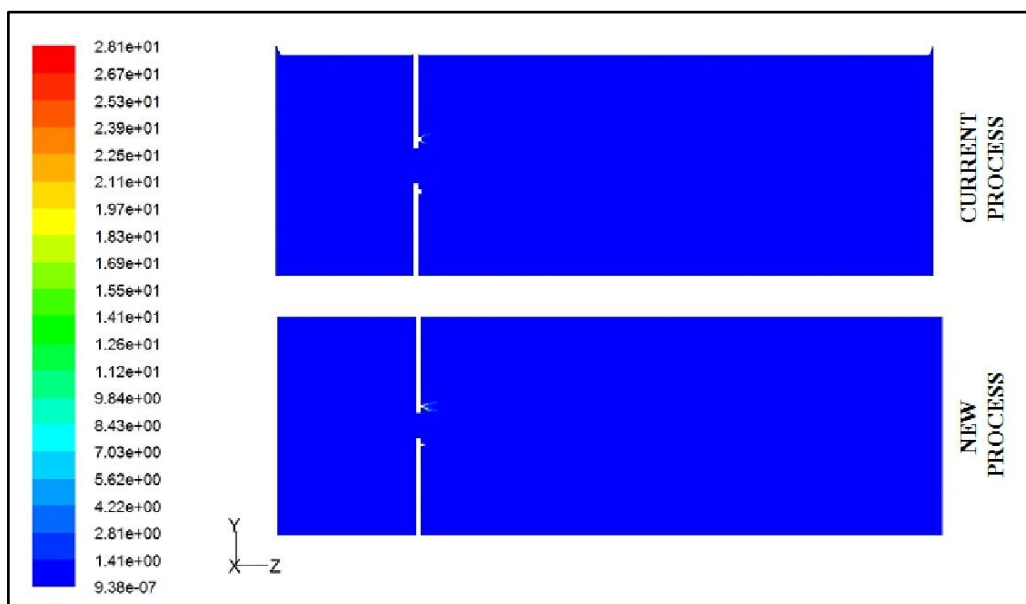


**Figure A15:** Contour for reaction equation (2.2)

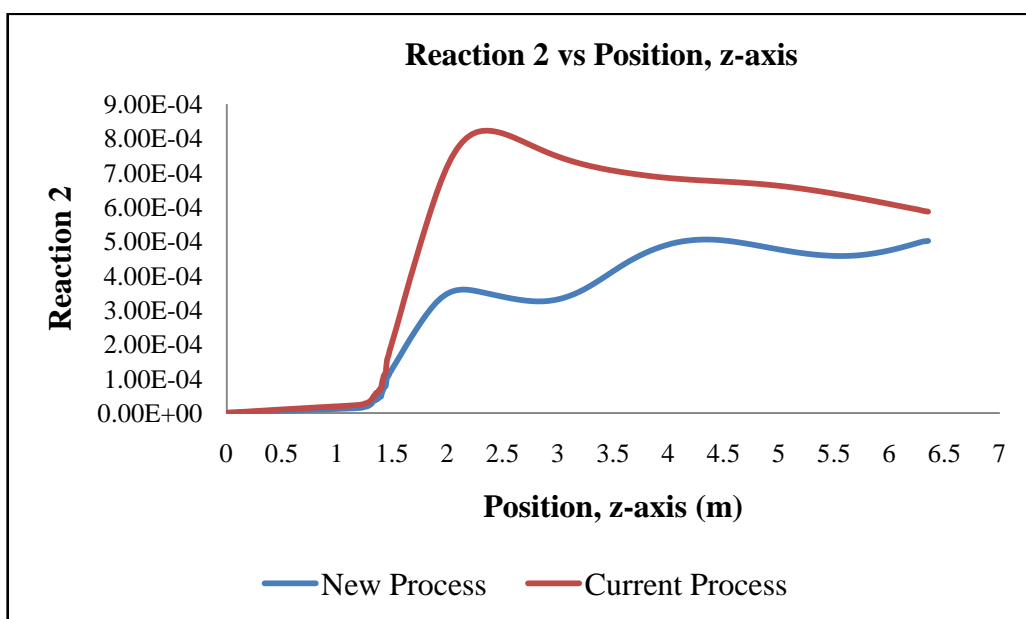


**Figure A16:** Graph for reaction equation (2.2)

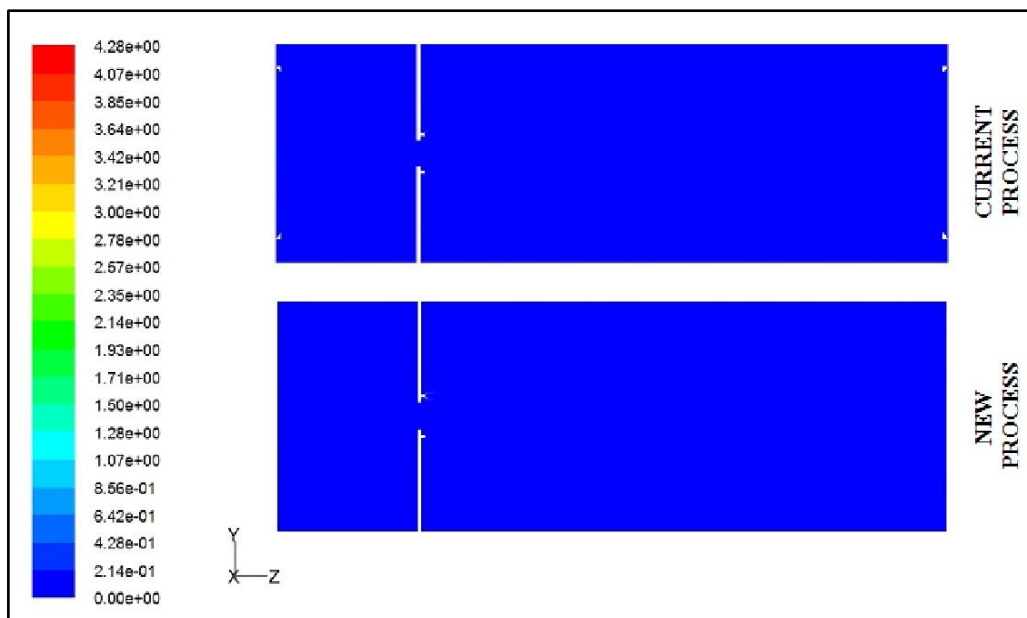


**Figure A17:** Contour for reaction equation (2.3)

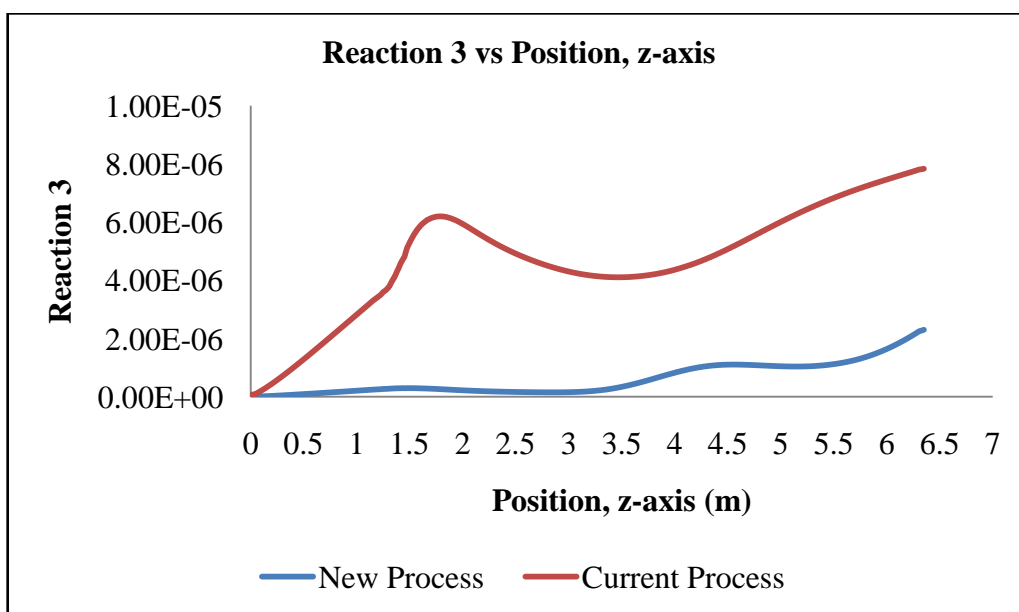


**Figure A18:** Graph for reaction equation (2.3)

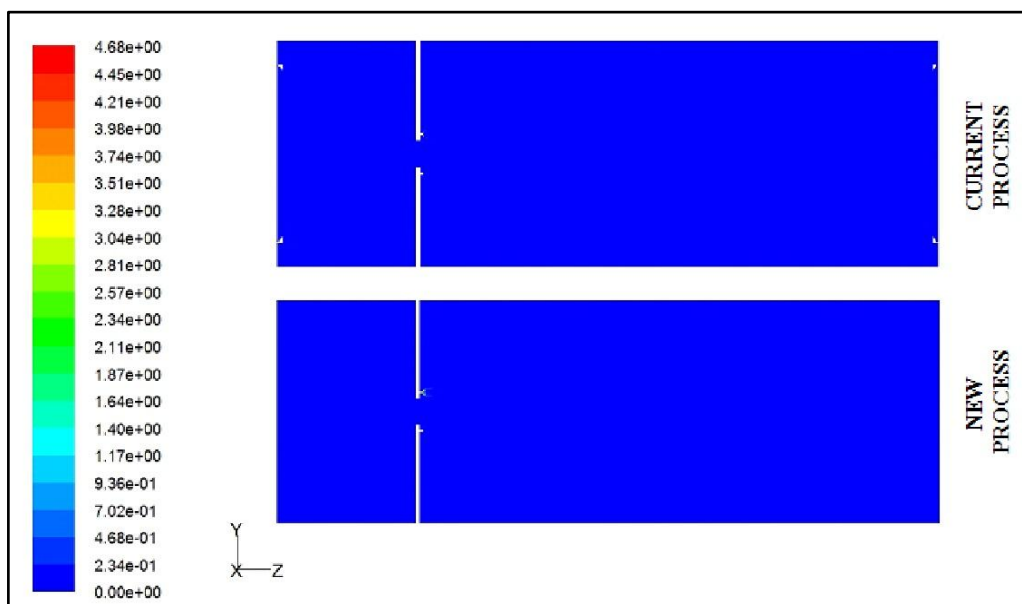
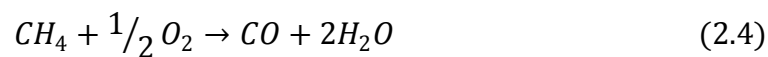


**Figure A19:** Contour for reaction equation (2.4)

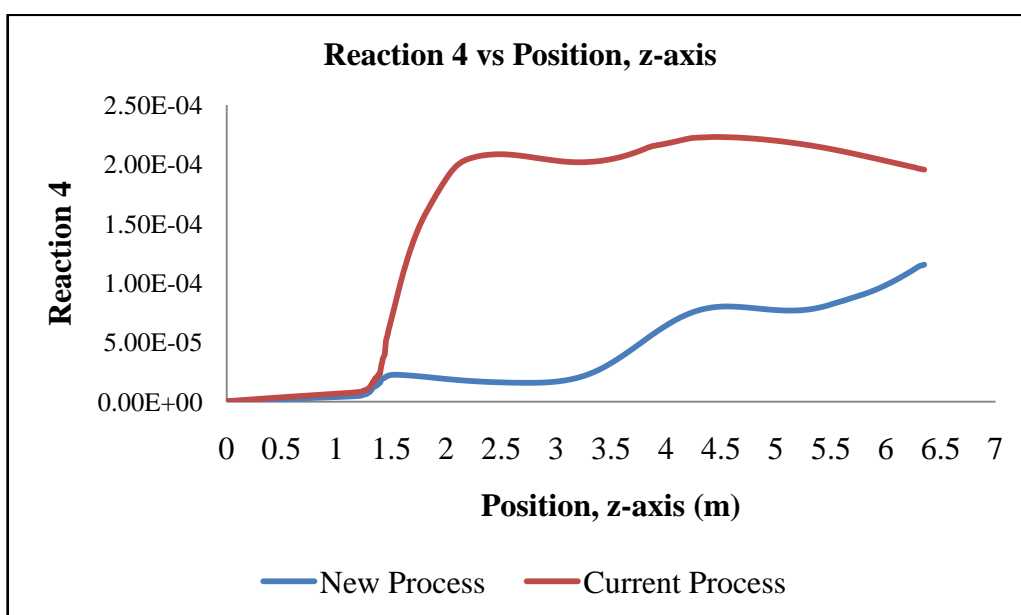


**Figure A20:** Graph for reaction equation (2.4)

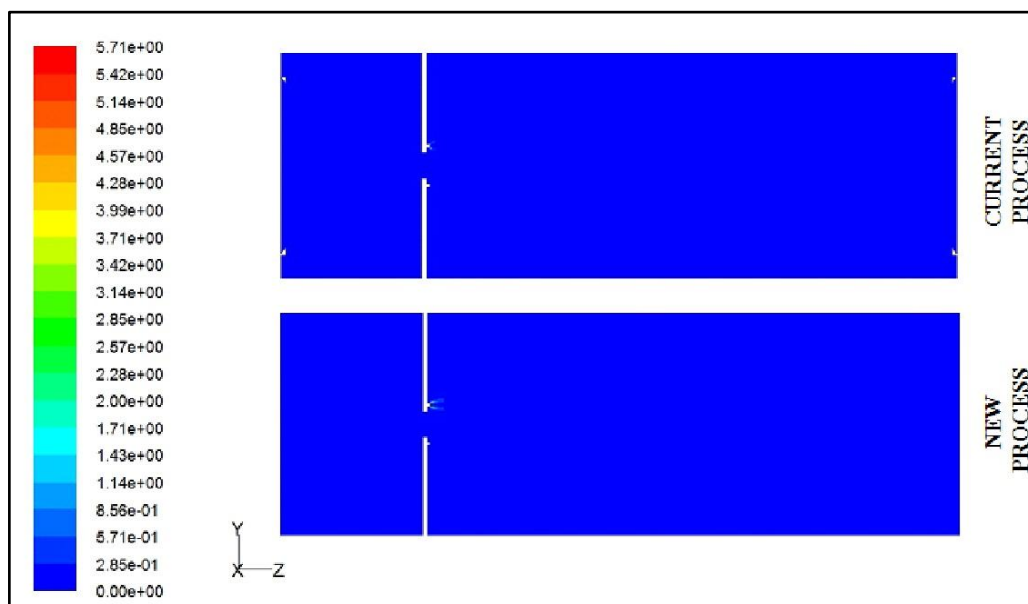


**Figure A21:** Contour for reaction equation (2.5)

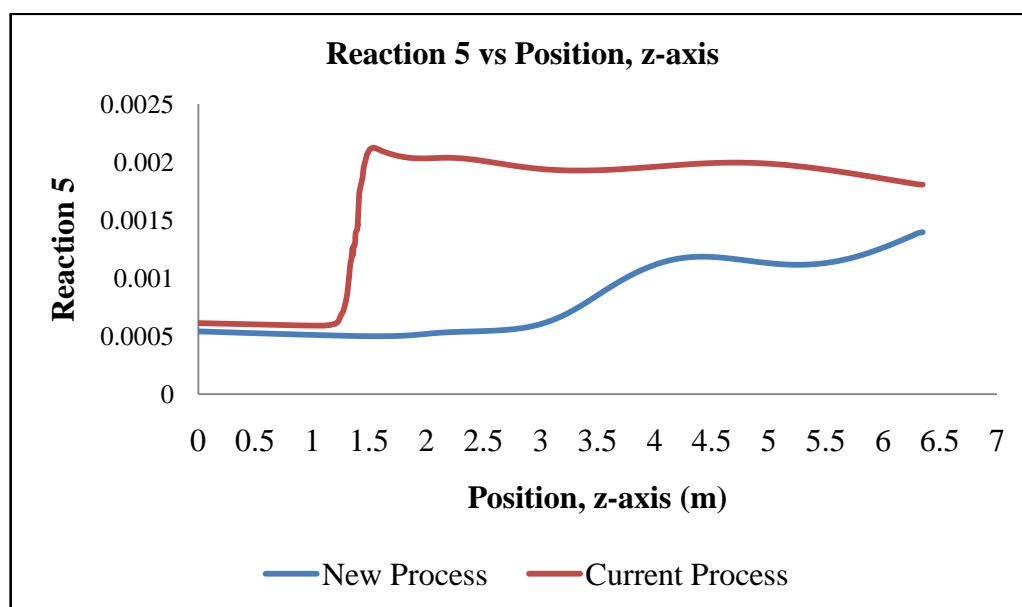


**Figure A.22:** Graph for reaction equation (2.5)



## APPENDICES B

### Supportive information for Simulation Study

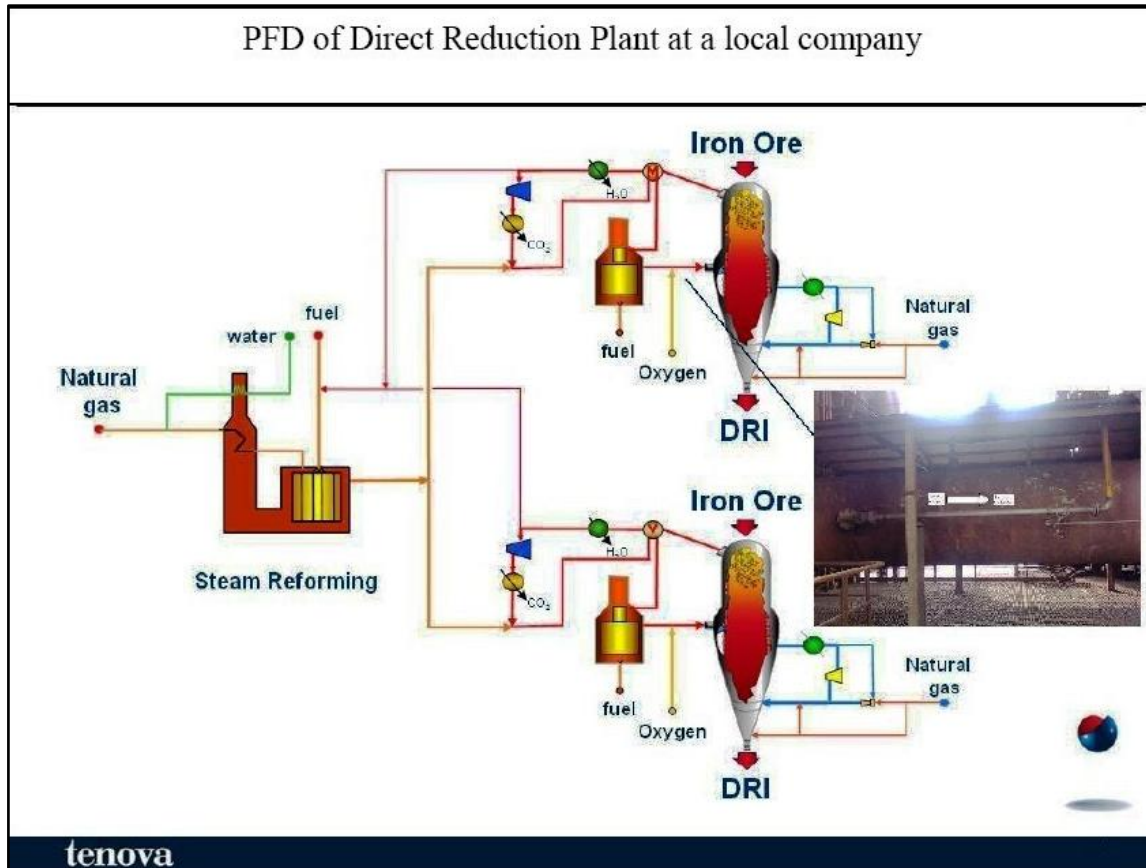


**Figure B1:** Process plant flow diagram

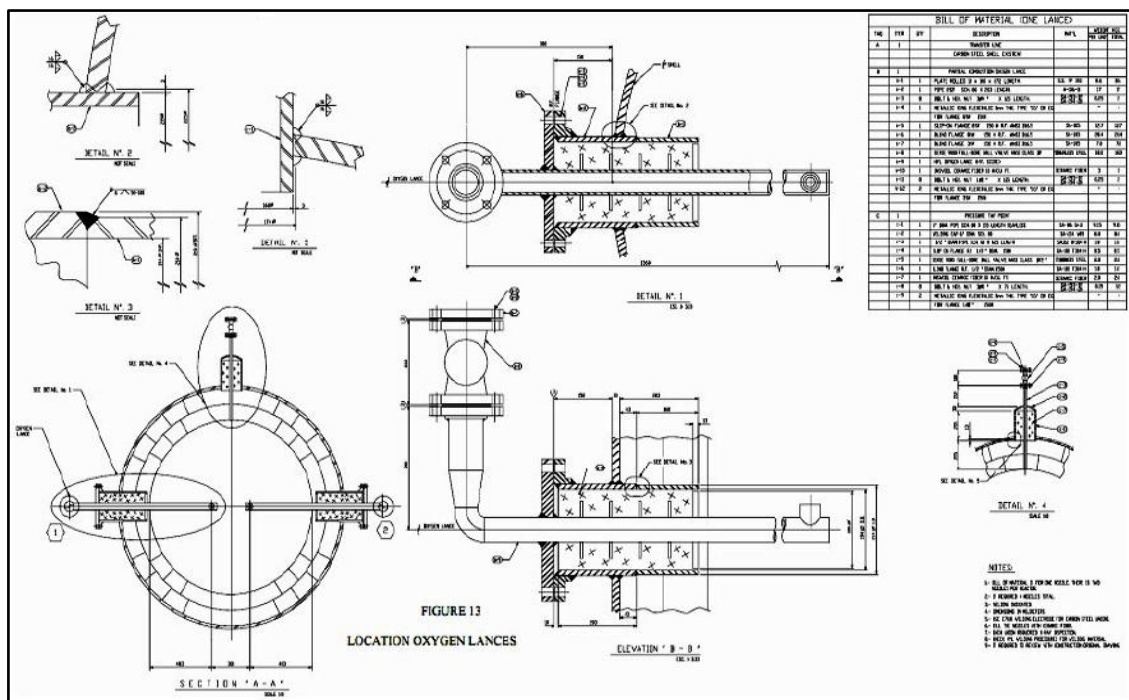


Figure B2: Details drawing on the transfer line

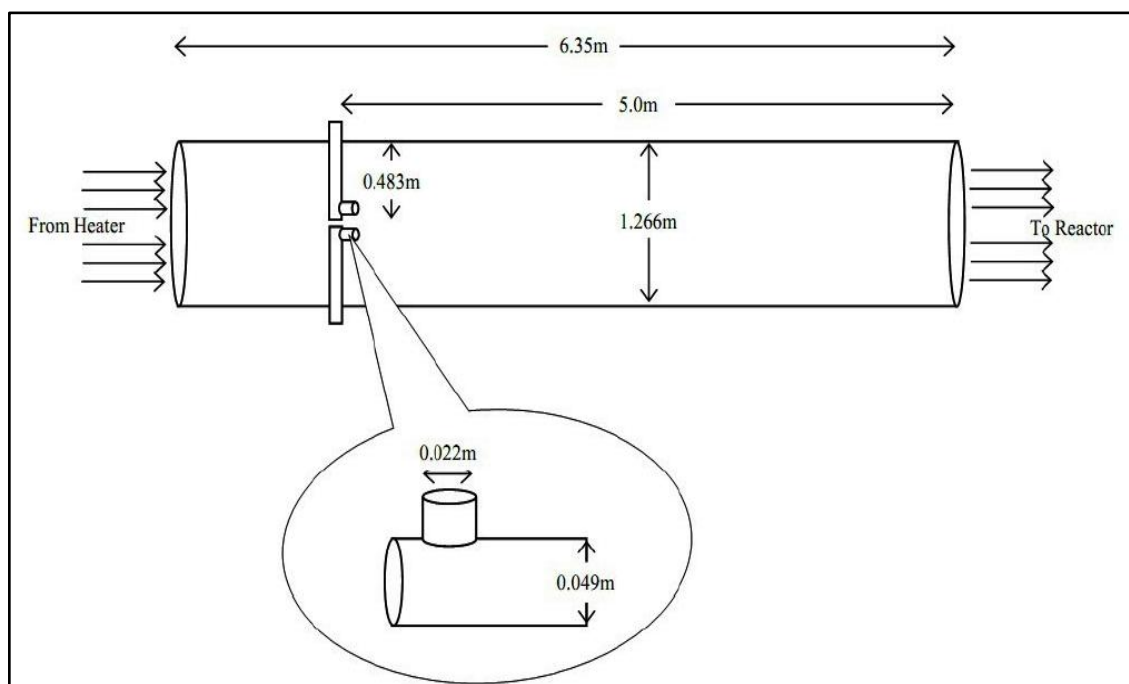
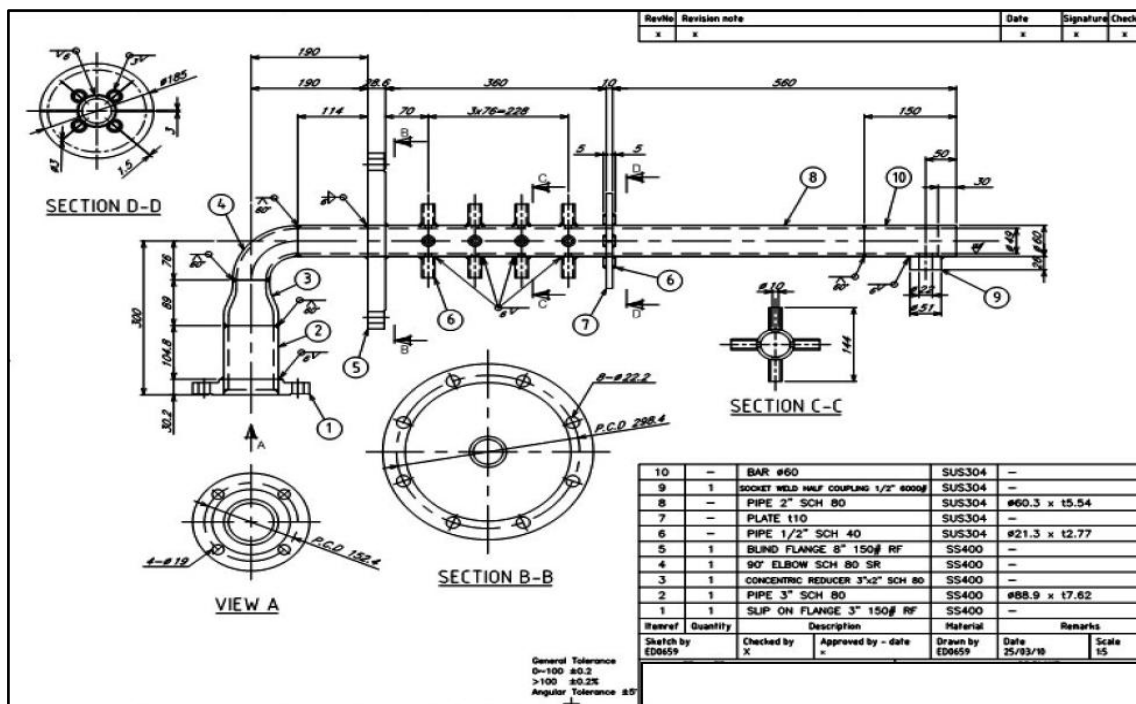
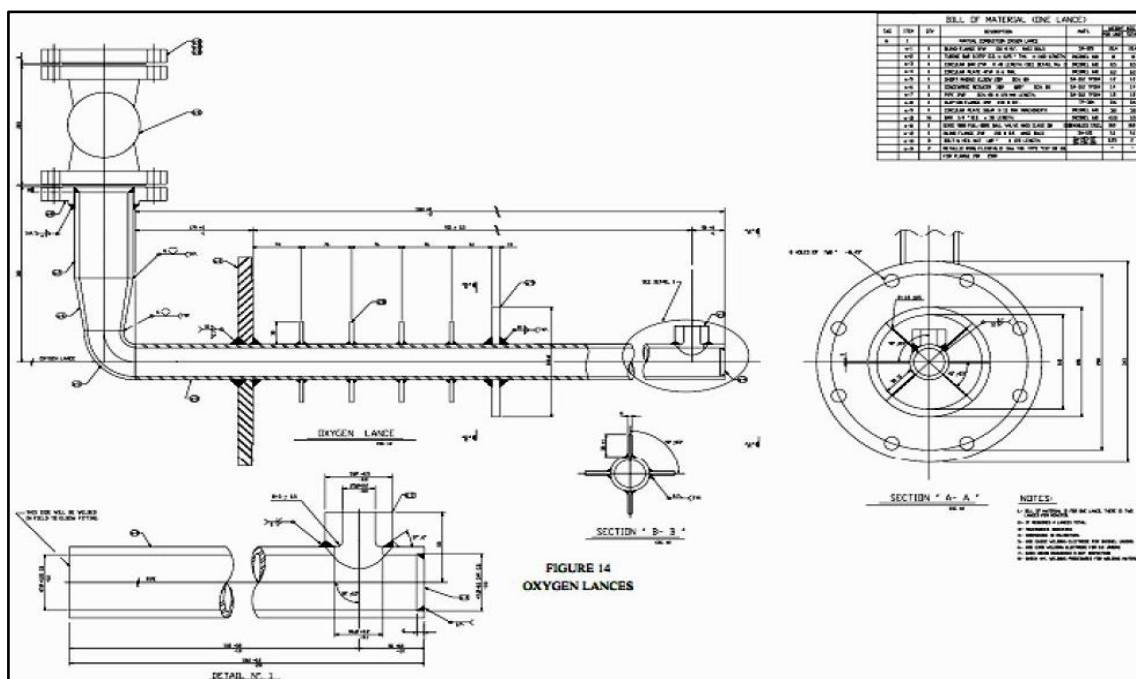


Figure B3: Overview drawing on the transfer line



**Figure B4 (a):** Details drawing on the oxygen lances



**Figure B4 (b):** Details drawing on the oxygen lances

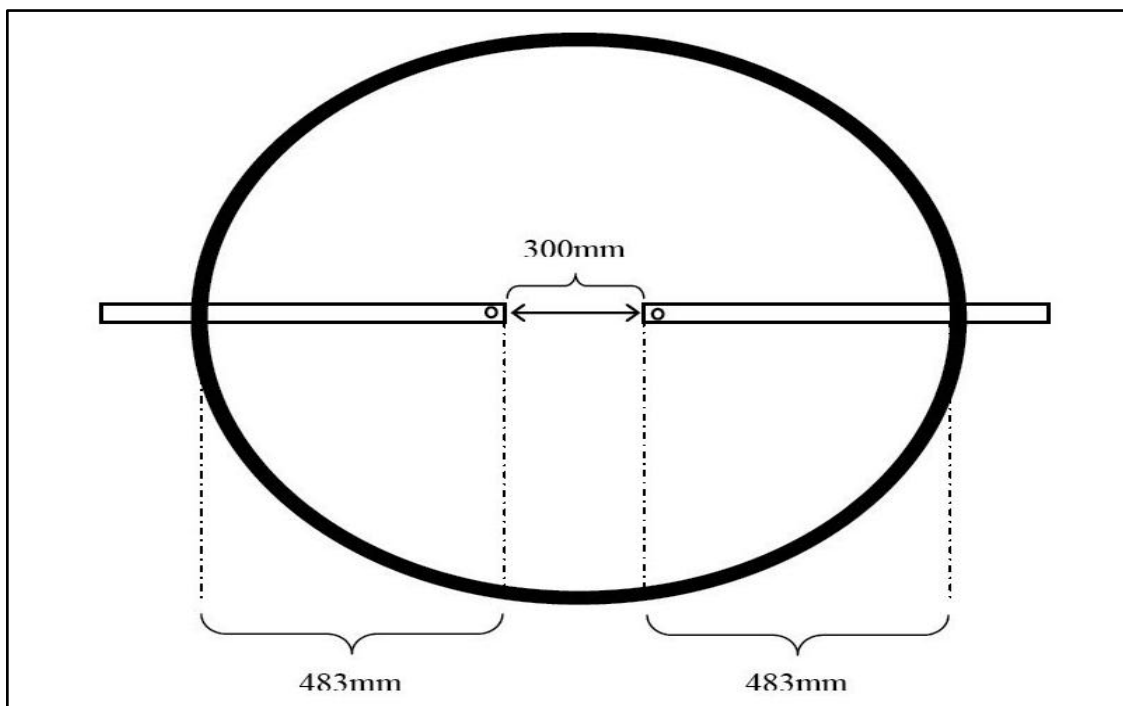


**Figure B5:** Overview drawing on oxygen lances

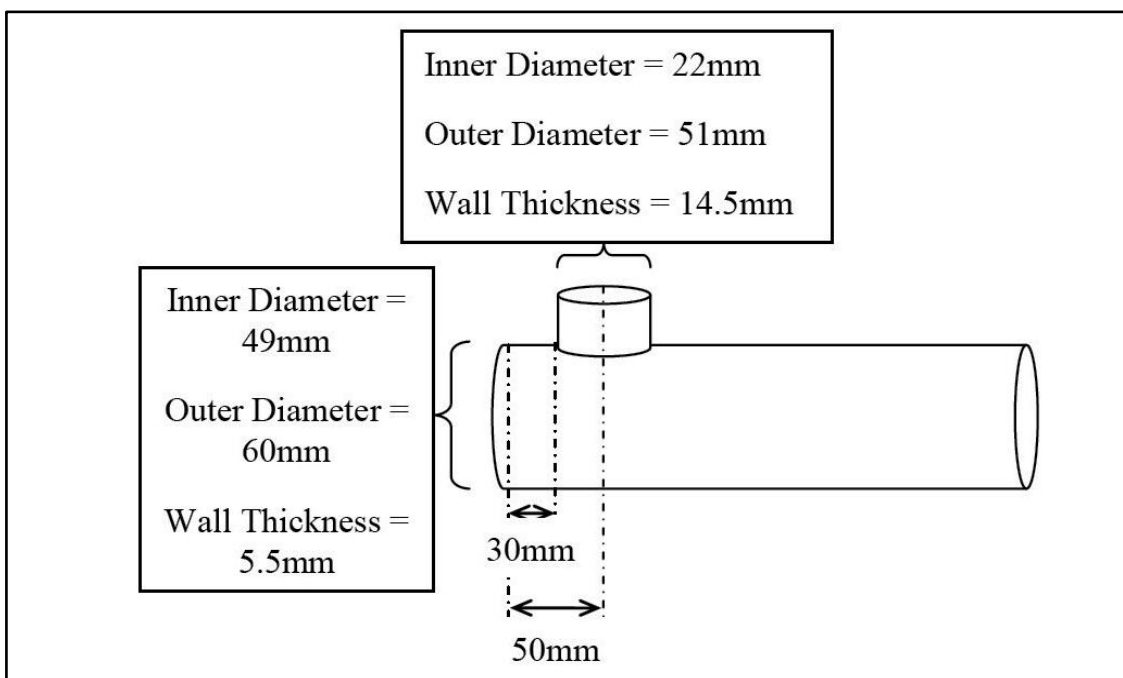


**Figure B6:** Overview drawing on nozzle oxygen lance

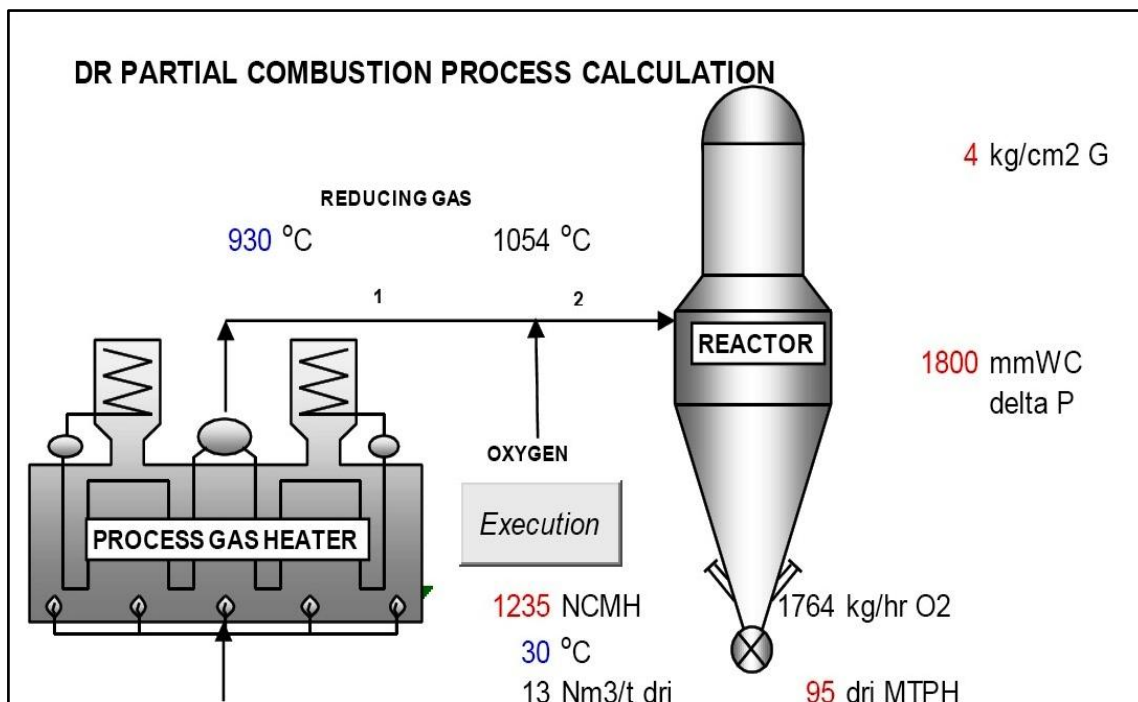


**Figure B7:** Excel simulation

**Table B1:** Mass fraction on the excel simulation

<b>Mass fraction</b>									
<b>STREAM</b>									
<b>No</b>	<b>1</b>					<b>2</b>			
	<b>MW</b>	<b>%</b>	<b>Mass fraction</b>			<b>%</b>	<b>Mass fraction</b>		
<b>H2</b>	2.01	69.63	1.40	8076.65	0.1538	67.7	1.36	7855.01	0.1447
<b>CO</b>	28.01	15.78	4.42	25498.15	0.4854	15.8	4.42	25498.15	0.4696
<b>CO2</b>	44.01	1.53	0.67	3873.00	0.0737	1.5	0.67	3873.00	0.0713
<b>CH4</b>	16.04	7.48	1.20	6925.45	0.1318	7.5	1.20	6925.45	0.1276
<b>N2</b>	28.02	4.07	1.14	6579.34	0.1253	4.1	1.14	6579.34	0.1212
<b>H2O</b>	18.01	1.52	0.27	1576.61	0.0300	3.4	0.62	3562.54	0.0656
<b>O2</b>	32.00								
			9.10		1.00		9.41		
<b>NCMH</b>	129263.00								
<b>kg/hr</b>	52529.20	=	52529.20		54293.49	=	54293.49		

**Table B2:** Mass balance on the excel simulation

<b>Mass Balance</b>								
<b>STREAM</b>								
<b>No.</b>		<b>1</b>		<b>O2</b>		<b>Mix</b>		<b>2</b>
	<b>%</b>	<b>NCMH</b>	<b>%</b>	<b>NCMH</b>	<b>%</b>	<b>NCMH</b>	<b>%</b>	<b>NCMH</b>
<b>H2</b>	69.6	90008.41			69.0	90008.41	67.7	87538.41
<b>CO</b>	15.8	20391.24			15.6	20391.24	15.8	20391.24
<b>CO2</b>	1.5	1971.26			1.5	1971.26	1.5	1971.26
<b>CH4</b>	7.5	9671.46			7.4	9671.46	7.5	9671.46
<b>N2</b>	4.1	5259.71			4.0	5259.71	4.1	5259.71
<b>H2O</b>	1.5	1960.92			1.5	1960.92	3.4	4430.92
<b>O2</b>			100.0	1235.00	0.9	1235.00	0.0	0.00
	100.0	129263.00	100.0	1235.00	100.0	130498.00	100.00	129263.00
<b>MW</b>	9.1		32.0		9.3		9.4	
<b>NCMH</b>		129263.00		1235.00		130498.00		129263.00
<b>kg/hr</b>		52529.20		1764.29		54293.49	=	54293.49
<b>kgmol/hr</b>		5770.67		55.13		5825.80		5770.67
						54293.49	=	54293.49

**Table B3:** Energy balance on excel simulation

Energy Balance			
Qin		Qout	
H1	Q1	H2	Q2
6594.59	26498614.48	7607.71	29730654.27
-19609.65	-17851114.62	-18614.39	-16945106.07
-83367.49	-7336565.41	-81649.44	-7185372.36
-5047.29	-2179225.88	-2626.92	-1134201.55
6734.55	1581329.77	7721.53	1813082.34
-49526.09	-4335565.96	-48209.50	-9536268.26
7130.59	393137.38		
	-3229390.22	=	-3257211.63

Tout	Qout	SUMMARY OUTPUT							
950	-8774196								
1000	-6155573	<u>Regression Statistics</u>							
1100	-796798.8	Multiple R	0.999984						
		R Square	0.999968						
1054	-3229390 =Qin	Adjusted F	0.999936						
		Standard E	32479.61						
		Observatio	3						
<u>ANOVA</u>									
		df	SS	MS	F	ignificance F			
		Regressior	1	3.31E+13	3.31E+13	31348	0.003596		
		Residual	1	1.05E+09	1.05E+09				
		Total	2	3.31E+13					
		Coefficient	standard Err	t Stat	P-value	Lower 95%	Upper 95%	ower 95.0%	pper 95.0%
		Intercept	-5.9E+07	306289	-193.837	0.003284	-6.3E+07	-5.5E+07	-6.3E+07
		X Variable	53240.52	300.7027	177.0537	0.003596	49419.73	57061.31	49419.73

**Figure B8:** Summary data from excel simulation